RIPRAP DESIGN FOR WIND-WAVE ATTACK

A laboratory study in random waves

September 1975

Hydraulics Research Station
Wallingford
Oxfordshire
England

Report No
EX 707

CONTENTS

CONTENTS (Cont'd)

CONTENTS (Cont'd)

CONTENTS (Cont'd)

FIGURES

CONTENTS (Cont'd)

PLATES

PREFACE

This report is the official Hydraulics Research Station (HRS) account of an investigation into riprap stability in random waves carried out in co-operation with the Construction Industry Research and Information Association. This laboratory study arose out of earlier work on riprap done by HRS for the Civil Engineering Research Association. Rather than extend the original study it was decided to take advantage of improved laboratory techniques and examine the stability of riprap in paddle generated irregular waves which could be directly related to irregular waves occurring in nature, thus avoiding the problem of relating natural waves to the regular waves largely used in the former study.

RIPRAP DESIGN FOR WIND-WAVE ATTACK

A laboratory study in random waves

INTRODUCTION

Riprap is graded quarry stone. This report considers its performance when dumped on an earth embankment to give protection from wind generated waves, a situation which occurs typically on the upstream faces of embankment dams. The waves are assumed to be in deep water which distinguishes this case from those of shallow water coastal environments. In any case the behaviour of graded riprap on an impermeable (to waves) embankment must be distinguished from that of single sized rock on the permeable (to waves) rubble mound breakwaters found in coastal situations.

The cost of the riprap, which can be considerable, is roughly proportional to the volume of stone required which is in turn directly dependent on the thickness of the protective layer (for a given slope and run-up the area to be protected is constant). In current practice the thickness depends on the D_{50}^{R} stone size which is simply related to wave height. Thus the cost of the riprap depends on the choice of design wave conditions and the method used to relate wave height to riprap size. In both cases there is considerable uncertainty.

In 1962 the Civil Engineering Research Association (CERA) sponsored laboratory tests which resulted in the publication of a report (1) giving design procedures for determining the riprap size required for given design wave conditions. The CERA work represents one of the first attempts to relate the results of tests using regular waves to those using irregular waves (laboratory wind generated in this instance). This relationship is a particular problem because most quantitative information on wave damage comes from laboratory generated regular waves rather than from irregular waves of the kind found in nature. Before an extension of the CERA work could be satisfactorily completed it became clear that the regular-irregular wave problem could be solved by using paddle generated irregular waves which had meanwhile become available. Thus it was decided to take advantage of improved techniques and make a new series of tests which covered parts of both the original CERA research programmes.

This report describes the tests and the resulting design procedures which apply to deep water waves. In brief, the volume of riprap eroded was measured as a function of the number of incident waves for each of three sizes of riprap for each of several significant wave heights at three mean wave periods. These measurements were made on slopes of 1 : 2, 1 : 3, 1 : 4 and 1 : 6. Throughout the work, in the planning, execution and reporting, discussions were held with practising engineers who formed the majority of a steering group (Appendix 1) set up by the Construction Industry Research and Information Association (successor to CERA) to guide the project.

CONCEPTUAL FRAMEWORK

In nature winds blowing over a reservoir formed by a dam generate waves. If these waves are incident on the dam then erosion will occur if the dam is not protected.

The growth of the waves depends on the wind velocity, the distance of water over which it blows (the fetch) and the time for which it blows (the duration). This means that the waves will be small at the up-wind end of the reservoir and that they will increase in height progressively with distance down-wind and be at a maximum at the down-wind end of the reservoir. At any point in the reservoir the waves also grow progressively in time (duration) until some limiting value is reached. In nature the wind velocities vary in time and space so that it is evident that the whole phenomenon of wave generation becomes very complex. It is usual to simplify the situation by assuming that the wind velocities are uniform and steady (ie non-varying in space and time) so that two cases can be distinguished; in the first the wave growth is limited by the fetch no matter how long the wind blows, and in the second the fetch is assumed to be so great that the growth is limited by duration. In a reservoir the waves are usually fetch limited.

The description of the waves remains a problem even when wave growth has ceased and equilibrium is assumed between the energy input to the waves by the wind and energy dissipated by waves breaking and by turbulence. This is because the waves are irregular in height, wave length and crest length. (Fig 2 includes a sample wind-wave record.) In effect the waves form a randomly changing surface which must be described statistically. To further simplify the situation it is usual to assume that the waves generated by the wind propagate only in the direction of the wind and have infinitely long crests. The randomly changing water surface can now be assumed to be the result of adding together a large number of sine waves with different heights and frequencies (frequency is the reciprocal of period) and random phase relative to one another (2). This leads to the fundamental description of the random sea, namely the wave or energy spectrum which specifies the amount of energy associated with the different wave frequencies. Thus in the typical energy spectrum in Fig 1a, the shaded area gives the energy between frequencies f_1 and f_2. Most of the energy in the waves is at frequencies in the region of the peak of the spectrum and this can be interpreted in terms of the constituent sine waves having the largest amplitudes at frequencies around those of peak of the spectrum. However it must be emphasised that these constituent sine waves which are used to get a theoretical understanding of the random sea cannot be directly observed or identified in the random waves. Indeed the individual observable waves are transient and are continually merging with other individual waves. Similarly the spectral ordinates (Fig 1a) do not represent wave height squared but wave height squared per frequency (ie the ordinate is not energy but energy density) and hence have no observable physical analogue in terms of individual wave heights in the random sea.

What the observer actually sees at a point in a random sea is a series of individual waves with heights and periods which vary randomly from wave to wave. This situation can only be described statistically by cumulative probability functions (Fig 1b). In Fig 1b, for example, q_1 is the probability that any wave at an observation point will exceed the value H_1 in height. It can be shown (2) that if the energy spectrum is known then the probability functions for wave heights and periods can be derived. Under steady wave conditions the energy spectrum does not change in time so that the derived probability distributions remain constant. Thus the waves can be defined by mean heights and periods which are simply derived from the probability distributions which are in turn calculated from the spectrum.

Generally the significant wave height (H_S) and the significant wave period (T_S) are the mean values used for defining waves. The significant wave height is the mean height of the highest third of the waves in the sea and the significant period is the mean period of the waves having the highest third of the heights. Historically these parameters were obtained directly from wave records by identifying individual waves and reading off the heights and periods. Much of the data for the Sverdrup–Munk–Bretschneider wave forecasting scheme were obtained by this method. Unfortunately, problems arise in the way that an individual wave in the record should be defined and some of the earlier methods do allow a degree of subjectivity (3).

However satisfactory definition schemes do exist. One such scheme defines the individual waves by zero crossings (see below). It can be shown (2) for a narrow spectrum (ie, one in which all the energy is restricted to a small range of frequencies as in Fig 2a) that the significant wave height $\overline{H}_3$, defined by zero crossings,

is given by $$\overline{H}_3 = 4.0\ m_0^{1/2} \quad \text{....(1)}$$

where m_o is the area under the spectrum (see Fig 2). There is good evidence for using this relationship with non-narrow spectra (4,5) such as those of wind waves (see Fig 2b) provided that the zero crossing definitions are used. In this scheme the individual wave height (H) is taken as the difference in level between the maximum and minimum water surface elevations between two successive down crossings of the mean water level (called zero crossings). The period (T) of the wave is taken as the time between the down crossings. Figs 2a,b give examples of the identification of individual waves on the zero crossing scheme of definition for two wave records with the same significant wave height and mean zero crossing period ($\overline{T}$) but different distributions of energy with frequency ie, different spectral shapes. This difference in shape is characterised by the spectral width parameter ϵ which varies from a value of zero for very narrow spectra to unity for the widest spectra and can be obtained by counting the number of zero crossings and the number of wave crests (6). Clearly $\overline{H}_3$ and $\overline{T}$ can be calculated once the H,T for the individual waves are known. (A practical method for getting $\overline{H}_3$ and $\overline{T}$ from a wave record is given in Reference 6). Thus waves can be characterised by $\overline{H}_3$, $\overline{T}$ and ϵ which are obtained either by counting individual waves using zero crossings or from the spectrum as outlined above. Bretschneider (3) shows that T_S is also related to the spectrum and subsequently (7) gives the relationship

$$\overline{T} = 0.91\ T_S \quad \text{....(2)}$$

between $\overline{T}$ and T_S. The zero crossing system will be used throughout this report.

In summary, it can be stated that in steady wind conditions the waves attacking the riprap will vary randomly in height according to a known probability distribution which is determined by the wave spectrum which in turn can be characterised by $\overline{H}_3$, $\overline{T}$ and ϵ.

If the waves attacking the riprap are large enough damage will occur as individual stones are dislodged and moved (generally) down the slope so that the thickness of the protective layer is reduced. In this report this damage is referred to as erosion damage and is initially quantified in terms of the volume (below the surface of the undisturbed riprap) eroded by the waves. This eroded volume usually takes the form of a depression in the riprap layer and failure is deemed to occur when a hole occurs somewhere in this depression which exposes the filter layer.

The attacking waves are random, and so is the riprap. Its shape and size is random between limits, it is dumped not placed. Hence it is described by a grading curve which is in effect a cumulative probability distribution function for size. It is often parameterized in terms of D^R_{50}, D^R_{85} etc. It is evident that the damage caused by a storm (a train of random waves) to the riprap (a random agglomeration of rock) will itself be random with an expected mean value. The designers' problem is to produce a safe and economical solution in the face of these statistical uncertainties. The following review of current practice sets out the published information currently available to the designer and forms an introduction to research described in this report.

REVIEW OF CURRENT PRACTICE

In discussing current practice no attempt will be made to set out the procedure of particular design offices but rather to collect together information available in the literature. This in turn may weight the discussion toward American practice which is the most widely published.

Wave prediction

The first step in designing the riprap is to determine from wind data the wave conditions on the upstream face of the dam. In all cases a derivative of the Sverdrup–Munk (8) method is used which relates measured wind speeds and fetches in deep water to measured significant wave heights and periods through dimensionless plots. Bertram (9), Sherard et al (10) and a recently revised US Army

Corps of Engineers' manual (11) use the earliest versions of this work whereas others (1,12-15) use the work of Saville et al (16,17) which is a revision of Bretschneider's (18) modification of the original method.

Saville et al (17) present design curves for fetches up to 40 miles after adding results of wind and wave recording on two reservoirs with fetches up to 6 miles to the earlier data which included data for fetches of the order of half a mile. The latest revisions of the Sverdrup–Munk method (19,7) are not so convenient to use for short fetches but can be used along with Saville's results as a check.

The most recent approach to the problem of fetch limited waves is that of JONSWAP (20) which uses spectral based methods and data different from that of the Sverdrup–Munk–Bretschneider (SMB) tradition. It can be shown that the JONSWAP results relate the surface wind speed at the 10 m elevation (U_{10}), the fetch (F), the acceleration due to gravity (g), the significant wave height ($\overline{H}_3$), the frequency of the peak of the wave spectrum (f_m) and the mean zero crossing period ($\overline{T}$) as follows:

$$\overline{H}_3 = 16 \times 10^{-4} \, (FU_{10}^2/g)^{1/2} \quad \ldots.(3)$$

$$f_m = 2.84 \, g^{0.7}/(U_{10}^{0.4} \, F^{0.3}) \quad \ldots.(4)$$

$$\overline{T} = 0.85/f_m \quad \ldots.(5)$$

The exact form of the JONSWAP spectrum can be calculated if required.

In both the SMB and the JONSWAP methods the data is scattered. This is inherent to some extent but the scatter of SMB is considerable. In addition there are difficulties in applying either method to reservoirs.

1. Both assume deep water conditions (depth greater than a quarter of the longest wave length (21)). Other methods are required in non-deep water situations (15).

2. The surface wind speed, direction and duration must be known at the reservoir site. How this is affected by topography is a very complex problem.

3. The over water wind speed is greater than the overland wind speed. Saville (16,17) gives data and this has considerable scatter.

4. The fetch width is usually finite and may vary rapidly with direction in an irregularly shaped reservoir. Saville (16) gives a method of calculating the effective fetch in these conditions which made his recorded data fall on the same line as the SMB data.

To summarise, the calculation of the wave conditions requires wind data in terms of wind speed, direction and duration which must be estimated or measured at the reservoir site. From this and the greatest plan area of the reservoir the effective fetch and over-water surface wind speed can be calculated (16). This information together with the duration can then be used in the design curves (7,16) to give the significant wave heights and periods for those particular wind conditions. If the waves are fetch rather than duration limited (7,16) the effective fetch and wind speed can also be used in equations (3-5) to give $\overline{H}_3$, f_m and $\overline{T}$ (NB $\overline{T}$ is the mean zero crossing period not the significant period) using the JONSWAP data.

Riprap design procedures

In this section procedures for relating the predicted wave heights to some average riprap dimension will be discussed. Riprap grades, thickness, filters etc will be dealt with in later sections.

Some experience based methods are self-contained; thus Bertram (9) predicts an undefined "maximum wave height" and from a survey of dams provides a table of minimum average rock sizes against maximum wave heights (note that Taylor (15) in a recent review suggests that these rock sizes

are too small). Sherard et al (10) follows Bertram whilst the US Bureau of Reclamation (USBR) (22) gives a table relating fetch to rock size. The US Army Corps of Engineers (11) imply that the Bertram "maximum wave height" should be used in the relationship

$$W_{50}^{R} = \gamma_R H_D^n / K_R (S_R - 1)^3 \cot a \quad \text{....(6)}$$

where W_{50}^{R} = median rock weight

γ_R = specific weight of rock

H_D = design wave height

n = 2

K_R = riprap "K factor" = 1.82

S_R = specific gravity of the rock

a = angle of embankment to the horizontal

(R as a superscript or subscript refers to riprap throughout this report).

Equation (6) was proposed by Hudson (23) with n = 3 for determining single size rock weights for breakwaters and was subsequently recommended (24) for riprap design with n = 3 for wave heights less than 1.5 m. K_R is a dimensionless variable which is measured in model tests and it is in the use of models that three problems are introduced:

1. The SMB and JONSWAP prediction methods give significant wave heights relating to the irregular waves in nature. Should these heights be set equal to height of the regular waves used in the model tests. In other words, how should the design wave height be chosen?

2. To what level of damage (if any) does any given value of K_R correspond and how is damage defined?

3. Are there scale effects between model and nature?

Although these questions are inter-related they can be used as a framework for discussion.

The design wave height is chosen variously. Some recommend that the protection should be designed for the worst storm (taking account of the fetch and orientation of the dam) predicted in the life-time of the dam and use these design wind conditions to get a design significant wave height H_S (see "Wave prediction"). Torum (12) tentatively suggests that following breakwater practice, H_D should be set equal to H_S in the Hudson version of equation (6) (n = 3). McConnell et al (14) also use $H_D = H_S$ but in non-Hudson type formula. Taylor (15) uses $H_D = 1.25\ H_S$ in equation (6). This puts H_D at the expected height of the highest wave in a group of 20 waves, ie, it suggests that regular waves of height $1.25\ H_S$ gives the same damage as irregular waves of significant height H_S. Burgess and Hicks (1) recommend from laboratory comparisons of the damage caused by regular and irregular waves that $H_D = 1.85\ H_S$ (with a safety factor included) in the graphs they present for relating H_D to riprap size.

A second approach for choosing the design wave height for use in a formula developed from regular wave tests is presented by Iverson and Ringheim (13). From a year's wind data they used the method of Saville et al (16) to get all the corresponding significant wave height and period combinations. They then used the known statistical distributions of individual wave heights in an irregular wave train of significant height H_S to get the frequency of occurrence of individual waves for a whole year. H_D was set to the wave height that would be exceeded by 100 individual waves in one year.

A further complication in the selection of H_D is the fact that the waves may not attack the riprap at normal incidence. It is usually assumed (implicitly) that waves at normal incidence cause the most damage. Burgess and Hicks (1) present limited experimental evidence supporting this view and suggest how allowance can be made for the effect when H_D is chosen. Other authors make no allowance.

The damage expected using the different procedures also varies. These self-contained methods based on experience give no specification of damage. Burgess and Hicks (1) allow a loss of 5% by weight of the riprap over a length of 4 H_D on the slope for $H_D = 1.67\ H_S$ and expect failure for $H_D > 1.67\ H_S$. Both Taylor (15) and Iverson (13) discuss the K_R value which can be used by making reference to (24) which quotes K_R (or K_D) values for no damage. Subsequently Beene and Ahrens (25) and Thomsen et al (26) use a riprap stability coefficient N_S related to K_R by the equation

$$K_R = N_S^3 \tan \alpha \qquad \text{....(7)}$$

for nominal "no damage". "No damage" is the point at which the erosion of the riprap shows a sharp increase with increasing wave height. These authors also quote a reserve stability at which failure occurs, failure being defined (as in (1)) as the exposure and erosion of the under-layer.

Scale effects are discussed by Thomsen et al (26) and are implicit in the work of Beene and Ahrens (25) which was done in regular waves at natural scale in a large flume. Thomsen et al (26) suggests that the linear dimensions of riprap specified on the basis of small scale laboratory tests may be up to 60% too large.

It is clear from the foregoing that the designer is currently faced with large areas of uncertainty.

Riprap size, grade and shape

In the foregoing section the way in which the design procedures specify the riprap was not discussed. The implicit assumption in all the methods is that riprap can be specified by a typical diameter and a grading. Model tests (1,26) show that median size by weight (W^R_{50}) can be used to relate damage to wave height independent of the grading. Many authors, particularly those following the Hudson type equation (6), use this method (11,15,24,26) and others specify a D^R_{50} size which is equivalent to the median size by weight. There are problems with this equivalencing; for example, Bertram (9) and Sherard et al (10) give no method (and in any case call D^R_{50} an average dimension rather than the median), Burgess and Hicks (1) use equivalent spherical diameter. Taylor (15) gives the formula

$$0.75\ D^3 = W/\gamma_R \qquad \text{....(8)}$$

Similarly there are various grading recommendations. Some (9,27) simply say "well graded". Burgess and Hicks (1) suggest that the smaller sizes should correctly match the filter layer. Other suggestions for maximum and minimum stone sizes are:

Reference 11
$$\begin{cases} W^R_{MAX} = 4.0\ W^R_{50} \\ W^R_{MIN} = 0.125\ W^R_{50} \end{cases} \qquad \text{....(9)}$$

Reference 24
$$\begin{cases} W^R_{MAX} = 3.6\ W^R_{50} \\ W^R_{MIN} = 0.22\ W^R_{50} \end{cases} \qquad \text{....(10)}$$

Reference 15
$$\begin{cases} W^R_{MAX} = 4.0\ W^R_{50} \\ W^R_{MIN} = 0.25\ W^R_{50} \end{cases} \qquad \text{....(11)}$$

$$\text{Reference 26} \begin{cases} \text{Narrow gradation} & 1.0 < (W^R_{85}/W^R_{15})^{1/3} < 1.3 \\ \text{EM–1110–2–2300 gradation} & 1.3 < (W^R_{85}/W^R_{15})^{1/3} < 2.5 \\ \text{Wide gradation ("quarry run")} & 2.5 < (W^R_{85}/W^R_{15})^{1/3} < 9.0 \end{cases} \quad \ldots.(12)$$

$$\text{Reference 10} \quad 1.5\ D^R_{50} \text{ down to 1 inch} \quad \ldots.(13)$$

Other information is available on grades actually used in the field (13,14,1), on grades for particular fetches (22), on recommended grading for 24 inch and 36 inch riprap (27) and rock quality (10,27).

So far as shape is concerned Burgess and Hicks (1) found in model tests that angular stones were more stable than rounded or flat stones which is also the case for single size breakwater stones (24). However, Thomsen et al (26) found that stone shape had no effect on stability over the range of shapes tested. The weight of the evidence favours cubical shapes.

Riprap thickness and placing

Two rules are given for riprap thickness;

1. The minimum thickness should be 1.5 D^R_{50} (1,9,10,13,15) or

2. The thickness should be sufficient to contain the largest rock (9,10,13,15). Taylor (15) gives the thickness (t_R) as

$$t_R = (W^R_{MAX}/\gamma_R)^{1/3} \quad \ldots.(14)$$

Thomsen et al (26) found no difference in laboratory performance for thicknesses of 1.4 to 2.9 D^R_{50} whereas Burgess and Hicks (1) found performance improved with thickness up to 2.75 D^R_{50} but suggested that there is no economic advantage in thicknesses greater than 2 D^R_{50}.

Construction methods are all aimed at producing a uniform, well knit unsegregated layer (10). Construction always begins at the toe of the slope and where the rock is of suitable size and quality it can be bulldozed up the slope (10). This gives compaction and ensures all the large rocks lie within the layer. More often the rock is tipped into place from above as the dam is built or by lowering vehicles down the completed slope (10). Sherard et al (10) recommend that there should be no bulldozing down slope because it produces segregation, a point confirmed by the experience of McConnell et al (14). The riprap can be directly placed by grab or dragline (13), equipment which is also used for trimming and reworking dump rock (1,10). Thomsen et al (26) describe an alternative method of construction where the riprap is tipped into place (down the slope) from a skip to minimise reworking.

Filter layer size, grading and thickness

A common problem with riprap protection is the erosion by wave action of the material underlying the riprap layer. To prevent this a filter layer of angular or rounded stone is interposed between the embankment andthe riprap. In some cases a double filter is required (sometimes referred to as a bedding layer and an upper coarser layer of spalls) to satisfy the design criteria which in many cases appear to be the same as those used for preventing the wash out of fine materials under steady hydraulic gradients. Many criteria have been suggested (R ~ riprap, F ~ filter, E ~ embankment):

(i) (Reference 9)

$$D^F_{85} > 50 \text{ mm}$$

$$D^R_{15}/D^F_{85} < 10$$

(ii) (Reference 10) $D^F_{85} > 50$ mm

$D^R_{15}/D^F_{85} < 10$

$D^F_{15}/D^E_{85} < 5$

(iii) (Reference 22) $D^F_{85}/(\text{Maximum opening of drain pipe}) > 2$

$D^F_{15}/D^E_{85} < 5$

$5 < D^F_{15}/D^E_{15} < 40$

The grain size curve for the filter and embankment should be roughly parallel.

(iv) (Reference 28) $D^R_{15}/D^F_{85} < 4$

$D^R_{15}/D^F_{15} < 20$

(v) (Reference 28) $D^R_{50}/D^F_{50} < 30$

$D^R_{15}/D^F_{15} < 15$

(vi) (Reference 29) $D^R_{15}/D^F_{85} < 5$

$D^R_{50}/D^F_{50} < 25$

$D^R_{15}/D^F_{15} < 20$

(vii) (References 1,27) $D^R_{15}/D^F_{85} < 5$

On minimum filter thickness opinions vary from 150 mm (300 mm for a double filter layer)(15) through 200 mm (11) to 300 mm (22) for single layer filters, the constraints being constructional. Alternatively 0.5 D^R_{50} has been suggested (1,22) and Burgess and Hicks (1) point out that a very porous filter can increase riprap stability.

Run-up and run-down

The run-up and run-down of the waves on a riprap protected slope affects the freeboard design and the lower limit of the protection. Sherard et al (10) give the run-up (measured vertically above still water level) as 1.5 times the undefined maximum wave height which is used for riprap design. Another self-contained method (22) tabulates freeboard against fetch.

The remaining methods use data from model tests in regular waves. Much of the data is American (24),relevant parts of which are presented by Saville et al (16) for freeboard design. Burgess and Hicks (1) supply similar data for run-up and run-down. Again the problems of design wave height and scale effects arise. Saville et al (16) recommend the use of H_S for the design wave height, acknowledging that there will be some overspill whereas Burgess and Hicks (1) use 1.67 H_S. McConnell et al (14) use 1.25 H_S. On scale effects Burgess and Hicks (1) supply correction factors which are already incorporated in the data of Saville et al (16).

It is clear from the preceding review that data is required which relates the damage and run-up directly to the wave parameters (significant wave height etc) used in wave prediction. This can be done by using paddle generated irregular waves as opposed to the regular waves formerly used. The following describes such a research programme.

PARAMETER LIST

It is convenient to list and define the parameters used in the experiments in terms of the independent and dependent variables. The former are those which can be varied independently (for example, wave height or rock size); the latter are those whose values are specified once the independent variables are fixed (for example, the erosion damage depends on the wave height and stone size amongst other things). The list of the independent variables must be comprehensive enough to describe uniquely an experiment.

Independent variables

The independent variables that must be considered have been largely determined by the "Review of current practice" and will now be dealt with systematically.

The waves when long crested and normally incident on the riprap are specified by the density ρ of water, the dynamic viscosity μ of water, the acceleration due to gravity g, the depth of water d, and the energy spectrum E(f) where f is the frequency in Hz. Although the energy spectrum E(f) completely specifies the waves it is inconvenient to use directly in the context of this report because the wave prediction methods used by engineers yield significant wave heights and periods rather than spectra. However it is possible to relate the characteristic wave heights and periods to the spectrum E(f) through the following general relationships (2):

$$\bar{H}_3 = 4.0\, m_0^{1/2} \qquad \text{....(15)}$$

$$\bar{T} = (m_0/m_2)^{1/2} \qquad \text{....(16)}$$

$$\epsilon^2 = (1 - m_2^2/m_0 m_4) \qquad \text{....(17)}$$

where

$$m_n = \int f^n E(f)\, df \qquad \text{....(18)}$$

with $n = 0, 2, 4.$

Hence if a standard spectral shape is assumed $\bar{H}_3$, $\bar{T}$ and ϵ can be specified and the spectrum E(f) deduced via equations (15-18). This allows the waves to be described in terms of engineering parameters which are simply related to the significant wave heights H_S ($\equiv \bar{H}_3$) and periods T_S ($\simeq 1.1\ \bar{T}$, see equation (2)) of the wave prediction. procedures.

The preliminary tests (Appendix 3) show that the damage does not depend critically on the spectral shape so the Moskowitz spectrum (30) which was developed for equilibrium wind waves in the deep ocean was used in this investigation. The spectrum is of the form suggested by Bretschneider (3) as part of his work on the Sverdrup–Munk–Bretschneider wave prediction scheme commonly used by engineers. It also has the advantage of being easily manipulated. In its original form it is written

$$E_M(\omega) = (Ag^2/\omega^5) \exp(-B(\omega_0/\omega)^4) \quad \text{for } \omega > 0$$

$$E_M(\omega) = 0 \quad \text{for } \omega < 0 \qquad \text{....(19)}$$

where ω is radian frequency, A (= 0.0081) and B (= 0.74) are dimensionless constants and $\omega_o = g/U_{10}$, U_{10} being the wind speed at 10 m elevation. If the spectrum is restricted to frequencies between $0.5\omega_o$ and $2.0\omega_o$ (31) to give a spectral width (ϵ) of 0.5 it can be rewritten after transformation to Hz as

$$E(f) = (0.122\ \bar{H}_3^2/(\bar{T}^4\ f^5))\ \exp\ (-0.46/(\bar{T}\ f)^4) \qquad ....(20)$$

which is a spectrum defined by $\bar{H}_3$ and $\bar{T}$ with a fixed spectral width.

It is also evident that the damage must be a function of the average number of zero crossing waves $\bar{N}$ incident on the riprap. Thus the parameter list for specifying the waves is

$$\rho,\ \mu,\ g,\ d,\ \bar{H}_3,\ \bar{T},\ \epsilon,\ \bar{N} \qquad ....(21)$$

provided a spectral shape of the form of equation (20) is used.

The riprap size is exactly specified by its grading but the "Review of current practice" suggests that the median size (D_{50}^R) by weight is sufficient to specify it from the point of view of damage. A more complete description of the grading includes D_{85}^R/D_{50}^R and D_{15}^R/D_{50}^R. The list is completed by ρ_R, the density of the rock, ρ_R^{BL} the bulk density of the riprap when laid, t_R the mean thickness of the riprap layer at right angles to the slope, S_h, a shape parameter and P, a parameter denoting the method of placing, ie,

$$D_{50}^R,\ D_{85}^R/D_{50}^R,\ D_{15}^R/D_{50}^R,\ \rho_R,\ \rho_R^{BL},\ t_R,\ S_h,\ P \qquad ....(22)$$

The filter does not contribute to the stability of the riprap by its weight but by its draining properties so that it is sufficient to specify its grading D_{50}^F, D_{85}^F/D_{50}^F, D_{15}^F/D_{50}^F, the bulk density ρ_F^B and the thickness t_F of the layer.

The embankment slope α completes the list of independent variables since the embankment is assumed impermeable.

Dependent variables

The dependent variables investigated are those which are of interest to the designer. There are two sets of variables, one describing the damage and one describing the run-up.

The damage is described by the erosion damage, the upper and lower limits of the damaged area, the erosion damage at failure and the minimum thickness of the riprap at failure (see Fig 3). The erosion damage is measured by N_Δ, the number of D_{50}^R sized spherical stones eroded from a 9 D_{50}^R width of the riprap slope (the 9 D_{50}^R width arises because the slope was surveyed for volume changes along 10 sections up the slope, each separated by D_{50}^R – the precise details are given in "Measurements and procedure"). The upper and lower limits of the damaged area l_u, l_l are measured vertically from still water (Fig 3), the minimum thickness t_R^{MIN} at failure is measured at right angles to the slope (Fig 3). Failure is said to have occurred when a $D_{50}^R/2$ sized hole appears through the riprap down to the filter layer.

The run-up and run-down, r_u and r_d, are the maximum and minimum water levels (with respect to still water – Fig 3) reached on the slope during the passage of a wave.

(The details of the measurement of these variables is set out in "Measurements and procedure".)

DIMENSIONAL ANALYSIS AND TEST PROGRAMME

Complete analysis

The controlling or independent variables defined in the previous section must be gathered into dimensionless groups for the conduct of the experiments so that the results can be interpreted for design information at natural scales. There are many equivalent sets of dimensionless groups that can be derived from any given set of independent variables. Usually a set is chosen which expresses the physics (ie, flow fields, forces and fluid) of the situation and gives experimental convenience. The latter point is important because the aim experimentally is to determine the dependence of any given variable (the damage for example) on the dimensionless groups in the set by varying each group one at a time. This can be done most easily by having each of the experimental variables in a separate group.

The dependent variable of greatest interest is the erosion damage N_Δ. By gathering together the independent variables from the previous section and performing the usual dimensional analysis N_Δ can be written

$$\begin{aligned} N_\Delta = f(&\bar{H}_3/D^R_{50},\ 2\pi D^R_{50}/g\bar{T}^2,\ 2\pi d/g\bar{T}^2,\ \rho\bar{H}_3 D^R_{50}/\mu\bar{T},\ \bar{N},\ \epsilon,\\ &a,\ D^R_{85}/D^R_{50},\ D^R_{15}/D^R_{50},\ \rho_R/\rho,\ \rho^{BL}_R/\rho,\ t_R/D^R_{50},\\ &S_h,\ P,\ D^R_{50}/D^F_{50},\ D^R_{15}/D^F_{85},\ D^R_{15}/D^F_{15},\ t_F/D^R_{50},\ \rho^B_F/\rho_R) \end{aligned} \qquad \ldots.(23)$$

The implication of equation (23) is that if values are given to all the ratios on the right hand side then the erosion damage N_Δ is uniquely specified. However it is evident that the experimental task of determining the dependence of N_Δ on each of the groups in turn is enormous. Consequently the values of many of the groups were fixed so that the experiments could be designed round a limited number of key variables. Before discussing the shortened list of groups (see "Variable groups" below) the values given to the fixed groups (see Table 1) will be discussed and specified.

Fixed groups

The preliminary tests confirmed the results (1,32) that a permeable embankment increases the riprap stability. Thus the assumption that the embankment of an earth dam is impermeable so far as the waves are concerned is both realistic and conservative. (However recent work (33) suggests that the steady pressure gradient set up in an "impermeable" earth dam by a rapid draw-down might reduce the riprap stability.)

On filters there is evidence (1), (not confirmed in the preliminary tests, Appendix 3), that a coarser material increases the stability of the riprap but it was decided that this point should not be further investigated and that the dimensionless properties of the filters with respect to the riprap would be kept constant throughout the tests. Following (1,22) the thickness t_F was set equal to 0.5 D^R_{50}. The bulk density ρ^B_F (which effectively controls the shape and placing) was also kept constant with respect to the riprap density. (See Table 1.) The choice of the grading was difficult. The "Review of current practice" gives a wide choice but preliminary tests with a filter similar to that of Burgess and Hicks (1) which had large values of the ratios D^R_{50}/D^F_{15} and D^R_{15}/D^F_{15} showed filter material being drawn through the riprap although D^R_{15}/D^F_{85} was less than 5 (Appendix 3). This was not serious but it occurred before the filter was exposed by erosion of the riprap and hence confused the then current failure definition which demanded the exposure and erosion of the filter. Although this failure definition was subsequently modified it was decided to find a filter that was not drawn through the riprap being tested. By examining the results of the preliminary tests with others (26,28 and 34) in terms of D^R_{15}/D^F_{85}, D^R_{50}/D^F_{50}, D^R_{15}/D^F_{15} it was found that

$$D^R_{15}/D^F_{85} < 4 \quad \text{....(24a)}$$

$$D^R_{50}/D^F_{50} < 7 \quad \text{....(24b)}$$

$$D^R_{15}/D^F_{15} < 7 \quad \text{....(24c)}$$

satisfactorily predicted whether or not filter losses would occur in 26 out of 32 cases. Of the remaining 6 cases no losses were found with the ratios (24b) and (24c) much higher than 7 (as high as 79 in one case). In all these cases the riprap grading curve had a long tail of fines which was not reflected in the above ratios. It is clear that the fines in the riprap prevented the erosion of the fine filter material. The riprap proposed for the present tests had no fine tail so the filter was designed within the limits (24).

These relationships have the disadvantage that (24a) and (24c) imply $D_{85} = 1.75\ D_{15}$ in the limit so that a flatter grading curve can only be obtained by having D^R_{15}/D^F_{85} smaller than 4, say 2. The filters for the tests were eventually made with $D^R_{15}/D^F_{85} = 2$ with their gradings parallel to those of the riprap thus:

$$D^R_{15}/D^F_{85} = 2.0$$

$$D^R_{50}/D^F_{50} = 4.5$$

$$D^R_{15}/D^F_{15} = 4.5$$

None of this filter was seen to be drawn through the riprap before its exposure by erosion. (See Appendix 2 for details of the filter materials.)

The riprap placing and thickness (t_R) also remained constant throughout the tests. The "Review of current practice" suggests a minimum thickness of D^R_{MAX} or $1.5\ D^R_{50}$. The riprap used had $D^R_{MAX} = 1.75\ D^R_{50}$ (see below). Hence it was decided that with $t_R/D^R_{50} = 2.0$ an even well mixed layer could be built without difficulty. Although the aim of an even layer of well mixed stone is common to model and nature, it is much more easily achieved in the model. Hence a conflict arises in the laboratory between the quality and consistency required for controlled experiments and the need to reproduce the sort of layer which is actually built in the field. Indeed, it is often impossible to reproduce the actual field methods of construction.

Two methods of slope construction were tested in waves in the preliminary tests (Appendix 3). Method A was an attempt to simulate the practice of pushing (or pulling) the riprap up the slope to the correct thickness. The model slopes were built in strips from the bottom upwards, each strip being adjusted in turn to the correct thickness by pushing stone projecting above the top of the layer after dumping up the slope, off the strip, on to the filter layer. This method has the effect of moving most of the largest stones into the layer (as recommended) and leaving small and medium sized stone on the surface (Plate 1). Method B followed the practice of constructing the whole slope in strips and subsequently trimming it to the correct thickness by removing projecting stones, usually the larger ones, into suitable holes. This produced a layer with the larger stones common on the surface in positions giving jamming and interlocking (Plate 1).

Repeat tests on the two methods showed that Method A gave reproducible results with an average erosion rate twice that of Method B, which whilst having overall reproducibility, showed more variations in detail. It is assumed that the jamming and interlocking was responsible for the variation and reduced erosion rate. However the difficulty of building a slope with consistent interlocking (as evidenced in the tests) and of ensuring such interlocking in nature lead to the adoption of Method A for giving consistent and conservative results.

A third method (C) was tried only for constructing (and not testing) the model bank. This method was the same as A except that the strips were built by tipping the material for each strip down the

slope rather than up the slope. This method produced a slope similar in appearance to A (Plate 1) but was not used because it caused more damage to the filter layer, led to stones rolling down on to already trimmed strips and was difficult to operate on the steeper slopes. The procedure adopted for laying the riprap is set out in Appendix 4.

An important feature of the adopted procedure was the control of the weight of material per unit area of slope (along the slope). Thus not only was the thickness ratio, t^R/D_{50}^R, controlled but so was ρ_R^{BL}/ρ_R, the ratio of the bulk density as laid to the stone density. (It should be noted that the bulk density as laid, 1300 kg/m^3, was less than that measured using a cubical box which averaged 1490 kg/m^3.)

Riprap size, grading and shape are considered in the "Review of current practice" where little advice is to be found on stone shape. It was decided not to investigate this parameter but to aim for cubical stone with a maximum dimension not more than twice the minimum. The largest grade used was hand sorted using this criterion, the smaller grades being partly hand sorted and partly mechanically screened. The resulting shapes of samples of stones from each grade are given in Appendix 2 which shows that 27% of the two smaller grades failed to meet the criterion with the smallest grade having values the ratio of the maximum to the minimum dimension up to 4.5. Of the largest grade only 12% of the sample failed to meet the criterion.

Since the review suggested that the riprap performance is independent of grading it was decided to keep the grading parameters D_{85}^R/D_{50}^R and D_{15}^R/D_{50}^R constant at the values 1.5 and 0.67. This gives $D_{85}^R/D_{15}^R = 2.25$, $D_{MAX}^R/D_{50}^R = 1.75$ and $D_{MIN}^R/D_{50}^R = 0.57$. These values show that the chosen grade is within the US Army Corps of Engineers' recommended limits (Thomsen (26)) and slightly outside the maximum and minimum values recommended by others (see "Review of current practice").

The density of the rock was 2700 kg/m^3 which is typical of that used in nature. (Natural densities are required because water is used in both model and prototype.) The ratio of ρ_R/ρ was thus constant at 2.70.

Details of the riprap are given in Appendix 2.

Variable groups

Having fixed the groups defining the riprap and filter layers it remains to discuss the variable groups which in effect describe the interaction of the waves with the riprap ie, equation (23) becomes

$$N_\Delta = f_1(\bar{H}_3/D_{50}^R,\ 2\pi\ D_{50}^R/g\bar{T}^2,\ 2\pi d/g\bar{T}^2,\ \rho\bar{H}_3\ D_{50}^R/\mu\bar{T},\ \bar{N},\ a,\ \text{constants}) \qquad \ldots.(25)$$

The group $\bar{H}_3/D_{50}^R$ is the linear scale of stone size to wave height which appears in one form or another in most studies of this kind. The ratio $2\pi\ D_{50}^R/g\bar{T}^2$ appears because of its experimental convenience and expresses the ratio of wavelength to stone size just as the group $2\pi d/g\bar{T}^2$, the relative depth, expresses the water depth to wavelength ratio. The ratio $\rho\bar{H}_3\ D_{50}^R/\mu\bar{T}$ is a Reynolds number where $\bar{H}_3/\bar{T}$ is the characteristic velocity.

The main programme of tests was designed on the assumption that the relative depth $2\pi d/g\bar{T}^2$ (the deep water wavelength $L_o = g\bar{T}^2/2\pi$) could be ignored because the tests were to be conducted for deep water ($d/L_o > 0.25$) where the influence of water depth on the waves is small. The Reynolds number was also neglected on the basis of previous laboratory experience. Hence the experiments were designed in terms of

$$N_\Delta = f_2(\bar{H}_3/D_{50}^R,\ 2\pi\ D_{50}^R/g\bar{T}^2,\ \bar{N},\ a,\ \text{constants}), \qquad \ldots.(26)$$

the object being to assess the effect of each group by changing one at a time. The basic experimental scheme was to choose a value of $\bar{T}$, D_{50}^R and $\bar{H}_3$ which fixed the first two groups and to measure the damage in terms of the mean number of waves, $\bar{N}$, in order to produce a damage history as in Fig 4a. By changing $\bar{H}_3$ and

rebuilding the riprap layer the experiment could be repeated for a different value of $\bar{H}_3/D^R_{50}$. Clearly a change of $\bar{T}$ would change only the group $2\pi\ D^R_{50}/g\bar{T}^2$. The results could then be presented in terms of the groups as in Fig 4b.

The practical constraints on the basic variables were as follows:

(i) Experimental time limited the maximum value of $\bar{N}$, the average number of waves incident on the riprap, to 5000 which is typical of a storm. In most cases this was too few waves to determine whether or not equilibrium damage was achieved or whether at the given value of $\bar{H}_3$ the slope would eventually fail.

(ii) $\bar{T}$ had to be chosen so that the waves were deep water waves. This condition was slightly relaxed by having $2\pi d/g\bar{T}^2 > 0.23$ which means that the waves were in the deep or intermediate class (there are wave periods in the spectrum up to 2.24 $\bar{T}$). This fixed the maximum value of $\bar{T}$ with the water depth in the wave flume at 0.61 m.
A further constraint was that values of $\bar{T}$ should be chosen so that $2\pi D^R_{50} g\bar{T}^2$ remained unchanged for changes of D^R_{50} so that "in scale" tests would be done as part of the programme.

(iii) The limits on $\bar{H}_3$ at a given period are either that the maximum stroke of the wave generator is too small to produce the required waves or that waves break. The latter constraint occurs with paddle generated random waves as follows. When the waves become too high they begin to break (even in deep water) because of excessive wave steepness (as in nature). This results in a change of the spectral shape and consequently in $\bar{T}$. It is rare for the steepness parameter $2\pi\bar{H}_3/g\bar{T}^2$ to exceed 0.05 in nature (35) which is the maximum value that can be generated in a paddle generated random sea without spectral changes. Wind generated waves in a deep water lake can be expected to have a similar maximum value of the steepness parameter which gives a practical (and natural) top limit for $\bar{H}_3$ at a chosen value of $\bar{T}$.

(iv) Having chosen the periods and heights of the waves the riprap size must be such that the smallest size can be efficiently handled and the largest size can be eroded by the chosen waves.

The above considerations led to the range of variables set out in Table 2: namely, up to four wave heights at each of periods 0.92, 1.13 and 1.3 s for riprap D^R_{50} = 20, 30 and 40 mm.

Slopes of cot α = 2,3,4 and 6 were considered typical of those likely to be encountered in design.

Scale tests in addition to the main programme of tests were subsequently made to determine whether the earlier neglect of the relative depth group and the Reynolds number was justified. This became necessary after

(i) the work of Thomsen et al (26) became available. This work suggests that Reynolds number scale effects should be found in laboratory tests of the kind being made;

(ii) tests on the 1:3 slope suggested that there were period effects which could not be explained by the dimensionless groups then in use.

Thus a series of tests was made with all the groups in equation (25) constant except for the Reynolds number $\rho\bar{H}_3\ D^R_{50}/\mu\bar{T}$. The absolute values of $\bar{T}$, D^R_{50} and d together with values of the groups are given in Table 3.

MEASUREMENTS AND PROCEDURE

Having specified the experimental programme it is convenient to describe first how the key variables were measured. All the experiments were made in a flume 45 m long, 1.2 m wide sub-divided into a calibration channel and a test channel which was 0.65 m wide (Fig 5). The dividing wall was terminated at the paddle end by a section of wall with permeability increasing towards the paddle which was intended to reduce the reflections caused by an abrupt termination. The maximum working depth was 0.61 m.

Waves

Irregular waves with the statistical properties of wind waves were generated by a wave paddle which is servo-controlled to follow in position a randomly varying voltage generated by an HRS spectrum synthesizer (36,37 and 38). This device synthesizes a time varying random voltage with the spectral and statistical properties appropriate to specified values of $\bar{H}_3$, $\bar{T}$ and ϵ (given a Moskowitz spectral shape (equation (20)). The synthesizer has the property that it can generate short repeating irregular sequences of waves with exactly the same spectra as the very long irregular wave sequences used for the damage tests. By doing a harmonic analysis on exactly one short sequence the wave spectrum can be calculated without statistical uncertainty and $\bar{H}_3$, $\bar{T}$ and ϵ derived from the spectral moments (equations (15-17)). Fig 6 gives examples of measured spectra.

The waves were recorded by a twin wire resistance probe placed in the calibration channel (Fig 5) which was terminated by a spending beach of coarse shingle (1:20 slope) to minimise reflections. The output of the probe was recorded on ultra-violet paper and digitally on magnetic tape for spectral computation.

The wave reflection measurements (see Appendix 5) were made in the test channel in front of the riprap slope (Fig 5) using a pair of twin wire wave probes and short repeating sequences of waves. The reflection coefficients were computed by a method equivalent to that of Kajima (39).

The mean number of zero crossing waves ($\bar{N}$) was obtained by dividing stop-watch timings by the nominal $\bar{T}$ of the experiment.

Run-up and run-down

The run-up and run-down were obtained from a capacitance wire stretched 10 mm above and parallel to the riprap slope (Plate 2). The output of the device at any instant gives the position of the intersection of the water surface and the wire with respect to the still water level. Knowing the angle of the slope this position can be given as a vertical distance above or below still water level (SWL). Thus the vertical run-up r_u above SWL and the vertical run-down r_d below SWL actually refer to a line 10 mm above the riprap slope. Because the riprap is rough it is assumed that the waves do not run up or down the slope under the wire and hence that the measurement of the intersection of the water surface and the wire adequately represents the position of the waves as they move up and down the slope. (There may also be small errors caused by air bubbles in the water surface and by splashing.)

The wire was supported between arms cantilevered out from a hinge at the side of the test slope (Plate 2) so that it could fold up and away from the slope except during measurements. Thus its presence did not prevent the erosion of the stones.

The output was recorded on ultra-violet paper and digitally on magnetic tape. The instantaneous position of water surface on the wire was recorded continuously over a time equivalent to 150 down crossings of the mean water level on the slope (the mean water level on the slope is different from SWL), and the maximum vertical run-up (r_u^{MAX}) and the maximum vertical run-down (r_d^{MAX}) was taken to be the maximum and minimum values of the instantaneous water surface (with respect to SWL) recorded in that time.

The values of r_u^{MAX} and r_d^{MAX} from such 150 wave samples are only estimates of the true value of the two statistics. In order to achieve better estimates eight such 150 wave samples were taken during each 5000 wave experiment (which had a random wave sequence much greater than 5000 waves) and the means $\bar{r}_u^{MAX}$ and $\bar{r}_d^{MAX}$ of the eight samples of r_u^{MAX} and r_d^{MAX} computed. The measurements were made without regard to any erosion damage that might have occurred.

Damage

All the information on damage was obtained from the surface profiler shown in Plate 2. Essentially, the profiler measures the level of a point on the riprap below a horizontal plane defined by the carriage rails. The profiler is relocatable in the horizontal plane by a system of two notched bars, one along the flume and the other transverse to it. As the profiler is lowered to the riprap a rack which is mounted on it, drives a potentiometer which produces a voltage proportional to the elevation of the probe. This is recorded on magnetic tape once the probe is stationary on the riprap.

A survey of the riprap consisted of recording the riprap levels over a square grid of positions (in plan) D_{50}^R apart. Ten sections (covering a 9 D_{50}^R width of slope) were taken up the slope with sufficient points to span the area of erosion. Successive surveys were taken at exactly the same points using the relocatability of the profiler. The foot of the profiler was a hemisphere of $D_{50}^R/2$ diameter.

The data for each riprap test consisted of a set of levels of the upper surface of the filter layer, a set for the undamaged riprap after the bedding in run (referred to below as the initial riprap survey) and a series of sets from surveys made after the generation of successive trains of 500 (or 1000) waves.

The computer was used to calculate volume for each set of levels, the ten values across the test section being first summed to give a mean profile (which could be plotted) which was then used to give the eroded volume using the trapezoidal rule.

The mean thickness t_R (Fig 3) of the riprap normal to the slope was calculated from the difference in levels between the filter layer and the first initial survey. This also gave the **laid bulk density ρ_R^{BL}** since the mass of riprap laid on unit area of the slope was known (and controlled).

The number N_Δ of D_{50}^R sized spherical stones eroded from a 9 D_{50}^R width of slope was obtained by differencing a given survey set with that of the initial riprap survey, and dividing the product of the bulk density ρ_R^B and the eroded volume by $\rho_R \pi (D_{50}^R)^3/6$, Fig 3. (The actual rather than the laid bulk density was used here because the former is more easily estimated in the field. The laboratory measurements of ρ_R^B are described in Appendix 2.)

The upper and lower limits of erosion damage l_u, l_l measured vertically from SWL (Fig 3) at failure or after 5000 waves were obtained by differencing the initial and final riprap surveys. The damage limits were set by finding the highest and lowest pair of adjacent transverse sections between which at least one equivalent spherical stone of D_{50}^R diameter was eroded in the 9 D_{50}^R width of slope. The upper limit was then defined as the level of the initial survey (with respect to SWL) at the position of the uppermost transverse section and the lower limit as the level of the initial survey (with respect to SWL) of the lowest transverse section.

The minimum thickness t_R^{MIN} at a transverse section at failure (Fig 3) measured normal to the slope was determined from the mean filter profile and the mean profile from the appropriate riprap survey.

Failure was said to have occurred if the $D_{50}^R/2$ diameter foot of a hand held gauge could touch the filter layer at any point (on or off the grid) after a sequence of 500 waves, whether or not filter material was eroded. Notes were also made of whether the foot of the gauge could touch the filter layer while waves were running and of any observed erosion of filter material.

Photographs were taken of the initial riprap layer and at failure or after 5000 waves.

Procedure

The details of the experimental procedure are given in Appendix 6. The main programme of experimental work involved tests on 4 slopes (1:2,3,4 and 6) with three riprap grades on each slope (D_{50}^R = 20, 30 and 40 mm, each with its own filter), each grade being subjected to three spectra ($\overline{T}$ = 1.3, 1.13 and 0.92 s), with at least 4 significant wave heights per spectra. The significant wave heights were chosen as far as possible to cover the spread of damage from failure with 5000 waves to negligible damage after 5000 waves. The basic test for a given slope, riprap, significant wave height and mean zero crossing period ($\overline{T}$) consisted of a survey of the filter layer (see above for measuring techniques), a survey of the riprap after a 1000 wave bedding in run and further surveys after successive sequences of 1000 waves up to a cumulative total of 5000 waves. The run-up and run-down was measured during the earlier 1000 wave sequences whereas wave reflections were measured as a completely separate exercise on the 30 mm D_{50}^R riprap only.

The main programme of tests (summarised in Table 2) was carried out at a water depth of 610 mm whereas depths of 461 mm and 305 mm were used in the scale tests (summarised in Table 3). Apart from the depth differences the procedure for the scale tests was the same as for the main programme of tests.

RESULTS AND DISCUSSION

Before dealing with the quantitative results of the tests a qualitative description will be given of the behaviour of the waves and riprap on the different slopes.

Qualitative description of riprap behaviour

This is of interest because it has been shown (25,40) that the stability of riprap in natural scale regular waves depends on the way in which the waves break. Galvin (41) classifies breakers in terms of an offshore breaker parameter $H \cot^2\alpha/L_o$ which shows that the wave break changes as the wave steepness (H/L_o) and the slope ($\cot\alpha$) changes. (Note that the values of the parameter for different classes of breaker are not the same in Galvin's (41) small scale experiments on smooth slopes as in Ahrens (25,26,40) large scale riprap experiments.) A wave of low steepness on a steep slope does not break but is said to surge up the slope. If the wave steepness increases or the slope decreases the wave crest sharpens as the wave moves up the slope. When the front face becomes vertical and the crest begins to curl over the whole face collapses to give a rapid uprush on the slope. These breakers are called collapsing breakers. Further steepening of the waves or flattening of the slope causes the waves to plunge. The crest curls over the vertical front face of the wave and traps a pocket of air before falling on to the slope or more usually into the run-down of the previous wave. Because the broken wave strikes near normally it generates large local pressures but relatively little run-up.

In an irregular wave train the steepness varies wave by wave and hence the individual waves break differently. This makes anything more than subjective descriptions of the breakers very difficult.

Regardless of breaker type, the overall picture on all the slopes was that very low significant wave heights ($\overline{H}_3$) could be found where no erosion occurred. At slightly higher values of $\overline{H}_3$ stones rocked and some were displaced. In all cases where erosion occurred the initial rate was greatest as the most readily removable stones were attacked. As a test continued either a steady (but reducing) erosion led to failure or, at the other extreme, fell to a very low level where only a rare group of very large waves gave further damage.

On the 1:2 slope most of the waves surged although a significant fraction of the highest waves were collapsing. In general the collapsing breakers did not cause any observable increase in stone movement. However very occasionally a very large well formed collapser did cause local slippages of the 20 mm and 30 mm D_{50}^R riprap. (Ahrens (25,40) found collapsing breakers to be the most damaging waves.)

Damage was caused predominantly by the run-down of the waves pulling stones down the slope. Only occasionally did the uprush cause displacement. The small and medium stones were first removed to leave the partially exposed larger stones to be pulled down by the biggest waves. There was little healing, the stones removed usually moved out of the damage zone to sit on a berm at the lower limit of damage (small values of $\overline{H}_3$) or to be spread uniformly over the lower part of the slope in medium and high wave conditions. Plate 3 shows typical initial and final conditions of a test which did not give failure.

On the 1:3 slope more collapsing waves were seen as the offshore breaker parameter predicts. Surging predominated at the lowest wave conditions and collapsing at the highest. The surging waves caused damage as on the 1:2 slope but the well formed collapsing plungers loosened the stone pack and the violent uprush displaced stone up the slope. The downrush then pulled these stones and others from the loosened pack down the slope. Again the small and medium stones on the surface of the layer were first eroded leaving the larger partially exposed stone to be prised out by repeated up and down rush. The eroded material moved down the slope more slowly than on the 1:2 slope and a little healing occurred when displaced stone fell into and remained in holes. The berm at the lower limit of damage was transient, occurring only when there was initially high erosion rates. Plate 3 shows typical initial and final conditions of a test which did not give failure.

On the 1:4 slope the reduced slope induced predominantly collapsing breakers with a significant fraction of plungers which increased with wave height. Most of the damage was caused by collapsers which loosened the pack and caused initial displacement up the slope in the high velocity uprush. The stones thus loosened oscillated up and down slope in the damage area with a net drift downwards. This oscillation caused healing as the small stones had many opportunities to fall into the holes caused by the removal (by prising) of the larger stones. This resulted in the large and medium sized stones moving down slope and being deposited on the lower part of the slope (without the formation of a berm). The plunging waves broke further "offshore" into the run-down of the preceding wave and apparently caused no damage or run-up. However inspection at the end of the tests showed that in areas where waves had repeatedly plunged the larger stones had been brought to the surface of the pack. This may be a result of the high local pressure field produced by the impact of the plunging wave instantaneously bringing a local area of the riprap into suspension and the small stones getting beneath the larger ones as they settled back into place. Plate 4 shows typical initial and final conditions of a test which did not give failure.

On the 1:6 slope the waves varied from predominantly collapsing to predominantly plunging. As on the 1:4 slope the majority of the readily visible movement was caused by the collapsing waves with their violent up and down rush. This resulted in an almost continuous movement of stones up and down the slope in the damage area with a very slow net drift downwards. This resulted in a high degree of healing. It was noticeable (particularly in high wave conditions) that the damage area was mostly occupied by small and medium stone with the larger stone down slope. Again the plungers broke further "offshore" than the collapsers and the largest collapsers and plungers appeared to do little damage. However, when the slope was stripped it was found that both the riprap and the filter were dented and ridged in the impact area of the plungers with the larger stones being brought to the surface of the layer. In the highest wave conditions a berm of small stones appeared for the first time at the upper limit of damage. The larger riprap drawn to the surface of the riprap produced a berm at the lower limit of damage. The stones from this berm were displaced both up and down the slope. Plate 4 shows typical initial and final conditions of a test which did not give failure.

Overall it is evident that the breaking of the waves and the movement of the stones is very dependent on the slope. The displaced stone moved quickly down the 1:2 slope with no healing whereas on the 1:4 slope the stone began to oscillate up and down the slope (with a net drift down the slope) so that healing occurred. This feature became very marked on the 1:6 slope where the stone movements began to take on the characteristics of those on a beach with little net erosion occurring although the stone was in motion.

Quantitative results for erosion damage

A typical series of damage histories recording the erosion of the riprap under steady wave conditions in terms of the mean numbers of zero crossing waves incident on the slope is shown in Fig 7. The curves have a characteristic form, showing relatively high erosion rates initially at all wave heights, the higher values of $\bar{H}_3$ giving more rapid erosion. In this form, the data for the different stone sizes and wave periods cannot readily be compared. Hence new plots in terms of N_Δ (the eroded number of spherical stones of D_{50}^R diameter per 9 D_{50}^R width) and $\bar{H}_3/D_{50}^R$ were plotted for the damage at 1000, 2000, 3000, 4000 and 5000 waves by reading from the interpolated damage histories, the $N_\Delta - \bar{H}_3/D_{50}^R$ combinations at the given number of waves. (See "Dimensional analysis and test programme – Main programme".)

The repeatability of the tests is important. The riprap is a random assembly of stones which is attacked by random waves. Hence the erosion damage must itself be a random variable which will vary from repeat test to repeat test about a mean value. Time was not available for the large number of repeat tests that are necessary to establish a standard deviation which formally expresses the variability of the results. Instead a much more limited number of repeat tests were performed which are discussed in Appendix 3. Figs 26 and 27 give an indication of the repeatability and it is evident there can be considerable variation from test to test.

The scale tests will be considered before the main programme of tests although they were performed as a later addition to the main programme (see "Dimensional analysis and test programme – Scale tests") because of doubts about the validity of assuming that the Reynolds number ($\rho H_3\ D_{50}^R/\mu T$) and the relative depths ($2\pi d/g\bar{T}^2$) could be ignored a priori. These doubts arose with the suspicion of an absolute period trend in the results for the 1:3 slope which could not be expressed by the dimensionless groups then being used (equation (26)). Further, Thomsen et al (26) strongly suggest that Reynolds number effects should occur in the present work. Their data, which covers a range of Reynolds number (as defined by them) from 2×10^4 to 1×10^6, predict that the results from the present tests, when scaled to prototype dimensions will give a D_{50}^R size 60% too big if Reynolds scaling is ignored. The range of Reynolds numbers (on Thomsen's definition) for the present work is 0.7×10^4 to 4×10^4 which suggests that the effect could be 30% of D_{50}^R over the range of D_{50}^R sizes used in this research, an effect which should be detectable.

This question is most important since it could lead to serious over-estimation of the size and hence cost of the riprap used in the field. For this reason additional tests were carried out so that all the dimensionless groups in equation (25) (the full set) except the Reynolds number remained constant whilst the latter was changed as much as possible. The same data was also used to look at the effect of varying the relative depths ($2\pi d/g\bar{T}^2$) only.

The results of the tests on the 1:2, 1:3 and 1:4 slopes are plotted in terms of N_Δ against $\bar{H}_3/D_{50}^R$ at 1000, 3000 and 5000 waves on Figs 8, 9 and 10. The basic data is summarised in Table 3 and detailed in Tables 4, 6–10, 12. Where Reynolds number alone was varied (Figs 8a, 9a and 10a) the Reynolds number for the 40 mm D_{50}^R riprap was about 3 times that of the 20 mm D_{50}^R at the same value of $\bar{H}_3/D_{50}^R$. On the 1:2 slope there is a possible trend towards most damage being associated with the lower Reynolds numbers (smaller D_{50}^R sizes), which is what would be expected if viscous effects were in operation. However the scatter of points is within those of the repeat tests (Figs 26 and 27) and a contrary trend (still within the scatter of the repeat tests) is found on the 1:4 slope (Fig 10a). The results for the 1:3 slope (Fig 9a) fall on one line. Thus there is no clear evidence in these results of a viscous scale effect as expressed by the Reynolds number.

Where the relative depth varied (Figs 8b, 9b,c and 10b) the Reynolds number also varied along the curve so that it was the same for all stone sizes at any value of $\bar{H}_3/D_{50}^R$. The relative depth varied between 0.23 and 0.46 for the different depths and only on Fig 8b is there an indication of a tendency for the points to follow separate curves. However this is within the repeatability and it is concluded that there is, as expected, no relative depth effect.

The overall weight of the evidence is that there are no Reynolds number or relative depths effect in the present series of tests. This is expected for relative depths but contrary to Thomsen et al (26) for viscous effects. It is possible that in the present results the relatively coarse filter maintained the turbulent flow regime or that the statistical uncertainties and the small range Reynolds numbers masked an effect which is present. Certainly the present results do not justify the reduction of two in the D^R_{50} design rock size. However, the possibility of such a reduction makes a strong case for large scale tests in irregular waves.

The main programme of tests will be discussed on the assumption that the Reynolds number and relative depths have no influence on the erosion damage, so that the damage becomes a function of $\bar{H}_3/D^R_{50}$, $2\pi D^R_{50}/g\bar{T}^2$, $\bar{N}$, the slope α and other groups whose values were fixed throughout (equation (26)).

The results for the 1:2, 1:3, 1:4 and 1:6 slopes are plotted in terms of N_Δ against $\bar{H}_3/D^R_{50}$ at 1000, 2000, 3000, 4000 and 5000 waves on Figs 11-14. The basic data is summarised on Table 2 and detailed in Tables 4-14. The 40 mm D^R_{50} riprap was not used on the 1:6 slope and at $\bar{T}$ = 0.92 s and 1.13 s on the 1:4 slope because the waves were not big enough to cause appreciable erosion. The results have five common features:

(i) The points all plot on broad curves which demonstrate that $\bar{H}_3/D^R_{50}$ is the dominant parameter. (The solid curves were drawn by eye to assist the user.)

(ii) There are threshold $\bar{H}_3/D^R_{50}$ values between 1.0 and 2.0 below which no erosion of stone occurs.

(iii) The gradient of the curves increases with $\bar{H}_3/D^R_{50}$ so that an increment in $\bar{H}_3/D^R_{50}$ at lower values produces a small change in the erosion, N_Δ, whereas the same increment at higher values of $\bar{H}_3/D^R_{50}$ produces much larger changes in N_Δ. This change in gradient is more rapid on the 1:2 and 1:3 slopes than on the 1:4 and 1:6 slopes.

(iv) On any slope the erosion N_Δ increases, as expected, with the mean number of zero crossing waves $\bar{N}$. The increase is relatively rapid at first but small between 4000 and 5000 waves.

(v) The erosion increases with increasing slope for a given $\bar{H}_3/D^R_{50}$ and $\bar{N}$.

The question arises of whether the curved bands of points show that N_Δ, the erosion damage depends only on $\bar{H}_3/D^R_{50}$ for any value of the slope and number of waves. In other words, do the results indicate any dependence on $2\pi D^R_{50}/g\bar{T}^2$ (equation (26))? It has already been pointed out (see "Repeatability") that repeated tests using exactly the same values of the independent variables should give a band of points because the experiments are intrinsically random in nature. Judgements on this point must therefore be made in the light of the repeatability tests, Figs 26 and 27. (The data points on Figs 11-14 are identified in terms of $\bar{T}$ and D^R_{50} rather than $2\pi D^R_{50}/g\bar{T}^2$, the appropriate values of the latter group are marked on the graphs.) Overall the curves show a strong dependence on $\bar{H}_3/D^R_{50}$ with no clear dependence on the other parameters evident on the plots. The general spread of the points is consistent with those of the repeat tests (Figs26 and 27). It might be argued on the 1:2 slope that a trend towards increasing damage with decreasing stone size is detectable on the graphs. If this trend is real, it is most likely to be a consequence of stone shape, which causes variations in the angle of repose of 1:1.38, 1.14, 0.97 for the 20, 30 and 40 mm D^R_{50} riprap (Appendix 2). Thus the 20 mm riprap is the least stable of the three sizes on the 1:2 slope. On the 1:3 slope there is a possible trend to a dependence on absolute period, a fact (among others) which led to the scale tests already discussed.

The apparent lack of dependence of the erosion, N_Δ, on the group $2\pi D^R_{50}/g\bar{T}^2$ is interesting because such a dependence was found by Thomsen et al (26) in regular waves. This dependence is explained by Beene and Ahrens (25,40), using the same data as Thomsen et al (26), in terms of breaker type. They found collapsing breakers (see "Qualitative description of riprap behaviour") most

damaging. These occur at a range of wave steepnesses between those which give rise to surging breakers (lower steepnesses) and plunging breakers (higher steepnesses). Plunging and surging waves were found to be equally damaging. In an irregular train of waves with a given $\bar{H}_3$ and $\bar{T}$ each wave has a different steepness and hence breaks in a different way. It has already been described (see "Qualitative description of riprap behaviour") how on a given slope two different types of breaker occurred so that the effect of one type may not be dominant. Hence it can be argued that the erosion damage on a given slope will show little or no dependence on the overall steepness $2\pi\bar{H}_3/g\bar{T}^2$, and hence on $2\pi D^R_{50}/g\bar{T}^2$, which is related to the steepness through the ratio $\bar{H}_3/D^R_{50}$. In other words, the overall effect of different types of breaker occurring in random order on a slope masks the fact that one of the breaker types is more damaging than the others.

In summary, it can be said that the erosion damage N_Δ (the equivalent number of D^R_{50} sized spherical stones eroded) increases with $\bar{H}_3/D^R_{50}$, the slope and the number of waves (Figs 11-14). It is evident from a consideration of the random nature of the phenomenon and the repeat tests that a scatter is to be expected in the results. Within this scatter there is no clear evidence from the plotted results of a Reynolds number ($\rho\bar{H}_3 D^R_{50}/\mu\bar{T}$) or relative depths ($2\pi d/g\bar{T}^2$) dependence (see "Scale tests, and Figs 8, 9 and 10). In the main programme of tests there is no clear evidence from the plotted results of a dependence on $2\pi D^R_{50}/g\bar{T}^2$ although such a dependence is known to occur in regular waves (26). This may be a result of the interaction of the different breaker types occurring in an irregular wave train. On all slopes there is a threshold value of $\bar{H}_3/D^R_{50}$ below which no damage occurs. This varies(not systematically) between 1.0 and 2.0 as the slope increases. Comparisons with the results of other workers, so far as they are possible, will be made in the section on "Worked example ".

Damage limits

The upper (l_u) and lower (l_l) vertical limits of the damage on the slope after 5000 waves (or less if failure occurred first) is shown scaled in terms of D^R_{50} in Figs 11-14. There is the expected scatter but no clear trends with parameters or groups other than $\bar{H}_3/D^R_{50}$. The curves show the vertical extent of the damage reducing with slope, the attack beginning in the zone D^R_{50} below still water level. The curves suggest (as do the erosion damages curves, Figs 11-14) that there is a value of $\bar{H}_3/D^R_{50}$ below which there is no damage after 5000 waves. The concept of no damage must be treated with caution in irregular waves because the no damage wave height must be a function of the number of waves as Figs 11-14 show to be the case. Even in the limiting case of waves with a small significant height incident for a very long time on relatively large riprap, there will be a few rare waves high enough to remove the smallest stones of the riprap pack and hence give damage. In practice there will be a no damage wave height but the problem of pinpointing it even after a precise number of waves in the random case can be seen from an examination of Figs 11-14. The damage limits for the scale tests are also plotted on Figs 11-14 where they fall amongst the main programme results.

The damage limit curves also show the $\bar{H}_3/D^R_{50}$ values for which failure first occurs during 5000 waves. (These failures are also marked on the erosion damage curves.) Again caution is necessary in interpreting the curves because, for example, the equivalent curves for 10 000 waves will show failure occurring at lower values of $\bar{H}_3/D^R_{50}$. Indeed it is conceivable that conditions giving very low rates of damage will lead to failure if a long enough time elapses. The very long preliminary tests (Fig 28a) give no certainty of the riprap eroding to a totally stable or equilibrium state even with low damage rates. Thus it is not safe to assume, as is often done in regular wave tests, that a slope will erode to stability. All that can be said is that the erosion rate may become small enough to be ignored in practice.

Failure

The failure conditions (see "Measurements and procedures") observed are presented in Table 15. The least variable parameter at failure is the minimum thickness t^{MIN}_R which averaged 1.1 D^R_{50}. This implies that with the failure criterion used, there is still substantial cover on the slope. No erosion of filter material was observed when the $D^R_{50}/2$ failure hole appeared. Typical initial and failure conditions are illustrated in Plates 5 and 6. Since both the minimum thickness and the vertical damage limits at

failure (Figs 11-14) appear to scale with D_{50}^R it might be expected that the damage N_Δ at failure is a constant. Table 15 shows large scatter for this parameter but this is quite consistent with the nature of the phenomenon and the difficulties encountered in finding an objective and meaningful definition (see Appendix 3). The mean failure values of N_Δ are marked on the damage curves (Figs 11-14). No failures were observed on the 1:4 and 1:6 slopes because of experimental wave height limitations. However, some estimate of N_Δ for these slopes is desirable from the point of view of design. Assuming that minimum thickness at failure is D_{50}^R and given that the vertical distance between the upper and lower limits of failure is 1 D_{50}^R (see Fig 3) then the number of spherical D_{50}^R stones eroded from the triangular wedge 9 D_{50}^R wide is

$$N_\Delta = 27\rho_R^B \, l/(\pi\rho_R \sin\alpha)$$

Using the known N_Δ values for the 1:2 and 1:3, l can be calculated as 5.96 and 5.75 respectively. These values are consistent with the damage limit curves (Figs 11,12). Assuming that a mean value of l = 5.86 is appropriate to the 1:4 and 1:6 slope (an assumption not inconsistent with the damage limit curves (Figs 13,14) then N_Δ values of 114 and 168 are the estimated values at failure on the 1:4 and 1:6 slopes. The fact that values of N_Δ considerably greater than 114 were measured without failure on the 1:4 slope suggests that these values are probably conservative.

Run-up and run-down

An examination of continuous run-up and run-down records on ultra-violet paper shows that the run-ups and run-downs are not symmetrical about the mean of the instantaneous water levels recorded. The distributions of run-upsand run-downs are different, the former have many more large excursions from the mean than the latter. This situation is further emphasised if the run-up and run-down is examined with respect to still water level which is always below mean water level on the slope because of the local raising of the mean water level caused by wave breaking. Thus the two parameters $\bar{r}_u^{max}$, $\bar{r}_d^{max}$ for run-up and run-down must be treated separately.

Fig 15 shows that the run-up (measured regardless of erosions) is best represented by

$$\bar{r}_u^{max}/\bar{H}_3 = f(\alpha) \qquad \ldots.(27)$$

independent of the other dimensionless groups. That is to say that $\bar{r}_u^{max}$ plots as a straight line against $\bar{H}_3$ the gradient of the line depending on the slope. Only on the 1:2 slope is there a suggestion of a slight bend in the $\bar{r}_u^{max}$ versus $\bar{H}_3$ line. It is difficult to say whether the bend is due to the scatter of the data or does reflect another run-up mechanism becoming active on the 1:2 slope. The general scatter of the run-up data is consistent with standard deviations of the data points.

The run-down (measured regardless of erosion) is best presented in terms of the parameter $\bar{T}(g\bar{H}_3)^{1/2}$ tanα suggested by Battjes (42) for breaking waves on smooth slopes (Fig 16). The scatter is large (rather larger than the standard deviations of the data suggest) and it is only when the data for all the slopes is combined (Fig 16) that a relationship appears as a straight line except very close to the origin. Thus

$$\bar{r}_d^{max}/(\bar{T}(g\bar{H}_3)^{1/2} \tan\alpha) = \text{const} \qquad \ldots.(28)$$

ie, the run-down expressed as above is independent of the groups in equation (25).

It might be argued that both equations (27) and (28) are inadequate because they do not express any roughness dependence which must exist. However, this is implicit in the experiments because the larger the D_{50}^R size, the larger the $\bar{H}_3$ required to cause damage.

As well as being asymmetrical about the mean water level on the slope, the mean period of the crossing of the mean level by the water surface is not the same as the T of the waves because the acceleration of the water on the slope depends on the slope. The periods on the slope are 1.14$\bar{T}$,

$1.18\overline{T}$, $1.20\overline{T}$ and $1.41\overline{T}$ respectively on the 1:2, 1:3, 1:4 and 1:6 slopes. The results of the scale tests are also included on Figs 15 and 16 where they lie with the main programme results.

Reflections

Wave reflection coefficients were measured with 30 mm D_{50}^R riprap on all slopes. Since these results are difficult to present in a satisfactory dimensionless form, they are included for information in model units in Appendix 5.

CONCLUSIONS

1. The erosion damage caused by irregular waves on a riprap slope is itself a random variable so that the expected scatter of results was found in repeat tests.

2. The erosion damage N_Δ, expressed as the number of D_{50}^R sized spherical stones eroded from a 9 D_{50}^R width of slope, depends principally on $\overline{H}_3/D_{50}^R$, the slope (a) and the mean number of zero crossing waves ($\overline{N}$) incident on the slope.

3. Within the scatter of the results, the tests showed no clear dependence of the erosion damage N_Δ on the Reynolds number ($\rho\overline{H}_3 D_{50}^R/\mu\overline{T}$) when it was varied by a factor of 3 within the range 320–3300 where Thomsen et al (26) showed that viscous scale effects are marked. (This scale effect would lead to the over-estimation of riprap sizes in the field.)

4. Within the scatter of the results the erosion damage showed no dependence on the relative depth ($2\pi d/g\overline{T}^2$) which is as expected for values of the parameter in the range 0.23–0.46.

5. Within the scatter of the results the erosion damage showed no clear dependence on the parameter $2\pi D_{50}^R/g\overline{T}^2$. This dependence which was found by Thomsen et al (26) in regular waves may not be apparent in irregular waves because the overall effect of different types of breaker occurring in random order on a slope masks the fact that one of the breaker types is more damaging than the others.

6. The erosion damage, N_Δ, increases with $\overline{H}_3/D_{50}^R$, the slope (a) and the mean number of zero crossing wave ($\overline{N}$) once a threshold value of $\overline{H}_3/D_{50}^R$ between 1.0 and 2.0 is exceeded. There is also a value of $\overline{H}_3/D_{50}^R$ above which N_Δ increases rapidly.

7. The movement of the stone is greatest on the flatter slopes although the net erosion is small. This movement results in self-healing by the smaller stones.

8. The physical limits of the damage on a given slope depends on $\overline{H}_3/D_{50}^R$.

9. With the filter layer criteria adopted for this research no filter material was drawn through the riprap before failure (defined as a $D_{50}^R/2$ sized hole through to the filter layer) occurred. The minimum riprap thickness at failure was 1.1 D_{50}^R on the 1:2 and 1:3 slopes.

10. The maximum run-up depends on the significant wave height ($\overline{H}_3$) and the slope whereas the best correlation for run-down depends on slope, $\overline{H}_3$ and the mean zero crossing period $\overline{T}$.

RECOMMENDED DESIGN PROCEDURES

Introduction

Several different kinds of information must be brought together in the formulation of design procedures for riprap. Wind data, methods for converting wind data into wave data and information from model tests are all required. To this must be added either the designer's judgement on acceptable damage levels or a more formal economic analysis. Strictly this report is concerned only with the results and interpretation of data from a model study, and consequently the step by step procedures finally presented only describe how to convert wind data for a single event into damage. Other information in the introductory sections is included to assist the designer.

Limitations of the model tests

The use of the results of this research in the recommended design procedures is subject to the limitations of the tests. For example, the effects of some variables such as the riprap thickness were not investigated. Hence the following procedures apply to the design of riprap protection of embankments subject to the attack of wind generated waves where:

(i) the embankment is effectively impermeable to waves (ie, earth embankments as opposed to the more permeable cored rubble breakwaters),

(ii) the waves are in deep or intermediate depths of water,

(iii) the specific gravity of the rock is 2.7,

(iv) the riprap thickness is 2 D^R_{50},

(v) the riprap grading is

$$D^R_{85}/D^R_{50} = 1.5$$

$$D^R_{15}/D^R_{50} = 0.67$$

(ie, it is a graded material as opposed to the single sized stone usual on a breakwater),

(vi) the in-situ bulk density is 1300 kg/m^3,

(vii) the filter layer is 0.5 D^R_{50} thick and

(viii) the filter grading is

$$D^R_{15}/D^F_{85} = 2.0$$

$$D^R_{50}/D^F_{50} = 4.5$$

$$D^R_{15}/D^F_{15} = 4.5$$

More details on the physical properties of the riprap can be found in Appendix 2. Table 1 gives an outline of the test conditions. The extent to which the results can be applied outside the above conditions will be discussed in the appropriate parts of the procedures.

Design criteria

The key step in any of the procedures is the determination of the ratio $\bar{H}_3/D^R_{50}$ where $\bar{H}_3$ is the significant wave height and D^R_{50} is the median stone diameter of the riprap. The test results give the erosion damage of the riprap, N_Δ, (as explained in "Conceptual framework" and "Parameter list – Dependent variables") corresponding to any given value of $\bar{H}_3/D^R_{50}$ so that the results can be used in either of two ways provided that $\bar{H}_3$ is known. Either

(a) the damage consequent on using a given value of $\bar{H}_3/D^R_{50}$ is determined or

(b) an acceptable level of damage can be specified which gives a value of $\bar{H}_3/D^R_{50}$ and thus determines the required D^R_{50}.

Alternative (a) would be used if the design procedure were incorporated in a formal economic analysis which anticipated that the costs could be minimised by designing for maintenance during the lifetime of the structure (43). Alternative (b) is more appropriate to the case where maintenance is not envisaged, the object being to find a D^R_{50} which will produce an acceptable level of damage over the lifetime of the structure.

There are many criteria which can be used to give acceptable levels of damage and the corresponding $\bar{H}_3/D^R_{50}$ values. All these are arbitrary and in putting forward the following criteria the aim

is to bring out some of the considerations involved in criteria selection so that the designer can determine new criteria to suit his own purposes. When selecting criteria the following points should be considered:

(i) The behaviour of the waves and riprap as described in the "Qualitative description of riprap behaviour".

(ii) The failure criteria used for the tests which is described in "Measurements and procedure" and discussed and illustrated under the "Failure" heading of the "Results and discussion". (Note that the per cent damage and failure definitions below are different from those of Burgess and Hicks (1).)

(iii) The fundamental randomness of the phenomenon as exemplified by the scatter of the erosion damage results in Figs 11-14. This scatter means that there is a range of possible values of the number, N_Δ, of D_{50}^R sized stones eroded for any slope, number of waves ($\bar{N}$) and $\bar{H}_3/D_{50}^R$ value. In the example in Fig 17e, the experimental values of N_Δ vary from 5 to 16 about a mean of 9 for $\bar{H}_3/D_{50}^R = 1.9$. In the discussion below the mean values of N_Δ are used.

(iv) The number of D_{50}^R sized stones eroded can be considered both absolutely and relatively. Absolutely, the number gives a picture of the amount of stone moved. It can be used with the damage limits (Figs 11-14) to give an idea of the scale of the resulting erosion hole. Relatively, the damage can be considered in many ways. Burgess and Hicks (1) related it to the amount of stone on a given area of slope but in this report it is related to the mean number of stones eroded at failure (as defined in "Measurements and procedure") so that the per cent damage is an expression of proximity to failure.

The following four criteria use the absolute and relative damage concepts to illustrate possible criteria from no damage to failure. Both the absolute damage Criterion B and the relative damage Criterion C can be used for situations intermediate between the no damage Criterion A and the failure Criterion D. The fact that Criterion C is associated with more damage than Criterion B in the illustration in no way implies that Criterion C inherently gives more damage than Criterion B.

Criterion A is the no-damage criterion. This is the most conservative design philosophy which is based on there being no erosion for a given significant wave height.The $\bar{H}_3/D_{50}^R$ values which give no-damage are given in Table 16 and plotted in Fig 17a for the different slopes in terms of the mean number of zero crossing waves, $\bar{N}$. The values of $\bar{H}_3/D_{50}^R$ were obtained from the solid lines drawn to represent the erosion damage results on Figs 11-14 (see (iii) above). As an example, the results for 1000 waves on the 1:2 slope are reproduced in Fig 17e showing an $\bar{H}_3/D_{50}^R$ value of 1.0 on the solid line for no damage. The curves on Fig 17a show that the no-damage values of $\bar{H}_3/D_{50}^R$ do not vary systemmatically with slope to the extent that those for the 1:6 slope are smaller than those of the 1:4 slope. These results emphasize the difficulty (discussed under "Damage limits") of defining a no-damage wave height in random waves. The problem can be avoided by designing for a small but acceptable amount of erosion.

Criterion B illustrates the absolute use of N_Δ by setting the damage to the erosion of an arbitrary number of D_{50}^R sized stones, say $N_\Delta = 9$.

~~Criterion A. Thus Criterion B is one which allows a small but acceptable amount of erosion for conservative design. As an illustration of the absolute use of N_Δ it is suggested that the tolerable limit of damage be set at the erosion of an arbitrary but small number D_{50}^R sized stones, say $N_\Delta = 9$.~~ This amounts to the erosion of one D_{50}^R sized stone per D_{50}^R width of the slope because the slope was surveyed over a 9 D_{50}^R width in these tests (see "Measurements and procedure"). Using the solid lines to represent the erosion damage results on Figs 11-14, the $\bar{H}_3/D_{50}^R$ values were read off at $N_\Delta = 9$ for the different slopes and numbers of waves and plotted on Fig 17b (Table 16). This process is illustrated in Fig 17e for the 1:2 slope at 1000 waves.

Seen in relative terms the damage level of $N_\Delta = 9$ is equivalent to the erosion of 14% of the mean number of stones eroded at failure on the 1:2 slope but only an estimated 5% of that number on the 1:6 slope (Table 16). These different per cent values reflect the relative stability of the slopes. The $\bar{H}_3/D_{50}^R$ values plotted in Fig 17b show a clear slope dependence which the Criterion A values do not.

Criterion C uses the idea of relative damage. It is assumed that it is undesirable to select values of N_Δ on the steeply rising portions of the solid lines on the results curves (Figs 11-14) where errors in the estimation of $\bar{H}_3$ could lead to large errors in the expected damage. An inspection of the curves with this requirement in mind leads on all slopes to the criterion of a maximum erosion of about 15% of the mean number of stones eroded at failure which is equivalent to the erosion of 9 and 13 D^R_{50} sized stones on the 1:2 and 1:3 slopes and an estimated 17 and 25 D^R_{50} sized stones on the 1:4 and 1:6 slopes. The corresponding $\bar{H}_3/D^R_{50}$ values were read from the solid lines on Figs 11-14 and plotted on Fig 17c (Table 16). It is interesting to note that this criterion is the same as Criterion B (see example on Fig 17e) on the 1:2 slope which shows that there is little room to manoeuvre on the steeper slopes. On the other slopes Criterion C gives more damage than Criterion B.

Criterion D is defined as a $D^R_{50}/2$ hole in the riprap through to the filter layer (see (ii) above) which was deemed to be failure in the model tests. The values of $\bar{H}_3/D^R_{50}$ were read from the results curves, Figs 11-14, (they were estimated for the 1:4 and 1:6 slopes; see "Results and discussion") at the N_Δ value equivalent to the mean number of stones eroded at failure. Strictly this is not intended as a design criterion by itself; it is included on Fig 17d to give a picture of the safety margins. Designers who think that the failure definition used in this report is too conservative should keep this in mind when considering safety margins and should also remember that designs using the steep portions of the results curves are inherently less safe than those using the flatter portions.

Wind data

Although not part of this research, for completeness and for the help of the designer, some comment will be made on wind data because the existence and form of these data have considerable influence on design procedures. In setting out procedures, it is impossible to provide rigid rules for handling wind data which will cover every circumstance. The aim is to give general outlines, the details of which must be resolved for particular cases by the designer. Ideally the designer requires the frequency of occurrence of storm events where the variation of wind velocity during the event is known. (In cases where reservoir levels vary appreciably it may be desirable to obtain these distributions for different ranges of reservoir level.) The frequency of events is necessary if the designer is to perform an economic analysis ("Design criteria", alternative (a)) and desirable if he is to assess the risks involved in using a design criterion of the kind illustrated by A to D above ("Design criteria" alternative (b)). These risks must be assessed in relation to the damage acceptable in the life of the structure.

The annual frequency of the occurrence of storms might be estimated from weather charts but will normally be calculated from measured data. Probably the best data for this purpose are mean hourly wind speeds and directions recorded over every hour for several years. Let a storm be defined as the maximum mean hourly wind speed occurring when the wind is consistently above Force 6 (say) in a direction that will generate waves on the dam (all waves are subsequently assumed to be at normal incidence, see Step 1.4 (i)). Then all such events in the wind records can be listed and the number of events of different magnitudes counted to give their frequency of occurrence per year. The storm shape, that is the way in which the wind speed varies during the storm must be determined by inspection of the wind record keeping in mind the durations required for the waves to grow over the fetches in question (see "Conceptual framework"). Wind speeds and directions meaned over half-hourly periods may be useful for rapidly changing tropical cyclonic storms.

If only a short wind record (say one year) is available then in general there will not be enough storms to obtain frequencies by the above method. In this case the concept of the storms must be abandoned and the annual frequencies of the mean hourly wind speeds computed. This is not a wholly satisfactory procedure because the frequencies of occurrence so computed are often used in the calculation of return periods of events which usually assumes that the frequencies of occurrence refer to statistically independent events, which strictly they do not. This is evident from an inspection of wind data which shows that adjacent values of mean hourly speeds are correlated rather than independent events. However this situation must be accepted if there is no alternative. Storm shape can be estimated as above.

The above discussion is also complicated by two facts. First, the wind data available may be so limited that it cannot justifiably be extrapolated to give information of the rare events of interest. Second, it is the frequencies of occurrence of waves rather than winds which are really of interest. The waves are a function of the wind speed and fetch, which depends on wind direction (see "Conceptual framework") if the reservoir is irregularly shaped. This can be dealt with by converting the wind record into waves storm by storm (or hour by hour) before the calculation of the frequencies is made. Whether this is reasonable or worthwhile is left to the designer's discretion. The calculation of the effective fetch F_E (16) for winds' directions at 10° or 20° intervals at the proposed dam site could help in this assessment.

Design procedures

Whether or not the designer calculates frequencies of occurrence of waves he must eventually decide how the wave data for a given event are to be used in relation to the laboratory results to get either the consequent damage or the safe D_{50}^R size. The use of the laboratory results requires a duration of wave attack in terms of the mean number of zero crossing waves ($\bar{N}$), a significant wave height, $\bar{H}_3$, and a mean zero crossing period $\bar{T}$. There appears to be three ways of formulating the wind data for a given event.

Method 1 assumes that the event (storm) has a steady wind velocity which produces waves of constant height $\bar{H}_3$ and period $\bar{T}$ over the duration of the event. This is the simplest model of a storm and will usually be the most appropriate one where wind data are inadequate.

Method 2 assumes that some detail is known about the variation of the wind within the event, that is to say that the storm shape is known in terms of the variation of the mean hourly wind speed during the storm.

Method 3 assumes that the damage may be allowed to accumulate over several events which must be compounded in terms of wind data to give one equivalent event before being applied to the laboratory results.

Note that by implication damage is repaired after each event in Methods 1 and 2.

The design procedures appropriate to the above methods are now set out in detail.

Method 1

Having chosen the wind speed, direction and duration appropriate to an event of interest, the method is as follows:

STEP 1.1 Use Saville (16) to calculate the effective fetch for the appropriate wind direction.
Note: (i) The above discussion on "Wind data".

STEP 1.2 Calculate the over-water wind velocity (16).

STEP 1.3 Calculate the significant wave height (H_S) and period (T_S) for the corresponding effective fetch and over-water wind speed (16). The result should be checked by using the most recent Bretschneider data (7) and checked independently by using the JONSWAP data given in equations (3) to (5).

Note: (i) The "Review of Current Practice – Wave prediction".

(ii) In STEP 1.3 the waves are generally limited by fetch and not duration. Duration is required because together with the wave period it gives the number of waves incident on the riprap.

(ii If the designer is using Method 1 to get a feel for a problem then it may be desirable to repeat STEPS 1.1–1.3 for several sets of wind speeds and directions to find that giving the biggest wave heights and periods.

STEP 1.4 Input H_S,T_S and the duration to the procedure by writing

$\bar{H}_3 \equiv H_S$

$\bar{T}$ = 0.91 T_S ($2\pi d/g\bar{T}^2 > 0.25$ for nominal deep water and the design curves to be valid).

$\bar{N}$ = duration/$\bar{T}$.

Note that:

(i) This step assumes that the waves are at normal incidence on the riprap. As far as is known there is no information on the behaviour of slope protection under the attack of oblique random waves. Limited data (44) for breakwaters in regular waves shows a reduction in damage only for angles of attack greater than 45° (to normal incidence) which is consistent with data of Burgess and Hicks (1) on riprap. The assumption of normal incidence so far as damage and run-up are concerned, is reasonable in the light of the lack of data.

(ii) The water depth, d, may be different from event to event giving damage to different parts of the slope.

(iii) If the JONSWAP wave data is used then equation (5) gives $\bar{T}$ directly.

STEP 1.5 Note the embankment slope, α, of interest.

In general the flatter the slope the more stable the riprap.

STEP 1.6 Select the required value δ, of $\bar{H}_3/D^R_{50}$, by either

(a) direct calculation if it is required to know the consequences of using a given D^R_{50}, or

(b) reading it from the erosion damage curves (Figs 11-14) at the appropriate α, $\bar{N}$ using a criterion giving acceptable damage.

Note:

(i) The above section on "Design criteria".

(ii) In the context of getting acceptable damage from one storm during the lifetime of the structure a low damage criterion must be used because the tolerance of too much damage in the design storm may lead to a D^R_{50} being selected which will allow damage in storms less intense than the design storm.

STEP 1.7 Using the value of δ obtained in STEP 1.6 either

(a) read off the damage N_Δ from curves (Figs 11-14) at the appropriate $\bar{N}$ and α if the damage consequent on using the given D^R_{50} is required, or

(b) calculate the D^R_{50} required to give the chosen level of acceptable damage from the equation

$$D^R_{50} = \bar{H}_3/\delta$$

Note that:

(i) The value of $2\pi D^R_{50}/g\bar{T}^2$ should be calculated to check that it is within the experimental range 0.0076–0.0303. Although the results show no clear dependence on this group it is advisable to note out of range values.

(ii) No allowance is made in the results for Reynolds number scale effects of the kind reported by Thomsen et al (26). Their work shows that in regular waves the prototype

D_{50}^R sizes predicted from small scale models of the size used in this research could be 60% too big. However, the present tests in random waves do not confirm this point. It can be argued that this is not unexpected because of the scatter of the results and the limited range of the Reynolds numbers used. Nevertheless the present tests were performed over a range of Reynolds numbers where the changes in the scale effect given in (26) are largest and hence most detectable. In view of the uncertainty an allowance for Reynolds scale effect (which is to the designer's advantage) cannot be recommended at this stage. (This point is important and further field and model work is now in hand.)

(iii) Data in Appendix 2 gives the relationship between stone diameter (as sieved), weight and specific weight as

$$(W/\gamma_R)^{1/3} = 0.82\ D$$

(iv) The D_{50}^R sizes obtained from the present results are for stone of specific gravity 2.7 (density 2700 kg/m^3) in fresh water. For stone density ρ_R' in water of density ρ' (sea water for example) the required D_{50}^{1R} is given by the semi-empirical relationship (26)

$$D_{50}^{1R} = (2700-1000)\rho' D_{50}^R/1000(\rho_R'-\rho')$$
$$= 1.7\ D_{50}^R/(\rho_R'/\rho' - 1)$$

(The value D_{50}^{1R} should be used for D_{50}^R in all that follows.)

(v) It has already been pointed out above (see "Limitations of model tests") that the use of the results implies that the thickness, shape, grading, in-situ bulk density, durability, filter layers etc used in the model can be reproduced in the field. (See Appendix 2 for full details on model riprap.) The practicability of this will be discussed below.

STEP 1.8 Model tests (1,26) show that the riprap grading is not critical. Various recommendations on grading are given in "Review of Current Practice" and it is probably sufficient at this step to check that the proposed grading lies in one of the classes quoted by Thomsen et al (26) – see "Review of Current Practice – Riprap size, grading and shape".
Note that:

(i) A large fraction of very fine material may adversely affect the performance of the riprap although a small amount (up to 10%) may be beneficial in protecting the filter layer. (There were no fines in the model riprap therefore the fines in any proposed riprap should be excluded in the measurement of D_{50}^R and bulk density.)

STEP 1.9 The "Review of Current Practice" gives contradictory evidence on the effect of stone shape whereas the present work suggests an influence and that it is desirable to have a cubical shape. A possible field criterion is that any stone with the long axis (see Appendix 2 for definitions) more than 2.5 times the short axis should be rejected.

STEP 1.10 In the present work the riprap thickness normal to the slope was set at 2 D_{50}^R (with an in-situ bulk density of 1300 kg/m^3 – see STEP 1.11). All the results are based on this. In the "Review of Current practice" a minimum thickness of 1.5 D_{50}^R or D_{MAX}^R is recommended with conflicting evidence on the effect of thickness. In general it must be expected that a thinner layer will fail more quickly than a thicker layer of a given stone size and that the number of stones eroded at failure will be less on a thinner layer than on a thicker layer. Hence Criteria C and D which are based on failure are likely to be dependent on layer thickness with reduced safety margins for thinner slopes. Criteria A and B are less likely to be dependent on thickness provided that the filter layer is adequately covered.

STEP 1.11 Decide on the method of placing the riprap. These methods are discussed in the "Review of Current practice". The aim is to produce a uniform, well knit, unsegregated layer. In the present work an in-situ bulk density of 1300 kg/m^3 (with rock of specific gravity 2.7) was achieved. The quality of construction is difficult to control in the field but it is evident that riprap with a lower bulk density will fail (on the definitions of this research) more quickly because the stone is less well packed.

Note that:

(i) It is suggested that the waves will cause the riprap to pack or consolidate to some "natural" bulk density. Compaction down the slope has been noted with artificial armour units on steep slopes but this occurred at the expense of gaps in the protection at the upper limit of run-up. Thus it is undesirable to rely on this effect to increase the bulk density of the in-situ riprap. Compaction normal to the slope may increase the bulk density but not the weight of riprap per unit area.

(ii) The preliminary tests showed that the interlocking or jamming of adjacent stones increases the durability (ie reduces the average erosion rate) of the protection.

(iii) Segregation of material (by size) during construction should be avoided. This appears to happen when material is bulldozed some distance down slope after dumping.

STEP 1.12 Select the filter material. The design recommendations in the "Review of Current Practice" are legion. In this work it was found that

$$D^R_{15}/D^F_{85} \leqslant 4$$

$$D^R_{50}/D^F_{50} \leqslant 7$$

$$D^R_{15}/D^F_{15} \leqslant 7$$

if the filter is not to be drawn through the riprap. This may lead to a coarse filter which will require an underfilter or bedding layer to prevent the erosion of the embankment. (This underfilter is unlikely to affect the riprap performance.) It is probably adequate to use conventional design relationships with their wider limits for the underfilter.

Note that:

(i) No shape specification is offered.

(ii) The use of riprap with some fines may allow the above recommended criteria to be relaxed, possibly at the expense of riprap stability (see STEP 1.8(i)).

STEP 1.13 Select the filter layer thickness. The "Review of Current Practice" suggests a minimum of 0.5 D^R_{50} or the minimum allowed by construction.

Note that:

(i) The thickness of the underfilter is not specified.

STEP 1.14 The upper and lower limits of damage l_u, l_l on the riprap slope (measured vertically from still water level) can be obtained from the damage limit plots (Figs 11-14) by reading off l_u/D^R_{50} and l_l/D^R_{50} for the appropriate value of δ and the slope, α. (See STEP 1.6.)

Note that:

(i) The damage limit curves are for 5000 waves which is adequate because these limits are established quickly.

(ii) If the lower damage limit is to be maintained at the levels given in the results then the riprap size below that level must not be reduced. The riprap might be reduced in size below a level 2 l_1 below minimum still water level.

STEP 1.15 The maximum run-up $\bar{r}_u^{max}$ and run-down $\bar{r}_d^{max}$ (measured vertically from still water level) can be calculated using $\bar{H}_3$ and $\bar{T}$ (from STEP 1.4) and the following formulae which are derived by fitting straight lines to the data plotted in Figs 15 and 16. The error introduced where the lines do not pass through the origin is small.

1:2 and 1:3 slopes

$$\bar{r}_u^{max} = 2.0\ \bar{H}_3 \qquad \text{....(29)}$$

1:4 slope

$$\bar{r}_u^{max} = 1.25\ \bar{H}_3 \qquad \text{....(30)}$$

1:6 slope

$$\bar{r}_u^{max} = 0.92\ \bar{H}_3 \qquad \text{....(31)}$$

All slopes

$$\bar{r}_d^{max} = 0.14\ \bar{T}(g\bar{H}_3)^{1/2} \tan\alpha \qquad \text{....(32)}$$

Note that:

(i) The run-up and run-down values are the expected values of the maxima in 150 zero crossings of the mean water level on the slope. This level is different from still water level because the waves cause a local elevation (or "set-up" which should be distinguished from set-up due to wind sieches or tides) of the mean water level on the slope. The mean period of the crossing of mean water level by the run-up and run-down is different from the mean zero crossing period, $\bar{T}$, of the waves. The mean period of the run-up is 1.14 $\bar{T}$, 1.18 $\bar{T}$, 1.20 $\bar{T}$ and 1.41 $\bar{T}$ on the 1:2, 1:3, 1:4 and 1:6 slopes respectively.

(ii) There is scatter on all the run-up plots; the above formulae refer to the mean lines as does that of the run-down where the scatter is large.

(iii) The run-up and run-down values plotted were measured at all stages of the experiments, that is, at all degrees of damage.

(iv) Designing to the maximum run-up in 150 crossings of the mean water level on the slope should be adequate for wave overtopping purposes. (As a guide, the overtopping discharge is of order 10^{-4} $m^3/s/m$ (45) with one wave in 50 overtopping a variety of smooth impermeable walls in a variety of random wave conditions.) It is possible that the discharge due to one run-up in 150 on a rough slope wall be an order of magnitude less and small enough to be absorbed in a soak-away.

(v) No allowance is made for scale effects which are not evident in this work. (For information, data on scale effects on smooth slopes are to be found in (24,25).)

Method 2

It is assumed in this method that some detail is known about the variation of the wind during the event (storm) of interest. In the following this information is taken to be in the form of a table of mean hourly wind speeds and directions.

STEP 2.1 Calculate the effective fetch F_E using Saville (16).

Note:

(i) The discussion on "Wind data".

STEP 2.2 Calculate the over-water wind velocities using (16) for each hourly step in the storm.

STEP 2.3 Calculate H_S and T_S for each hourly step in the storm using (16), (7) or equations 3 to 5.

STEP 2.4 Calculate the $\bar{H}_3$, $\bar{T}$ and $\bar{N}$ for each hourly step (duration = 1 hour) as in STEP 1.4. See example on Fig 18a.

STEP 2.5 Note the embankment slope, α.

STEP 2.6 Either note

(a) the size D_{50}^{RI}, for which the designer requires the consequent damage (see "Design criteria, (a)), or

(b) select the design criteria giving acceptable damage and note the value of N_Δ, the average number of stones eroded using the chosen criteria (see "Design criteria, (b)).

Note:

(i) The discussion of "Design criteria".

(ii) In the context of getting acceptable damage from one storm in the lifetime of the structure a low damage criterion must be used because the tolerance of too much damage in the design storm may lead to a D_{50}^R being selected which will allow damage to occur in storms less intense than the design storm.

STEP 2.7 Either

(a) where the damage consequent on using a given D_{50}^R is required use the noted value D_{50}^{RI} to calculate the value of $\bar{H}_3/D_{50}^R$ for each step in the storm; in the example in Fig 18 these values are ${}_1\bar{H}_3/D_{50}^{RI}$, ${}_2\bar{H}_3/D_{50}^{RI}$ and ${}_3\bar{H}_3/D_{50}^{RI}$. Turn to the damage curves for the appropriate slope α, Figs 11-14, and for each of the calculated $\bar{H}_3/D_{50}^R$ values read off the number of stones eroded ${}_1N_\Delta$, ${}_2N_\Delta$, etc at 1000, 2000, 3000, 4000 and 5000 waves as in the damage curves in the example on Fig 18b (notice that the damage curves in Fig 18b for 1000, 2000, etc waves are plotted on one graph whereas the experimental curves, Figs 11-14 are plotted separately). Reconstruct the damage histories for each $\bar{H}_3/D_{50}^R$ by plotting the ${}_1N_\Delta$, ${}_2N_\Delta$, etc at the appropriate number of waves as in Fig 18c. These reconstructed damage histories show how much erosion will occur for the riprap size D_{50}^{RI} in waves of height ${}_1\bar{H}_3$, ${}_2\bar{H}_3$ and ${}_3\bar{H}_3$. Now read off the total damage for the storm by plotting the storm on the damage histories as in Fig 18c. That is, N_1 waves of height ${}_1H_3$ produces the erosion given by point A on the ${}_1\bar{H}_3$ curve. Move horizontally from A on the ${}_1\bar{H}_3$ curve to B on the ${}_2\bar{H}_3$ curve so that the $\bar{N}_2$ waves of height ${}_2\bar{H}_3$ give additional damage equivalent to moving from B to C on the ${}_2\bar{H}_3$ curve. The final step is to move horizontally from C on the ${}_2\bar{H}_3$ curve until the intersection of the ${}_3\bar{H}_3$ curve is reached. In the example the intersection is at some point X, outside of the range of the data. However the actual additional damage due to $\bar{N}_3$ waves of height ${}_3\bar{H}_3$ will be less than that obtained by going from points D to E on the ${}_3\bar{H}_3$ curve because the curve gets flatter as $\bar{N}$ increases. Thus the total damage for the storm is that read off at point C plus that between points D and E, or

(b) where it is required to find D_{50}^R so that the chosen level of damage is obtained (see STEP 2.6 (b)), then use an iterative procedure with different trial values of D_{50}^{RI} in STEP 2.7 (a) until a D_{50}^R value is found which gives the required damage level. A first trial value

of D_{50}^R can be found by estimating average values of $\bar{H}_3$ and $\bar{N}$ for the whole storm and reading off from the damage curves (Figs 11-14) at the appropriate $\bar{N}$,α the $\bar{H}_3/D_{50}$ value (δ say) equivalent to the required design criteria. The trial D_{50}^R size is then $\bar{H}_3/\delta$. (See STEP 1.6 (b), 1.7 (b) for example.)

Note:

(i) That if $\bar{H}_3$ varies little throughout the storm then Method 1 may be adequate.

(ii) That if the peak value of $\bar{H}_3$ in the storm is so much greater than the other $\bar{H}_3$ values the damage only occurs for the peak $\bar{H}_3$ value then Method 1 is adequate.

(iii) The assumptions given under STEP 1.7 (i)–(v).

STEPS 2.8–2.15 are exactly STEPS 1.8–1.15 with δ set equal to the largest $\bar{H}_3/D_{50}^R$ value in the storm.

Method 3

This method is an attempt to deal with the situation where damage is left to accumulate over several events. It involves compounding the damaging events expected during the period of interest (the lifetime of the structure for example) into a single equivalent event. The implication is that the frequency of occurrence of mean hourly wind speeds for relevant directions (see "Wind data") is known for the period of interest. This Method is the same as Method 2 except

(i) that the table of mean hourly wind speeds for one storm event required in Method 2 is replaced by a table of all the mean hourly winds great enough to cause damage together with their frequency of occurrence in the period of interest. The minimum wind speed giving damage is obtained by reading the no-damage $\bar{H}_3/D_{50}^R$ value for the appropriate slope from Figs 11-14 (see "Design criteria") and using the trial value of D_{50}^R (see STEP 2.7) to obtain the minimum value of $\bar{H}_3$. This is converted to a wind speed for the appropriate effective fetch using Saville (16) or (7) or equations 3-5.

(ii) that in reading the damage from the damage histories (Fig 18b) in STEP 2.7 the waves are assumed to attack the riprap in steps of ascending order of magnitude (clearly the final damage depends on the order of occurrence of the waves (see Fig 18c); it seems reasonable to apply the lowest waves first),

(iii) when calculating the damage in STEP 2.7 the damage done for each wave height step must be multiplied by the number of times that particular wave height (ie mean hourly wind speed) is expected in the period of interest.

COMPARISONS AND WORKED EXAMPLES

It is of considerable interest to compare the use of the procedures set out in this report with those of other workers, particularly Burgess and Hicks' (1) CERA Report 4 and those of the Coastal Engineering Research Center (CERC) in America where the natural scale tests of Thomsen et al (26) were done. Although no exact comparisons are possible because the various definitions, experimental methods and criteria are so different, an attempt will be made to make comparisons with CERA Report 4 because it is widely used. The large scale work of Thomsen et al (26) has not yet been incorporated in design procedures so comparisons are inappropriate at this stage.

Even general comparisons are very difficult. Probably the most readily apparent difference is the effect of wave period on erosion damage. In this report there is no clear evidence of any influence of the mean zero crossing wave period $\bar{T}$ on damage in irregular waves whereas both Burgess and Hicks' (1) CERA Report 4 and Thomsen et al (26) find a dependence on the wave period in regular waves (note that the CERA Report 4 and Thomsen et al have different period dependences). As stated in

"Quantitative results for erosion damage" this difference between the irregular and regular wave situation might be more apparent than real because in any sea state there are individual waves of a wide range of periods, the damage being the result of the total action of all of them. Hence results from irregular waves characterised by a mean period $\overline{T}$ might well mask variations in damage caused by individual waves.

Because of the difficulties of general comparisons, a worked example of the procedures in this report will be given which will be followed by a few particular examples using both these and the CERA Report 4 methods.

Worked example

Since the main aim of this work is the relation of wave conditions to riprap sizes, examples of manipulating wind data will not be given. It is useful to take an example from the earlier CERA report (1) which is

$H_S = 1.37$ m (4.5 ft)

$T_S = 4.8$ s

Duration 4.65 hours (3500 waves of 4.8 s period)

and follow Single Storm Method 1 from STEP 1.4

$\overline{H}_3 = 1.37$ m

$\overline{T} = 0.91 \times 4.8 = 4.4$ s

$\overline{N} = 4.65 \times 3600/4.4 = 3800$

(no depth, d, is available to check the relative depth).

STEP 1.5 The slope is 1:2.

STEP 1.6 Use Criterion B with $N_\Delta = 9$ because only a minimal amount of damage is tolerable. In addition a new criterion equivalent to that of CERA (1) can be calculated. This criteria is 5% damage by weight of the stone on a 4 H_D length of slope. Assuming a thickness of 2 D^R_{50} and a width of 9 D^R_{50} (to match this work) then the mass of stone on the slope is

$$2\ D^R_{50} \times 4\ H_D \times 9\ D^R_{50} \times \rho^B_R = 72\ H_D (D^R_{50})^2 \rho^B_R$$

and the mass of a D^R_{50} size spherical stone is

$$\rho_R\ \pi (D^R_{50})^3/6$$

whence the number of stones eroded at 5% damage is

$$N_\Delta = 0.05 \times 432 \times \rho^B_R\ H_D/(\pi \rho_R\ D^R_{50})$$

$$= 21.6\ \rho^B_R\ H_D/(\pi \rho_R\ D^R_{50}) \qquad \ldots(33)$$

Using H_D and D^R_{50} from (1) and densities from this research this criterion is $N_\Delta = 12$ stones. Hence $N_\Delta = 12$ is suggested as a criterion equivalent to that of CERA in this case.

STEP 1.7 From Fig 11 $\delta = 1.6$ for Criterion B with $N_\Delta = 9$

From Fig 11 $\delta = 1.7$ for the CERA Criteria

Hence D^R_{50} = 0.9 m Criterion B

or D^R_{50} = 0.8 m CERA Criterion

The dimensionless group $2\pi\, D^R_{50}/g\bar{T}^2 = 0.028$ or 0.027 which is within the experimental range.

STEP 1.14 From Fig 11 the upper and lower damage limits are

$$l_u/D^R_{50} = 3.0 \quad l_l/D^R_{50} = 3.2 \text{ for } \delta = \bar{H}_3/D^R_{50} = 1.6$$

and $$l_u/D^R_{50} = 3.2 \quad l_l/D^R_{50} = 3.4 \text{ for } \delta = \bar{H}_3/D^R_{50} = 1.7$$

giving l_u = 2.7 m l_l = 2.9 m for D^R_{50} = 0.9 m

l_u = 2.6 m l_l = 2.7 m for D^R_{50} = 0.8 m

STEP 1.15 The maximum run-up $\bar{r}_u^{max}$ is 2.0 $\bar{H}_3$, vertically above still water level, hence

$$\bar{r}_u^{max} = 2.0 \times 1.37$$

$$= 2.7 \text{ m}$$

The run-down below SWL is = 1.1 m.

Those steps which depend on the details of stone grading etc which are specific to particular cases are omitted.

Comparison with the CERA work (1)

Using equation (33) to calculate a damage criterion equivalent to that of CERA (1), the following comparisons can be made for a riprap 2 D^R_{50} thick, using the same wave conditions as above.

On the 1:2 slope:

	Present research	CERA (1)
D^R_{50}	0.80 m	0.80 m
Upper limits of damage	2.6 m	2.5 m
Lower " " "	2.7 m	1.6 m
Run-up	2.7 m	2.3 m
Run-down	1.1 m	–

(excluding scale compensation, waves at normal incidence).

On the 1:3 slope:

	Present research	CERA (1)
D^R_{50}	0.65 m	0.53 m
Upper limits of damage	1.2 m	1.7 m
Lower " " "	1.5 m	1.2 m
Run-up	2.7 m	2.0 m
Run-down	0.75 m	–

On the 1:4 slope:

	Present research	CERA (1)
D_{50}^{R}	0.49 m	0.40 m
Upper limits of damage	0.7 m	1.3 m
Lower " " "	1.1 m	0.9 m
Run-up	1.7 m	1.7 m
Run-down	0.6 m	--

These comparisons show that the present work predicts the same or larger design values of D_{50}^{R} for the particular wave conditions used.

FUTURE RESEARCH

This investigation and the drafting of design procedures has highlighted the need for research to determine:

1. Whether there are Reynolds number scale effects which lead to the over-estimation of D_{50}^{R} sizes when laboratory damage results are extrapolated to full scale. Field experiments aimed at resolving this problem are now in hand.

2. What kind and duration of wind recording is desirable at a site for satisfactory wave prediction and how wave prediction methods can be improved particularly for enclosed bodies of water in hilly areas.

3. The effect of oblique wave attack on stability.

4. The effect of riprap thickness on stability.

5. The effect of stone and water density on stability.

6. The depth below the minimum water level which requires protection.

7. The effect on stability of slopes flatter than 1:6.

8. The effect on stability of relatively shallow water approaches of the type found in estuarial and coastal environments.

9. Satisfactory field grading procedures particularly for large riprap and their relation to laboratory sieve size gradings.

ACKNOWLEDGEMENTS

This report was prepared in Mr W A Price's Division by D M Thompson and R M Shuttler. Thanks are due to those members of the section who operated the model through a long experimental programme and to the CIRIA Project Steering Group for their help and comments throughout.

REFERENCES

1. BURGESS J S and HICKS P H Riprap protection for slopes subject to wave attack. Civil Engineering Research Association, Research Report 4, 1966.

2. CARTWRIGHT D E and LONGUET-HIGGINS M S The statistical distribution of the maxima of a random function. Proceedings of the Royal Society A 237, 1956.

3. BRETSCHNEIDER C L Wave variability and wave spectra for wind-generated gravity waves. US Army Corps of Engineers, Beach Erosion Board, Tech Memo 118, 1959.

4. WILSON J R and BAIRD W F A discussion of some measured wave data. Thirteenth Coastal Engineering Conference, 1972.

5. GODA Y Numerical experiments on wave statistics with spectral simulation. Report of the Port and Harbour Research Institute of Japan, 9 (3), September 1970.

6. TUCKER M J Analysis of sea wave records. Proceedings of the Institution of Civil Engineers, 26, 1963.

7. Shore protection manual, US Army Corps of Engineers, Coastal Engineering Research Centre, 1973.

8. SVERDRUP H U and MUNK W H Wind, sea and swell: Theory of relations for forecasting. US Navy Department, Hydrographic Publication HO 601, 1947.

9. BERTRAM G E Slope protection for earth dams. Fourth International Congress on Large Dams, Vol 1, 1951.

10. SHERARD J L et al Earth and earth-rock dams. Wiley, 1963.

11. Earth embankments. Corps of Engineers, Department of the Army, Engineering Design Manual, EM 1110-2-2300, March 1971.

12. TORUM A Riprap design against wind generated waves. Technical University of Norway, Rivers and Harbours Laboratory, November, 1971.

13. IVERSON N L and RINGHEIM A S Upstream slope protection of Gardiner and Qu'Appelle river dams. Eleventh International Congress on Large Dams, Vol 3, 1973.

14. McCONNELL A D, SEEMEL R N and O'BEIRNE H J Freeboard and slope protection of dykes for Churchill Falls Project, Eleventh International Congress on Large Dams, Vol 3, 1973.

15. TAYLOR K V Slope protection on earth and rockfill dams, Eleventh International Congress on Large Dams, Vol 3, 1973.

16. SAVILLE T, McCLENDON E W and COCHRAN A L Freeboard allowances for waves in inland reservoirs, ASCE, 88 (WW2) 1962.

17. Waves in inland reservoirs; US Army Corps of Engineers, Beach Erosion Board, Tech Memo 132, 1962.

18. BRETSCHNEIDER C L Revised wave forecasting relationships. Second Coastal Engineering Conference, 1952.

19. BRETSCHNEIDER C L Revisions in wave forecasting: Deep and shallow water. Sixth Coastal Engineering Conference, 1957.

20. HASSELMANN K et al Measurements of wind wave growth and swell decay during the Joint North Sea Wave Project (JONSWAP), Erganzungsheft zur Deutschen Hydrographischen Zeitschrift Reihe A (8°), Nr 12, 1973 and correspondence.

21. KINSMAN B Wind waves. Prentice-Hall, 1965.

22. Design of small dams. US Bureau of Reclamation, 1960.

23. HUDSON R Y Laboratory investigation of rubble mound breakwaters. ASCE, 85 (WW3), 1959.

24. Shore protection planning and design, US Army Corps of Engineers, Coastal Engineering Research Centre. Tech Report 4, 1966 Edition.

25. BEENE R R W and AHRENS J P Wave tank studies for the development of criteria for riprap. Eleventh International Congress on Large Dams, Vol 3, 1973.

26. THOMSEN A L, WOHLT P E and HARRISON A S Riprap stability on earth embankments tested in large and small scale wave tanks. US Army Corps of Engineers, Coastal Engineering Research Centre, Tech Memo 37, June 1972.

27. ESMOIL E E Rock as upstream protection for earth dams – 149 cast histories. US Department of the Interior, Bureau of Reclamation, Report DD-3, May 1968.

28. DAMSGAARD A et al Northumberland Causeway, model tests on filters. Technical University of Norway, Rivers and Harbours Laboratory, Bulletin 13E, 1972.

29. HYDRAULICS RESEARCH STATION Banksmeadow breakwater. Report EX 538, 1971.

30. PIERSON W J and MOSKOWITZ L A proposed spectral form for fully developed wind seas based on the similarity theory of S A Kitaigorodskii, Journal of Geophysical Research, 69 (24) 1964.

31. THOMPSON D M Tests on a discrete-frequency irregular wave generator. Hydraulics Research Station, Report INT 82, April, 1970.

32. BRUUN P M Damage function of rubble mound breakwaters. Discussion ASCE (WW2) 1970.

33. JOHANNESSON P and BRUUN P M Hydraulic performance of rubble mound breakwaters: reasons for failure. Proceedings of First International Conference on Port and Ocean Engineering in the Arctic, Vol 1, 1971.

34. AHRENS J In correspondence.

35. BATTJES J A Long term wave height distribution. National Institute of Oceanography, Internal Report No A44, July 1970.

36. FRYER D K, GILBERT G and WILKIE M J A wave spectrum synthesizer. J Hydraulics Research 11 (3), 1973.

37. DEPARTMENT OF THE ENVIRONMENT Hydraulics Research 1972, HMSO.

38. HYDRAULICS RESEARCH STATION Wave spectrum synthesizers, Tech Memo 1/1972, June 1972.

39. KAJIMA R Estimation of an incident wave spectrum under the influence of reflection. Coastal Engineering in Japan, 12, 1969.

40. AHRENS J P The influence of breaker type on riprap stability. Twelfth Coastal Engineering Conference, 1970.

41. GALVIN C J Breaker type classification on three laboratory beaches. Journal of Geophysical Research 73 (12), 1968.

42. BATTJES J A Run-up distributions of waves breaking on slopes, ASCE, 97 (WW1), 71.

43. KREEKE VAN DE J and PAAPE A On optimum breakwater design. Ninth Coastal Engineering Conference, 1964.

44. KREEKE VAN DE J Damage function on rubble mound breakwaters. Discussion, ASCE, 95 (WW3) 1969.

45. HYDRAULICS RESEARCH STATION Maplin seawalls, a model study. Report EX 653, July 1974.

NOTATION

d	water depth
f	frequency in Hz
f_m	the frequency (Hz) of the peak of the JONSWAP (20) energy spectrum
g	the acceleration due to gravity
l	the number of D_{50}^R (vertically) between the upper and lower limits of the erosion area
l_l	lower limit of the damaged area measured vertically from still water level
l_u	upper limit of the damaged area measured vertically from still water level
m_o	mean square water surface elevation (or variance of the surface), $m_o = \int E(f)df$
m_n	n^{th} spectral moment
r_u	run-up; measured vertically from still water level
r_d	run-down; measured vertically from still water level
t	layer thickness measured normal to the slope
A,B	dimensionless constants (0.0081, 0.74) of Moskowitz spectrum
B	superscript; bulk (density)
BL	superscript; in-situ bulk (density)
D	nominal stone diameter
D_n	the diameter of a stone which exceeds that of n% of the stone by weight; where measured in this report it refers to a sieve size; in other work it may be an equivalent diameter
E	superscript; embankment
E(f)	energy density spectrum (synonymous with spectrum, wave spectrum, energy spectrum). Dimensions – L^2T
$E_M(\omega)$	Moskowitz energy spectrum in radian frequency
F	fetch; the distance for which the wind blows over water.
F	superscript or subscript; filter material
F_E	effective fetch; the effective distance for which the wind blows over water when the up-wind boundary is irregular. See Saville (16).
H	zero down crossing wave height; defined as the vertical distance between the highest and lowest instantaneous water surface elevations between two successive down crossings of the mean water level by the instantaneous water surface (Fig 2)
H_D	the design wave height, the height of a regular wave which best characterises the irregular sea for design purposes
H_s	the significant wave height; the mean height of the highest third of the waves, the symbol used in wave prediction schemes

H_3	the mean height of the highest third of the waves defined by zero down crossings. Fig 2.
K	'K factor', see (24)
L_0	deep water wavelength; $gT^2/2\pi$
MAX	subscript; maximum
MIN	subscript; minimum
N_Δ	the damage expressed as the equivalent number of spherical stones of D_{50}^R diameter eroded from the slope
N_S	stability coefficient, see (26)
N	mean number of zero crossing waves
R	superscript or subscript; refers to riprap
P	a placement parameter
S	specific gravity
S_h	a shape parameter
T	zero crossing wave period; the time between two successive down crossings of the mean water level by the instantaneous water surface
T	mean zero crossing wave period
T_S	the significant period; the mean period of the waves associated with the highest third
U_{10}	wind speed at an elevation of 10 m
W	weight of an individual stone
W_n	the weight of a stone which exceeds that of n% of the stone by weight
α	the slope of the embankment from the horizontal
γ	specific weight
δ	the design value of $\bar{H}_3/D_{50}^R$
ϵ	the spectral width parameter defined by equations 17 and 18 in text or by counting waves as in Reference 6
μ	dynamic viscosity of water
ω	radian frequency
ω_0	parameter of the Moskowitz spectrum
ρ	density (mass per unit volume) of water unless otherwise subscripted
σ_N	standard deviation of number of D_{50}^R stones eroded at failure
	superscript; mean

APPENDICES

APPENDIX 1

Members of the CIRIA Steering Group

R G T Lane	Sir Alexander Gibb and Partners
G F Olliver	Wimpey Laboratories Limited
B H Rofe	Rofe, Kennard and Lapworth
E P Sephton	Sir M MacDonald and Partners
E H Taylor*	Sir M MacDonald and Partners
R G Taylor	Sir William Halcrow and Partners
L Summers*	Sir William Halcrow and Partners
A R Thomas	formerly Binnie and Partners
D M Thompson	Hydraulics Research Station
D E Wright	CIRIA (Chairman)

* Occasional member

APPENDIX 2

Description of model riprap and filter materials

The riprap

The agreed grading curves for the riprap shown on Fig 19 are straight lines on a log-linear plot with D^R_{85}/D^R_{50} = 1.50 and D^R_{15}/D^R_{50} = 0.67. To obtain these gradings crushed Carboniferous Limestone was sieved through square mesh screens into a range of sizes such that each riprap grade could be mixed from at least five different sizes. The stone however was very flaky particularly at the smaller sizes. It was decided (arbitrarily) that the stone shape would be acceptable provided that the ratio of the maximum to minimum dimension did not exceed 2.0. To achieve this sieved sizes greater than 20 mm were sorted by hand, the assessment being made by eye. The smaller stone sizes were resieved through flakiness screens which had rectangular slots of a width about 0.7 times that of the mean stone size. The riprap grades were mixed in the proportions by weight as shown in Table 17.

In order to assess the stone shape a representative sample of about 200 stones was taken from each grade. The weight and dimensions of the enclosing cuboid of each stone was measured. (The stones were positioned so that the maximum and minimum dimensions were the greatest and least that could be obtained.) Figs 20, 21 and 22 show the scatter diagrams for each grade, obtained by plotting the ratios maximum/median dimension and minimum/median dimension for each stone. Superimposed on each plot are lines of constant maximum/minimum dimension from which the exceedance curves on Fig 23 were obtained by counting the numbers of stones in the bands formed by the lines of constant maximum/minimum dimension.

The 40 mm riprap grade which was sorted entirely by hand most nearly approaches the shape requirement with 11.7% of the stones exceeding the limit of 2.0. The 20 and 30 mm grades are similar to each other except below the 5% exceedance level and give 27.1% and 26.3% exceeding the limit of 2.0. In all cases the stones with the largest ratio of maximum to minimum were among the smallest stones in the samples.

At the conclusion of the test programme a representative sample of the 30 mm riprap was analysed for shape as above. The results are plotted on Figs 24 and 25. The comparison between the two 30 mm riprap samples is good. The small divergences are probably sampling variations. This confirms the visual comparison of stones used throughout the tests with unused stones which did not indicate any significant wear. Possibly some of the sharpest corners were slightly rounded but not appreciably.

Samples were taken from each sieve cut used to construct the riprap grades and the average weight and mean sieve size for each cut used to calculate the dimensionless ratio $(W_R/\gamma_R)^{1/3}/D^R$ which relates stone weight to sieve size. The average value of this ratio was 0.82 (Table 18).

The stone used for the riprap had a density of 2700 kg/m^3. The bulk density for the 20, 30 and 40 mm riprap grades was 1510, 1480 and 1480 kg/m^3 respectively. This was measured by filling a box (0.5 m)^3 with layers of well mixed riprap, and weighing the stone required to fill the box. The bulk density of the stone laid to the correct thickness on the model slope was 1300 kg/m^3. This was obtained by surveying the surfaces of the filter layer and the laid riprap to obtain the volume of the layer and using the known weight of material on the slope.

The natural angle of repose of each riprap grade was measured by piling the dry material against a vertical wall. Well mixed loads were placed at the top of the pile and allowed to roll down. Sufficient material was used to give a final surface area of at least 10 x D^R_{50} wide and 30 x D^R_{50} long. A flat board was then laid on this surface and its angle measured. For the 20, 30 and 40 mm riprap grades the natural angle of repose was 1 : 1.38, 1.14 and 0.97 respectively. The measurement was repeated for the 20 mm grade completely immersed in still water and gave an angle of 1:1.38 (as for the dry condition).

For all the main series of tests the riprap was laid on the filter layer to the instructions detailed in Appendix 4.

The filters

The grading curves for the filter materials used are shown on Fig 19. To obtain these smooth rounded shingle and coarse grit were sieved through square mesh screens to give a range of sizes such that each grade could be mixed from at least three different sizes. The mixing proportions are given in Table 17.

No attempt was made to apply a shape criterion to the filter material. Plate 7 shows the three filter grades 4/20, 4/30 and 4/40 used for the main test series.

The bulk density of each grade was measured by weighing the stone required to fill an $(0.25\ m)^3$ box. The values are given in Table 17. No attempt was made to measure the laid bulk densities of the filter grades.

For each test the filter material was well mixed and laid roughly in position. It was then lightly tamped and screeded to profile working from the bottom of the slope. Plate 7 shows the appearance of the filter grades when so laid.

APPENDIX 3

Preliminary tests

Introduction

Prior to the main test programme described in the body of this report a preliminary series of tests was made with the general aim of checking the viability of the experimental procedures, the measuring techniques and the failure criterion. In addition it was hoped that some reduction of the number of dimensionless parameters might be achieved. To keep this series as short as possible the tests were limited to one slope (1 : 3), one period ($\overline{T}$ = 1.3 s), one riprap grade (D_{50}^R = 30 mm) and a water depth of 610 mm. The thickness of the riprap and filter layers was 2 D_{50}^R and 0.5 D_{50}^R for all these tests.

Facility and measuring equipment

The test facility and measuring equipment were exactly as for the main test programme and are described in the body of the report.

Measurements and analysis

The measurements to be made consisted of wave data, run-up data, surveys of the riprap surface and an assessment of the failure of the riprap slope.

The run-up data and the surveys of the riprap surface were measured and analysed in basically the same way as the corresponding data for the main test programme. The procedures are described in Appendix 6.

The measurement and analysis of the wave parameters $\overline{H}_3$, $\overline{\overline{T}}$ and ϵ was different from the main programme methods in that the wave data was recorded with the run-up data and analysed by picking the zero crossing waves directly from the record rather than by computing the energy spectrum.

Failure of the riprap was initially defined as occurring when a grain of filter material moved through the riprap on to the riprap surface. It was expected that this would only happen when the filter layer had been exposed by the erosion of the riprap.

Test programme

Table 19 gives a summary of the preliminary test programme and the main changes made. Tables 20-22 give the detailed results. The main constructional change to the model occurred after Tests 1-7. For Tests 1-7 a porous embankment of 20 mm single sized shingle was used. A fine mesh nylon net was laid on the surface of the shingle to prevent the loss of filter material into the embankment. The mesh was not fine enough to prevent the free access of water into and out of the embankment. For the remaining tests the embankment was impermeable.

Test procedure

Before the tests the synthesizer was set up to give waves with a Moskowitz spectral shape at $\overline{\overline{T}}$ = 1.30 s and the riprap profiler and the run-up meter were calibrated (see "Measurements and procedure" and Appendix 6).

The basic procedure for each test is set out below as originally conceived. In brief, each test was to be run in steps of 500 waves and as much wave and run-up data collected as possible. During the course of the preliminary tests procedural changes were made based on the results obtained and these are noted below for the tests in which they occurred.

Basic procedure for a test

1. Screed the filter layer to profile working up the slope.

2. Survey the surface of the filter layer. (This was done for the first test only, on the assumption that careful screeding for each test would produce the same results.)

3. Lay the riprap slope. (No formal laying procedure had been decided at the start of the tests apart from the need to have the riprap well mixed and laid as compactly as possible without undue damage to the filter layer.)

4. Fill the flume to the working level.

5. Take the zero reading of the riprap profiler with the hemispherical foot just on the water surface.

6. Set the initial conditions on the synthesizer to give small waves for the bedding-in run.

7. Run the small waves. (For all the preliminary tests this wave train was 2000 zero crossing waves long and of such a height that stones might be rocked but not displaced.)

8. Survey the riprap surface. (This gave the initial riprap levels from which all the erosion volumes for the test were calculated.)

9. Calibrate the wave probe.

10. Note the zero reading of the run-up meter.

11. Run 500 waves at the chosen value of $\bar{H}_3$ and record wave and run-up data.

12. Survey the riprap slope.

13. Reset initial condition of the synthesizer to the state at the end of the previous 500 waves.

14. Repeat 11-13 above until failure occurred.

15. Drain the flume.

16. Strip out the riprap.

17. Go to 1 for the start of the next test.

Tests 1-4: Laying and repeatability

Aim

Since the attacking waves and the riprap are both random phenomena it was expected that the damage history (ie the variation of absolute erosion with time) would also be a random phenomenon and that some variability for identical tests could be expected. This is obviously crucial to the accuracy of the results and their use for predictive purposes. To assess this Tests 1-4 were made in what were intended to be identical conditions.

Procedure change

A procedure change was made after Test 3. Instead of recording one block of combined wave and run-up data per 500 waves two shorter blocks were recorded. The length of each block was such that at least 150 zero crossing run-ups of the mean water level on the slope were recorded.

Discussion

The damage histories for the four tests are shown on Fig 26 (Table 20). There are two distinct sets of results, one for Tests 1 and 4 and the other for Tests 2 and 3. It was realised after Test 2

that different operators had used different techniques for laying the riprap. The operators (who were unaware of the situation) were each asked to rebuild and repeat the tests. The first laid the slopes for Tests 1 and 4, and the second for Tests 2 and 3.

In Test 1 the method (A) of laying the riprap was an attempt to simulate the practice of pushing or pulling the riprap up the slope to the correct thickness. The model slope was built strip by strip from the bottom upwards, each strip being trimmed to level by raking the surface and projecting stones up the slope and off the strip to sit on the filter layer. This method had the effect of moving most of the larger stones to the bottom of the riprap layer leaving the surface covered mostly with small and medium sized stones (Plate 1).

Test 2 (method B) followed the practice of roughly laying the whole slope and then trimming it to the required thickness by replacing individual stones. In the model the slope was again covered with the riprap material strip by strip from the bottom upwards but no adjustment was made until the slope was complete. Then projecting stones which were usually the large ones were removed and placed in suitable holes. This method produced a slope with large stones common on the surface in positions giving some interlocking and jamming (Plate 1).

The results for Tests 1 and 4 (Method A) give reasonably smooth and repeatable damage histories while Tests 2 and 3 are very erratic although there was overall repeatability of the number of waves to failure and the number of stones eroded at failure. The scatter in the damage histories for Tests 2 and 3 was largely due to the jamming of several large stones. This jamming occurred between 0 and 2000 waves in Test 2 and 2000-3000 waves in Test 3 and resulted in an uneven erosion pattern across the width of the test slope. In Tests 1 and 4 the removal of stone was uniform across the width of the test slope.

These tests indicated that the method of laying the riprap was important both for repeatability of identical experiments and for the consistency of all the experimental results. In nature and in a model the aim is to produce a uniform thickness of well mixed stone. This is feasible on a model but very difficult in nature and hence a conflict arises. For controlled experimental work it is desirable to have the uniform thickness of well mixed stone which can be laid and relaid quickly to give repeatable results. This degree of control is not possible on-site and hence the model is not a precise copy of field practice.

A compromise solution was therefore required to give a method of laying a controlled reproducible riprap slope in a short time using methods which reasonably parallel site techniques. The laying procedure finally agreed is given in Appendix 4. It was based principally on Method A (Tests 1 and 4 above) for the following reasons:

1. The damage history curves for method A are reasonably smooth and free from the irregularities which arise from large stones jammed together as in method B.

2. This method gives the most rapid damage and hence the results are likely to be conservative.

3. The jamming of large stones in method B would be difficult to control from test to test and hence less repeatability could be expected.

4. Method A is quicker to lay because it requires no movement of individual stones.

In both method A and B the skip holding the stone was tipped out up the slope. In practice the material is more often tipped into position down slope, hence two trial slopes were built (but not tested in waves) using method A, one with stone tipped up the slope and the other with stone tipped down the slope. Photographs of the finished slopes (Plate 1) show that the appearance of the two slopes is very similar. For the model tests it was agreed to use up slope tipping for the following reasons:

1. Both methods give similar results in terms of the laid bulk density, thickness and appearance. There was therefore no reason to expect any difference in performance.

2. Down slope tipping caused more damage to the filter layer during laying. This was due to the difficulty of controlling the fall of stones from the skip which had to be held higher above the slope than when tipping up the slope.

3. Down slope tipping resulted in stone rolling down the slope on to completed areas and necessitated the reworking of these areas.

4. Handling the skip was likely to be particularly difficult on the steeper slopes so that the problems noted under 1 and 2 would be increased.

Tests 1 and 4 show that with the method A laying procedure good repeatability of identical tests can be achieved. No further tests on repeatability were attempted at that stage. However some repeats occurred between Tests 25-28 of the preliminary series and Tests 33-36 in the main series. A comparison between these sets of tests was made by drawing smooth curves through the data points for each test on the damage history plots and then reading off the number of D^R_{50} sized stones eroded at 1000, 3000 and 5000 waves for each value of $\overline{H}_3$. These values were then plotted as erosion versus $\overline{H}_3/D^R_{50}$ for each number of waves (Fig 27). Figs 26-27 give a measure of the repeatability that can be expected.

Tests 5-7: Effect of significant wave height

Aim

These tests were made to establish the dependence of the rate of erosion upon the significant wave height. For this purpose an attempt was made to choose four wave heights which would cover erosion rates from those giving failure in about 500 waves to those giving small erosion rates leading to stability. Tests 1 and 4 combined were taken as one of these wave heights.

Procedure change

The laying procedure detailed in Appendix 4 (ie Method A) was used for all these and subsequent tests. During the tests the restraint of running in 500 wave steps was relaxed first to 1000 wave steps and then later to 2000 wave steps when the erosion rate was very small. This reduced the number of surveys and hence saved some time. This choice was left to the operator's discretion and could be changed during the test. For a 1000 wave step four records of wave and run-up data were taken such that each record had at least 150 zero crossing run-ups about the water level on the slope. For the 2000 waves step only 4 records were taken in the first 1000 waves. This was to reduce the excessive amount of data which accumulated during the longer tests. For those tests which did not produce a failure a limit of 20 000 waves was set.

Discussion

The damage histories (Table 20) are plotted on Fig 28a and show a strong dependence on the significant wave height. Except for the largest wave height the erosion rate is not linear but reduces with time and increasing damage. At the lowest wave height the erosion is initially fast but becomes very small. The plotted points for this test give an indication that after the initial erosion, which is probably the loss of the smallest stones on the surface, the subsequent erosion occurs in steps rather than gradually. These steps could be the result of the arrival of one or more of the largest waves in the wave train. The general picture is one of relatively rapid erosion of the easily removable material in the upper layer followed by ever reducing erosion rates as the more secure material in the lower layers is attacked.

Tests 8-11: Core permeability

Aim

These tests were made with an impermeable core to show by comparison with Tests 4-7 the effect of core permeability on the erosion rates.

Procedure change

None.

Discussion

The four wave heights used for these tests were nearly the same as those of Tests 4-7 (Table 20) and the resulting damage histories are shown in Fig 28b. For a given wave height the rate of erosion for the impermeable core is greater than for the permeable core and this is particularly so at the intermediate wave heights where the erosion rate is more than twice as great. For Tests 1, 4-7 the failure erosion volumes varied from 60-92 stones and for Tests 8-11 it varied from 72-88 stones. It appears that the influence of core permeability is variable with wave height. At the lowest wave heights the wave run-up is low and hence the flow of water into and out of the core is small. Thus only small changes would be expected. With increasing wave height the effect of permeability on erosion rates and damage limits increase. With further increasing wave height the effect of core permeability on erosion decreases probably due to a limit on the rate at which water can flow into and out of the core.

These tests verify the assumption that an earth embankment, impermeable to waves, gives conservative results.

Tests 12-15: Spectral width

Aim

These tests were made with a narrow spectrum (Fig 2) to establish by comparison with Tests 8-11 the effect of the spectral width parameter on the performance of the riprap.

Procedure changes

None.

Discussion

The damage histories for the four wave heights tested with the spectral width parameter, $\epsilon \sim 0.1$, are plotted on Fig 29a (Tables 20 and 21). A comparison with the results for the Moskowitz spectrum ($\epsilon \sim 0.5$) (Fig 29b) shows that narrow spectra give initially higher rates of erosion. The only test that lasted an appreciable time showed that the final erosion rate was lower for the narrow spectrum as was the absolute damage.

In these tests particularly at the three highest wave heights the movement of the riprap was different from that caused by the Moskowitz spectrum. In the latter the stones moved as individual units even when heavy damage was occurring. With the narrow spectrum the large damaging waves arrived at the beach in groups and produced slides of riprap material down the slope. These slides tended to drag down the filter material which became mixed into the riprap, producing early failure. The failure volumes ranged from 48-92 stones compared with 72-88 for Tests 8-11. More comparisons on spectral width occur below, Tests 21-24.

Tests 16-20: Filter grading

Aim

These tests were made with a coarse grade of filter material (grade 4/30, Fig 19, Table 17) to assess the effect of the filter grading on the performance of the riprap.

Procedure changes

The maximum length of any run was reduced from 20 000 to 15 000 waves with the last 5000 being run continuously and with only one block of combined wave and run-up data being recorded at the beginning of it. For the lowest wave height tested the run could be terminated at 5000 waves or any point after that at the judgement of the operator.

Discussion

The damage histories (Table 21) plotted on Fig 29b compare well with those for Tests 8-11 (Fig 28b). Replotting the data as erosion versus $\bar{H}_3/D_{50}^R$ at 1000, 3000 and 5000 waves (Fig 30) shows that the riprap stability was unaffected by the change of filter material.

The only obvious change is in the volume of erosion at failure. For Tests 8-11 the failure volume ranged from 72-88 stones and for these tests from 105-115 stones. Thus failure as defined by filter material being drawn out through the riprap is delayed by the use of a coarser filter. The filter layer was much more exposed at failure in these tests than in Tests 8-11 with the fine filter.

Tests 21-24: Spectral width and filter grading

Aim

These tests were made with the narrow band spectrum used in Tests 12-15 above. The first object of these tests was to further assess the effect of the spectral width parameter on the performance of the riprap by comparison with Tests 16-20. The second object was to further assess the effect of the filter grade on the performance of the riprap by comparison with Tests 12-15.

Procedure changes

To further reduce the amount of run-up and wave data being collected a limit was imposed from Test 24 onwards such that 16 blocks of data would be recorded in the normal way (ie up to 4000 waves) and thereafter only 1 block of data irrespective of the number of waves in a step.

Discussion

The damage histories (Table 21) are plotted on Fig 31. Comparisons with Tests 16-20 (Fig 29b) are difficult because the wave heights are different. However replotting in terms of $\bar{H}_3/D_{50}^R$ (Fig 32a) shows that the erosion rate was unaffected by spectral width. The failure erosion volumes were increased from 105-115 stones for Tests 16-20 to 115-160 stones for these tests.

A comparison of the damage histories of these tests with Tests 12-15 through the plots of erosion versus $\bar{H}_3/D_{50}^R$ at 1000, 3000 and 5000 waves (Fig 32b) does not reveal any influence of the filter grading upon the erosion rates. This confirms the similar conclusion above from Tests 8-11 and 16-20 made with the Moskowitz spectrum. The failure erosion volume for these tests ranged from 115-160 stones compared with 48-92 stones for Tests 12-15 with the finer filter, again confirming that the coarse filter delays the failure of the slope.

Tests 25-28: Failure criteria

Aim

These tests were made with identical conditions to Tests 16-20 and were to test a new failure criterion which was intended to remove the dependence of failure on the filter grading found above.

Procedure changes

For all the previous tests failure of the slope was defined as occurring when at least one particle of filter material was eroded. This was expected to occur after the erosion of the riprap and the exposure of the filter but in practice the filter was drawn through the riprap before the filter was exposed. The criterion for these tests was that an area of filter of diameter $D_{50}^R/2$ should be clearly visible at a whole number of 500 waves. This was tested with a cylindrical gauge and failure was judged to have occurred when the gauge could be slid through the riprap layer to touch the filter layer without disturbing any riprap material.

A camera was fitted above the riprap slope and a photograph taken of the damaged riprap at the end of each test.

The surface profile of the riprap was more rigorously controlled to attain the required layer thickness of 60 mm.

Discussion

Tests 16-20 and these tests (Table 21) were intended to be repeats in all but failure criteria. However the decision was made to trim the riprap thickness more closely to the nominal 2 D_{50}^R. Hence the value for Tests 16-20 was 66.3 mm as against 60.2 mm for Tests 25-28. The damage histories, Figs 33a, 29b, are difficult to compare directly and are compared in terms of $\bar{H}_3/D_{50}^R$ in Fig 33b. There is possibly a tendency for the thinner riprap to suffer less erosion at higher values of $\bar{H}_3/D_{50}^R$ (cf repeatability tests Fig 27).

However the new failure criterion resulted in a decrease from 105-115 stones (Tests 16-20) to 55-67 stones (Tests 25-28) at failure and hence is more conservative. The new criterion was easy to apply. The old criterion was difficult because a constant watch was required particularly with the finer filters because any particle drawn out on to the surface of the riprap was quickly washed back and could easily be missed. No filter material was seen to be washed out before failure occurred with the new definition.

Plate 8 shows the riprap surface at the end of each of the tests with the exposed filter layer indicated for Tests 25-27 which failed. Note that for Test 28 where erosion appeared to have stopped after 10 000 waves the filter layer cannot be seen.

Tests 29-32: Filter grading

Aim

These tests were made with a very fine filter (grade 5/30) as a further check on the effect of filter grading on the performance of the riprap by comparison with Tests 25-28.

Procedure changes

None.

Discussion

The damage histories (Table 22) for these tests are plotted on Fig 34. A comparison with the results for Tests 25-28 (Fig 33a) shows that Tests 25 and 29 repeat well but that Tests 28 and 32

show some divergence. Unfortunately an undetected fault in the surface profiler produced results for Test 30 which although plotted are very suspect and results for Test 31 which were manifestly wrong. This fault was rectified before Test 32. However in view of the observed filter behaviour Tests 30 and 31 were not repeated.

The fine filter material came out through the riprap layer with ease and tended to migrate down the slope both under and through the riprap. This made testing with the new failure criterion difficult. Plate 9 shows the riprap slopes at the end of each of the four tests. For Tests 29-31 the filter can be seen clearly. In Test 32 the filter emerged freely through the riprap but tended to be washed back again so that the photograph for this test shows only a little filter on the riprap surface.

The tests showed that too fine a filter can be severely damaged by erosion through the riprap and that its use should be avoided. These tests were inconclusive on the influence of filter grading on riprap stability.

Conclusions

The preliminary tests described above were made with one slope, stone size and zero crossing period and thus the conclusions drawn should not be generalized. The following points have emerged from these tests:–

1. The rate of erosion of the riprap is, as expected, strongly dependant upon $\overline{H}_3$.

2. The rate of erosion decreases with time and hence the damage history curves flatten out. At the lower wave heights the curves can become nearly horizontal giving an apparently stable riprap slope.

3. The method of laying the riprap has a significant effect upon the damage history. The laying method adopted and detailed in Appendix 4 gives conservative repeatable results within a scatter which is to be expected with random waves attacking randomly placed stone.

4. Increasing the embankment permeability gives increasing riprap stability. Tests with an impermeable embankment are therefore conservative.

5. The spectral shape as specified by the width parameter, ϵ, does not affect the erosion rates when measured in terms of the number of zero crossing waves although initial erosion rates can be higher at the higher waves heights.

6. The filter grading has no influence on the riprap stability.

7. Filter gradings need to be carefully designed. A filter (grade 4/30, Table 17) with a grading parallel to the riprap and $D^R_{50}/D^F_{50} = 4.5$ was not removed by erosion through the riprap. Filters with flatter gradings had the finer material drawn out through the riprap even when substantially covered.

8. The failure criterion requiring a given area of exposed filter layer was easier to assess than that requiring the observation of the erosion of filter material and gave erosion volumes at failure which were independent of the filter grades used.

9. The measuring techniques and test procedures were viable.

APPENDIX 4

Procedure for laying riprap

The riprap was laid in position on the filter layer in strips across the test flume from the bottom to the top of the slope; each strip being adjusted for level before the next strip was laid. The operators were given the following instructions:

1. Mix the riprap material thoroughly.

2. Fill skip with about 5 kg of mixed material. Try to ensure that each 5 kg load is a representative sample.

3. Tip the contents of the skip in one strip evenly across the leading edge of the riprap already placed.

4. Repeat 2 and 3 above placing the second strip across the leading edge of the first strip.

5. Using the fingers as a rake, pull the material in an upwards direction until the general level is correct when checked by a screed placed across the slope.

NB. During this operation very large stones which are pulled up the slope may be repositioned across the flume if they fall next to a group of very large stones already on the filter.

6. Where obvious 'holes' show in this surface of the riprap after completing 5 above, fill in with stone from the front face of the riprap. Do not be fastidious and waste time.

7. The riprap is correctly laid if all the material fits exactly into the slope length.

This procedure was followed with the following modifications.

1. For the 20 mm riprap grade step 4 above was omitted. Thus one strip at a time was laid and graded.

2. In the early series of tests the riprap slope was laid to the top of the flume to ensure that the maximum run-up was contained on the riprap. The maximum run-up was much less than expected and thus much of the laid riprap was redundant. For the main test programme the riprap slope was laid to a point approximately 250 mm (along the slope) above the expected maximum run-up. When a new grade of riprap was first laid the upper limit was marked on the sides of the flume. The check in step 7 above then became that the relaid riprap should reach these marks.

APPENDIX 5

Wave reflections

Wave reflections are best understood in terms of sine waves. A certain fraction of the energy of a sine wave at normal incidence on a slope is reflected as a sine wave of the same period with a lower height. The reflection coefficient at that period is defined as the reflected wave height divided by the incident wave height.

If irregular waves are regarded as a sum of sine waves at different frequencies (periods) then the reflection coefficients can be calculated (39) for all the frequencies in the incident wave spectrum. Measurements were made with 30 mm D^R_{50} riprap on the 1:2,3,4 and 6 slopes for Moskowitz spectra with $\overline{T}$ = 0.92 s, 1.13 s and 1.30 s over a range of steepnesses $2\pi\overline{H}_3/g\overline{T}^2$ from 0.01–0.046. Over this range of steepness the results for the riprap slopes depend only on frequency and embankment slope. The results show that the reflection coefficient is largely independent of the spectrum and the wave-steepness. Fig 35 shows the results for a wave-steepness value of 0.02 on all slopes in terms of model frequencies. As expected from regular wave results the reflection coefficient increases with slope and wave-length.

The results are presented in model units because of the problem of finding a suitable length scale for converting frequency to prototype values. This is done by dividing the model value of frequency by the square root of the ratio of a typical length dimension in the prototype to the corresponding length dimension in the model (the process is Froudian). This dimension might be D^R_{50} or $\overline{H}_3$ or even the water depth.

Once the frequencies have been scaled to prototype values the reflection coefficients can be used as follows to calculate the reflected wave properties.

The incident wave spectrum must be known and from this $\overline{H}_3$, $\overline{T}$ and ϵ can be determined (see "Conceptual framework"). The reflected wave spectrum can be calculated by multiplying the ordinates of the incident spectrum at each frequency by the square of the reflection coefficient at the appropriate frequency. The reflected $\overline{H}_3$, $\overline{T}$ and ϵ can be calculated from the reflected spectrum as above (see "Conceptual framework"). If the reflection coefficient is more or less constant across the range of frequencies in the spectrum then the above manipulations give the reflected $\overline{H}_3$ as the incident value multiplied by the coefficient (not squared) and leaves $\overline{T}$ and ϵ unchanged.

APPENDIX 6

Test procedure

The complete programme of experimental work involved tests on 4 slopes (1:2,3,4 and 6) with 3 riprap grades on each slope (D_{50}^R = 20, 30 and 40 mm), each grade being subjected to 3 spectra ($\overline{T}$ = 1.3, 1.13 and 0.92 s), with at least 4 wave heights per spectra. The wave heights were chosen as far as possible to cover a spread of damage on each slope from a failure within 5000 waves to negligible damage after 5000 waves.

The following flow chart shows the basic order of both the test programme and each test and indicates where calibrations of instruments and changes in the test parameters were made. The chart is written on the assumption of tests of 5000 wave duration in 1000 wave steps. Some small variations occurred during the programme and these are mentioned at the end of the flow chart.

1. Calibrate riprap profiler. (The calibration did not vary throughout.) Tests for each slope begin here.

2. Set up side cheeks for screeding the slope. Tests for each riprap grade begin here.

3. Screed in the impermeable base for riprap grade to be tested.

4. Mix and lay the appropriate filter material for the riprap grade to be tested, screeding up the slope.

5. Fit appropriate foot to vertical probe of the riprap surface profiler.

6. Survey the filter layer.

7. Mix and lay the riprap material to the instructions given in Appendix 4.

8. Photograph the newly laid riprap.

9. Place the run-up meter in position and calibrate by slowly filling and emptying the flume and noting the water level and data logger reading at appropriate intervals.

10. Set the correct water level in the flume.

11. Take the zero reading of the profiler with the hemispherical foot just touching the water surface.

12. Decide the test conditions ie $\overline{T}$ and $\overline{H}_3$. Tests for each spectrum begin here.

13. Set up the synthesizer for the chosen $\overline{T}$. Tests for each wave height begin here.

14. Set up the initial conditions on the synthesizer. (This ensures that all tests for a given water depth and spectrum start at the same point in the irregular wave train.)

15. Run a 1000 zero crossing waves with $\overline{H}_3/D_{50}^R \simeq 1.0$ to bed in the riprap.

16. Survey riprap slope. (This is the initial riprap survey from which all the damage volumes are calculated for the test.)

17. Lower wave absorbing beach in front of riprap slope to protect the riprap.

18. Calibrate wave probe.

19. Record wave data for calculating the test value of $\overline{H}_3$ using the short sequence length facility of the synthesizer. This value of the wave height remains unchanged until the riprap is rebuilt.

20. Raise wave absorbing beach.

21. Reset synthesizer to long sequence length.

22. Position run-up wire above the riprap slope and note the logger reading for the still water level.

23. Run 1000 zero crossing waves and during the run record 4 blocks of run-up data. (The times used ensured that each block of run-up data had at least 150 zero crossing run-ups about the mean water level on the slope.)

24. Survey the riprap surface.

25. Reset the initial conditions of the synthesizer to the state of the synthesizer at the end of the previous 1000 waves.

26. Repeat 23-25. (This ensures that 8 blocks of run-up data are recorded.)

27. Reset the initial conditions of the synthesizer to the state of the synthesizer at the end of the previous 1000 waves.

28. Run a further 1000 zero crossing waves.

29. Survey the riprap surface.

30. Repeat 27-29 above until 5000 waves have been completed or failure occurs (see "Measurements and procedure").

31. Drain flume.

32. Photograph damaged riprap.

33. Strip out riprap taking care not to unduly disturb the filter layer.

34. Rescreed the filter layer.

35. Mix and relay the riprap material to the instructions given in Appendix 4.

36. Photograph the newly laid riprap.

37. Fill flume to the correct level.

38. Choose a new value for $\overline{H}_3$.

39. Repeat 14-38 above until at least 4 values of $\overline{H}_3$ have been tested.

40. Choose a new value for $\overline{T}$.

41. Repeat 13-40 above until 3 values of $\overline{T}$ have been tested.

42. Choose the next grade of riprap.

43. Repeat 3-42 above until the 3 grades of riprap have been tested.

44. Choose the next slope.

45. Repeat 2-44 above until the 4 slopes have been tested.

Throughout each test a close watch was kept of the riprap to observe the progress of damage, to note if and when failure occurred and to observe if there was any movement of the filter layer material.

Wave reflection measurements were made with the 30 mm riprap in place usually after a test giving negligible damage so that the slope did not have to be specially rebuilt.

During the course of the test programme additional scale tests were made with the different water depths. These were incorporated into the test programme at the most convenient point.

The main modifications to the procedure outlined above occurred when the rate of damage to the riprap was either negligible or large enough to produce failure before 5000 waves. With negligible damage rates the test was run for the first 1000 waves as above and then completed in two steps of 2000 waves each. When the rate of damage was rapid the test was run in steps of 500 waves with two blocks of run-up data being recorded per 500 waves. In some cases failure occurred before 2000 waves and the required 8 blocks of run-up data were not obtained.

TABLES

TABLE 1

Variable list

		ABSOLUTE	DIMENSIONLESS
Slope	a	1 : 2, 3, 4, 6	1 : 2,3,4,6
Filter thickness	t_F	10,15,20 mm	t_F/D^R_{50} = 0.5
Filter bulk density	ρ^B_F	1666 kg/m^3	ρ^B_F/ρ_R = 0.62
Filter grades	D^F_{50}	4.5, 6.6, 8.9 mm	D^R_{15}/D^F_{85} = 2.0
		See Appendix 2 for detailed gradings	D^R_{50}/D^F_{50} = 4.5
			D^R_{15}/D^F_{15} = 4.5
Riprap placing		See Appendix 4	Method A
Riprap bulk density	ρ^B_R	1490 kg/m^3	ρ^B_R/ρ_R = 0.55
Riprap bulk density as laid	ρ^{BL}_R	1300 kg/m^3	ρ^{BL}_R/ρ_R = 0.48
Riprap shape		See Appendix 2 and Figs 20-23	
Riprap size	D^R_{50}	20, 30, 40 mm	D^R_{85}/D^R_{50} = 1.5
			D^R_{15}/D^R_{50} = 0.67
Riprap density	ρ_R	2700 kg/m^3	ρ_R/ρ = 2.70
Riprap thickness	t_R	40, 60, 80 mm	t_R/D^R_{50} = 2.0
Spectral width	ϵ	0.5	ϵ = 0.5
Number of waves	$\bar{N}$	5000 (MAX)	$\bar{N}$ = 5000 (MAX)
Significant wave height	$\bar{H}_3$	23.1–121.7 mm	$\bar{H}_3/D^R_{50}$ = 1.0–5.88
Mean zero crossing wave period	$\bar{T}$	0.92, 1.13, 1.30 s	$2\pi D^R_{50}/g\bar{T}^2$ = 0.0076–0.0303
Depth	d	0.61 m	$2\pi d/g\bar{T}^2$ = 0.23–0.46
Density of water	ρ	1000 kg/m^3	$\rho\bar{H}_3/D^R_{50}/\mu\bar{T}$ = 322–3293
Dynamic viscosity	μ	1.137 x 10^{-3} kg/ms	

TABLE 2

Range of parameters for main test programme

SLOPE 1 : –	D_{50}^R (mm)	$\bar{T}$ (Nominal) (s)	$\bar{H}_3$ (Range tested) (mm)	$\bar{H}_3/D_{50}^R$ (Range tested)	$\frac{2\pi D_{50}^R}{g\bar{T}^2}$	TEST NUMBERS
2	20	1.3	23.1 – 42.6	1.16 – 2.13	0.0076	69 – 72
		1.13	28.7 – 48.2	1.44 – 2.39	0.0100	73 – 77
		0.92	28.4 – 52.7	1.42 – 2.64	0.0152	78 – 81
	30	1.3	29.9 – 67.7	1.00 – 2.26	0.0114	86 – 89
		1.13	30.1 – 74.8	1.00 – 2.49	0.0152	90 – 94
		0.92	35.6 – 76.9	1.19 – 2.56	0.0227	94 – 97
	40	1.3	52.7 – 93.4	1.32 – 2.34	0.0152	98 – 101
		1.13	69.1 – 90.3	1.73 – 2.26	0.0201	102 – 104
		0.92	64.4 – 87.9	1.61 – 2.20	0.0303	105 – 107
3	20	1.3	37.5 – 65.9	1.88 – 3.30	0.0076	49 – 53
		1.13	35.5 – 74.5	1.78 – 3.73	0.0100	54 – 57
		0.92	31.2 – 71.7	1.56 – 3.59	0.0152	58 – 61
	30	1.3	54.3 – 92.4	1.81 – 3.08	0.0114	33 – 36
		1.13	55.0 – 100.5	1.83 – 3.35	0.0152	37 – 40
		0.92	51.0 – 84.7	1.70 – 2.82	0.0227	41 – 46
	40	1.3	58.7 – 88.9	1.47 – 2.22	0.0152	62 – 64
		1.13	56.7 – 82.1	1.42 – 2.05	0.0201	65, 66
		0.92	51.6	1.29	0.0303	67
4	20	1.3	53.2 – 80.9	2.66 – 4.05	0.0076	117 – 119
		1.13	53.7 – 85.5	2.69 – 4.28	0.0100	120 – 123
		0.92	56.8 – 71.3	2.84 – 3.57	0.0152	124 – 127
	30	1.3	45.2 – 99.8	1.51 – 3.33	0.0114	128 – 131
		1.13	45.5 – 88.5	1.52 – 2.95	0.0152	132 – 135
		0.92	51.2 – 72.7	1.71 – 2.42	0.0227	137 – 140
	40	1.3	69.5 – 121.7	1.74 – 3.04	0.0152	170 – 173
6	20	1.3	40.5 – 117.6	2.03 – 5.88	0.0076	141 – 145
		1.13	48.6 – 90.5	2.43 – 4.53	0.0100	146 – 149
		0.92	46.8 – 70.6	2.34 – 3.53	0.0152	150 – 152
	30	1.3	41.9 – 109.2	1.40 – 3.64	0.0114	153 – 156, 163
		1.13	55.3 – 90.9	1.84 – 3.03	0.0152	157 – 160, 164
		0.92	51.9 – 78.2	1.73 – 2.61	0.0227	161 – 162, 165

d = 610 mm for all tests

$\bar{N}$ = 5000 maximum

TABLE 3

Range of parameters for scale tests

SLOPE 1 : –	D_{50}^{R} (mm)	$\overline{T}$ (Nominal) (s)	d (mm)	$\overline{H}_3$ (Range tested) (mm)	$\overline{H}_3/D_{50}$ (Range tested)	$\rho\overline{H}_3 D_{50}^{R}/\mu\overline{T}$ (Range tested)	TEST NUMBERS
2	40	1.3	610	52.7 – 93.4	1.32 – 2.34	1426 – 2528	82 – 85
	20	0.92	305	20.8 – 47.4	1.04 – 2.37	398 – 906	98 – 101
3	40	1.3	610	58.7 – 88.9	1.47 – 2.22	1589 – 2406	62 – 64
	30	1.13	461	74.0 – 87.7	2.47 – 2.93	1727 – 2047	113 – 116
	20	0.92	305	45.0 – 63.0	2.25 – 3.15	860 – 1204	108 – 112
4	40	1.3	610	69.5 – 121.7	1.74 – 3.04	1880 – 3293	170 – 173
	20	0.92	305	38.5 – 60.8	1.93 – 3.04	736 – 1162	166 – 169

$2\pi d/g\overline{T}^2 = 0.231, 0.306, 0.462$

$2\pi D_R^{50}/g\overline{T}^2 = 0.0152$ } For all tests.

$\overline{N}$ = 5000 Maximum }

TABLE 4

Experimental data for 1:2 slope, 20 mm D_{50}^{R}

TEST NO	69	70	71	72	73	74	75	76	77	78	79	80	81	82	83	84	85
$\bar{H}_3$ (mm)	33.6	42.6	23.2	38.3	37.6	47.7	48.2	32.8	28.7	46.8	52.7	38.0	28.4	41.6	31.0	20.8	47.4
$\bar{T}$ (s)	1.31	1.31	1.31	1.31	1.15	1.15	1.15	1.16	1.15	0.96	0.98	0.95	0.96	0.99	1.00	1.00	0.99
ϵ	0.50	0.50	0.50	0.49	0.49	0.50	0.49	0.49	0.49	0.48	0.48	0.49	0.50	0.47	0.46	0.46	0.48
d (mm)	610	610	610	610	610	610	610	610	610	610	610	610	610	305	305	305	305
BEDDING IN $\bar{H}_3$ (mm)	14.9	15.2	12.8	11.4	12.8	14.5	14.5	15.4	17.6	17.6	15.5	16.6	19.3	10.4	11.3	13.8	15.4
D_{50}^{R} (mm)	20	20	20	20	20	20	20	20	20	20	20	20	20	20	20	20	20
INITIAL t_R (mm)	46.0	43.7	42.4	40.7	43.5	43.6	43.1	47.7	41.8	42.8	39.6	40.3	41.2	40.2	41.1	45.6	42.4
WATER TEMP. °C	10.0	10.0	9.3	10.0	9.3	9.0	9.5	9.5	10.0	10.2	10.0	10.5	10.3	6.3	–	–	5.0
N_Δ – NO OF WAVES																	
500											24.0						
1000	9.9	27.3	2.0	13.1	16.0	33.1	46.2	11.6	1.1	18.1		15.0	2.6	13.2	4.2	0.9	38.6
1500											65.0*						
2000	10.0	44.1	2.4	12.3	25.7	30.3*	71.4	16.9	4.3	20.4		22.0	4.6	22.7	6.6	1.3	47.1
2500																	
3000	12.3	59.0*	1.5	15.6	26.2		89.4*	22.2	4.4	20.5		26.4	5.2	32.3	11.0	1.3	49.7
3500																	
4000	11.2		0.9	25.9	42.3			23.4	5.3	38.2		30.3	5.0	45.1	14.2	5.5	51.6
4500																	
5000	15.6		1.3	25.7	44.0			(LOST)	7.3	42.4		32.6	(LOST)	51.0*	16.6	3.7	57.8

* RIPRAP FAILED

TABLE 5

Experimental data for 1:2 slope, 30 mm D_{50}^R

TEST NO	86	87	88	89	90	91	92	93	94	95	96	97
$\bar{H}_3$ (mm)	60.9	29.9	67.7	42.5	74.8	64.4	45.7	30.1	76.9	64.4	52.7	35.6
$\bar{T}$ (s)	1.31	1.31	1.31	1.30	1.16	1.15	1.15	1.15	1.04	1.01	0.97	0.94
ϵ	0.50	0.51	0.51	0.51	0.50	0.50	0.49	0.49	0.43	0.46	0.48	0.50
d (mm)	610	610	610	610	610	610	610	610	610	610	610	610
BEDDING IN $\bar{H}_3$ (mm)	21.3	24.4	27.4	27.8	26.8	24.0	20.7	17.2	26.1	26.1	26.1	26.1
D_{50}^R (mm)	30	30	30	30	30	30	30	30	30	30	30	30
INITIAL t_R (mm)	59.6	57.8	56.9	58.4	58.0	59.6	58.9	60.8	61.7	56.8	59.3	59.8
WATER TEMP °C	5.7		6.2	6.6	6.2	5.6	6.4	7.4		5.7		6.2
N_Δ – NO OF WAVES												
500												
1000	22.7	0.1	34.9	0.6	27.6	25.0	4.2	0.2	36.2	13.3	5.8	3.1
1500												
2000	37.9	0.0	44.7	1.1	45.4	26.8	13.6	1.6	52.7	23.1	4.7	3.7
2500												
3000	46.9	1.2	59.9	6.2	56.8*	35.5	20.6	4.2	73.1	24.3	6.1	3.8
3500												
4000	48.7	0.4	63.0	6.3		48.1	24.4	4.1	84.9	29.1	5.1	3.9
4500												
5000	55.1	0.2	73.4*	12.5		50.6	24.4	6.7	88.2*	32.1	6.1	3.3

* RIPRAP FAILED

TABLE 6

Experimental data for 1:2 slope, 40 mm D_{50}^{R}

TEST NO	98	99	100	101	102	103	104	105	106	107
$\bar{H}_3$ (mm)	93.4	76.0	72.2	52.7	90.3	79.9	69.1	87.9	78.2	64.4
$\bar{T}$ (s)	1.31	1.31	1.31	1.31	1.20	1.19	1.19	1.07	1.04	1.00
ϵ	0.51	0.50	0.50	0.50	0.48	0.48	0.48	0.42	0.44	0.46
d (mm)	610	610	610	610	610	610	610	610	610	610
BEDDING IN $\bar{H}_3$ (mm)	31.4	31.4	31.4	31.4	33.8	33.8	33.8	31.8	31.8	31.8
D_{50}^{R} (mm)	40	40	40	40	40	40	40	40	40	40
INITIAL t_R (mm)	79.6	78.4	82.0	79.2	79.9	81.6	83.3	81.3	77.6	81.2
WATER TEMP °C			6.8	7.0		8.0	8.3	8.1	8.2	7.8
N_Δ – NO OF WAVES										
500										
1000	25.0	5.2	8.1	0.8	11.5	10.7	4.8	10.4	6.7	1.3
1500										
2000	36.9	11.2	10.4		20.2	10.6	4.7	20.3	10.7	1.6
2500										
3000	46.5	13.8	11.5	2.6	28.1	13.1	6.6	31.6	10.8	1.1
3500										
4000	55.3*	14.5	12.2		36.7	14.7	10.1	35.8	17.1	1.8
4500										
5000		15.8	12.1	1.9	40.1	14.7	11.4	38.6	18.0	1.9

* RIPRAP FAILED

TABLE 7

Experimental data for 1:3 slope, 20 mm D_{50}^{R}

TEST NO	49	50	51	52	53	54	55	56	57	58	59	60	61	108	109	110	111	112
$\overline{H}_3$ (mm)	37.5	44.0	52.4	57.8	65.9	74.5	54.7	35.5	65.4	71.7	31.2	55.4	60.4	59.3	52.3	45.0	55.8	63.0
$\overline{T}$ (s)	1.30	1.30	1.31	1.29	1.29	1.14	1.13	1.13	1.13	1.01	0.92	0.95	0.98	0.99	0.99	0.97	0.99	1.01
ϵ	0.51	0.51	0.51	0.51	0.51	0.48	0.50	0.50	0.51	0.44	0.48	0.49	0.46	0.50	0.50	0.50	0.50	0.50
d (mm)	610	610	610	610	610	610	610	610	610	610	610	610	610	305	305	305	305	305
BEDDING IN $\overline{H}_3$ (mm)	25.0	25.0	25.0	25.0	25.0	22.0	20.0	20.0	18.0	20.0	20.0	22.0	24.0	16.0	16.0	16.0	16.0	16.0
D_{50}^{R} (mm)	20	20	20	20	20	20	20	20	20	20	20	20	20	20	20	20	20	20
INITIAL t_R (mm)	38.0	35.9	41.6	41.1	41.3	38.9	39.2	40.1	41.5	42.1	42.4	42.1	43.4	44.6	43.0	43.0	42.6	42.9
WATER TEMP °C	16.6	17.9			20.0	20.0	20.0	18.8	18.5	18.0	19.0	17.4	17.3	4.0	7.0	8.2		7.9
N_Δ – NO OF WAVES																		
500			21.1	22.0	44.4	65.5	5.9		28.0	30.2		8.9	12.5					
1000	4.1	21.6	33.3	48.3	100.0*	77.1	22.5	11.4	60.1	48.6	8.8	19.1	24.5	23.6	16.2	9.6	19.1	53.8
1500				51.2		111.1*			70.0	65.8								
2000	9.1	25.9	37.2	70.0			25.2	6.1	85.3*	66.0	4.9	23.4	39.0	31.5	23.2	16.3	34.0	76.2
2500																		
3000	20.2	33.0	55.6	71.0*			44.4	10.2		87.4*	13.7	24.7	48.8	48.3	34.2	21.4	43.3	108.2
3500																		
4000	18.0	34.3	62.6				43.5	8.4			12.3	28.3	50.9	70.1	46.3	21.2	57.5	119.4
4500																		
5000	18.7	46.1	73.7				50.7	9.3			12.0	19.8	63.8	73.2	47.6	19.8	56.4	119.5

* RIPRAP FAILED

TABLE 8

Experimental data for 1:3 slope, 30 mm D_{50}^{R}

TEST NO	33	34	35	36	37	38	39	40	41	42	43	44	46	113	114	115	116
$\bar{H}_3$ (mm)	54.3	82.9	92.4	70.3	55.0	89.0	100.5	78.8	51.0	73.5	84.7	54.7	70.3	84.0	79.6	74.0	87.7
$\bar{T}$ (s)	1.29	1.31	1.32	1.31	1.13	1.18	1.21	1.16	0.96	1.03	1.06	0.95	1.04	1.18	1.17	1.20	1.18
ϵ	0.52	0.52	0.52	0.51	0.52	0.50	0.49	0.50	0.50	0.46	0.45	0.50	0.45	0.50	0.50	0.46	0.50
d (mm)	610	610	610	610	610	610	610	610	610	610	610	610	610	461	461	461	461
BEDDING IN $\bar{H}_3$ (mm)	40.0	40.0	40.0	40.0	40.0	35.0	35.0	35.0	30.0	30.0	30.0	30.0	30.0	38.6	38.6	38.6	38.6
D_{50}^{R} (mm)	30	30	30	30	30	30	30	30	30	30	30	30	30	30	30	30	30
INITIAL t_R (mm)	59.9	57.9	55.3	56.0	60.7	62.5	60.9	60.4	63.4	62.7	63.1	65.4	63.6	64.5	62.9	63.9	62.4
WATER TEMP °C	12.3	13.3	15.2	14.7	17.4	18.5		17.8	18.8	19.1	19.3	19.0	18.7	7.7	7.3	7.0	6.8
N_Δ – NO OF WAVES																	
500		28.3	54.0			25.1	39.7				11.2						
1000	9.2	45.0	81.0	10.4	5.2	48.3	52.5	11.7	7.4	7.7	18.3	5.3	8.6	15.0	14.8	14.2	22.7
1500		46.6	84.0			54.2	69.8										
2000	9.3	53.6	86.0	15.5	6.4	58.5	81.2*	21.3	9.1	8.2	26.3	7.1	11.4	27.3	22.5	17.1	35.3
2500		55.8	87.0														
3000	12.6	65.8	98.0*	22.0	10.5	78.1		27.9	13.0	9.3	29.9	7.2	13.7	45.6	30.0	32.0	49.3
3500																	
4000	14.8	75.2*		26.8	8.8	81.9		35.2	12.8	11.9	41.3	9.3	21.0	49.9	35.2	32.3	69.5
4500																	
5000	13.4			28.6	11.1	91.7		27.9	14.2	11.0	43.2	13.8	22.2	51.5	38.3	33.1	75.7

* RIPRAP FAILED

TABLE 9

Experimental data for 1:3 slope, 40 mm D_{50}^{R}

TEST NO	62	63	64	65	66	67
$\overline{H}_3$ (mm)	58.7	88.9	61.3	82.1	56.7	51.6
$\overline{T}$ (s)	1.30	1.31	1.31	1.17	1.16	0.96
ϵ	0.51	0.50	0.50	0.49	0.49	0.48
d (mm)	610	610	610	610	610	610
BEDDING IN $\overline{H}_3$ (mm)	40.0	38.0	41.0	36.0	40.7	40.0
D_{50}^{R} (mm)	40	40	40	40	40	40
INITIAL t_R (mm)	85.1	81.0	78.5	82.2	81.2	80.5
WATER TEMP °C	13.4	13.7	13.0	12.0	12.7	13.8
N_Δ – NO OF WAVES						
500						
1000	0.6	11.6	4.3	8.0	1.1	3.6
1500						
2000	1.8	10.8	7.8	12.7	1.6	4.0
2500						
3000	2.3	15.3	7.6	9.8	2.4	5.5
3500						
4000	4.9	15.2	7.7	15.3	1.6	6.0
4500						
5000	2.7	19.0	6.8	15.4	1.7	5.8

TABLE 10

Experimental data for 1:4 slope, 20 mm D_{50}^{R}

TEST NO	117	118	119	120	121	122	123	124	125	126	127	166	167	168	169
$\overline{H}_3$ (mm)	62.8	71.3	56.8	61.5	73.0	85.5	53.7	60.1	71.2	53.2	80.9	60.8	53.4	46.4	38.5
$\overline{T}$ (s)	1.00	1.02	0.98	1.14	1.15	1.17	1.14	1.31	1.31	1.31	1.31	1.01	0.99	0.99	0.98
ϵ	0.46	0.45	0.47	0.51	0.50	0.49	0.50	0.51	0.51	0.51	0.51	0.48	0.48	0.48	0.48
d (mm)	610	610	610	610	610	610	610	610	610	610	610	305	305	305	305
BEDDING IN $\overline{H}_3$ (mm)	21.0	21.0	21.0	20.2	20.2	20.2	20.2	19.5	19.5	19.5	19.5	20.9	20.9	20.9	20.9
D_{50}^{R} (mm)	20	20	20	20	20	20	20	20	20	20	20	20	20	20	20
INITIAL t_R (mm)	44.2	41.4	44.6	43.1	42.2	43.8	42.7	41.8	45.3	42.7	42.0	37.1	39.6	43.3	43.6
WATER TEMP °C	6.4	8.3		9.5	10.6	11.0	12.4	10.5	10.5		10.1	16.5	16.6	17.5	17.7
N_Δ – NO OF WAVES															
500															
1000	17.6	30.6	10.7	19.1	24.7	56.7	16.0	25.6	47.0	14.4	47.4	8.8	7.5	3.2	2.5
1500															
2000	22.9	46.4	14.0	25.8	30.2	93.6	18.8	32.3	63.6	15.3	85.5	11.6	7.8	5.2	
2500															
3000	21.6	50.7	18.7	29.4	51.6	106.0	24.3	40.8	86.7	18.4	106.9	13.9	13.2	6.2	2.4
3500															
4000	29.9	54.7	22.4	35.1	57.6	122.1	33.0	51.0	104.9	17.8	127.5	24.4	16.5	8.2	
4500															
5000	28.4	59.5	17.2	37.3	61.0	129.7	27.0	50.1	119.7	20.7	145.2	20.4	17.1	10.4	3.3

TABLE 11

Experimental data for 1:4 slope, 30 mm D_{50}^{R}

TEST NO	128	129	130	131	132	133	134	135	137	138	139	140
$\bar{H}_3$ (mm)	99.8	84.3	70.3	59.7	88.5	77.7	62.4	45.5	72.7	61.1	51.2	45.2
$\bar{T}$ (s)	1.32	1.32	1.31	1.31	1.17	1.15	1.14	1.14	1.01	0.99	0.96	1.31
ϵ	0.51	0.51	0.51	0.50	0.49	0.50	0.50	0.50	0.47	0.47	0.48	0.51
d (mm)	610	610	610	610	610	610	610	610	610	610	610	610
BEDDING IN $\bar{H}_3$ (mm)	29.3	29.3	29.3	29.3	28.1	28.1	28.1	28.1	28.1	28.1	28.1	29.3
D_{50}^{R} (mm)	30	30	30	30	30	30	30	30	30	30	30	30
INITIAL t_R (mm)	64.0	62.3	64.4	63.1	62.4	63.3	64.9	65.4	63.5	64.8	63.8	63.4
WATER TEMP °C	10.5	10.1	10.5	10.5		12.0	13.6	15.0	15.3	14.4	13.8	13.7
N_Δ – NO OF WAVES												
500												
1000	31.9	9.8	7.0	3.6	11.2	8.3	8.1	0.8	4.0	4.7	0.4	0.5
1500												
2000	32.5	15.2	5.3	5.2	14.3	13.1	9.6	0.5		8.0		
2500												
3000	37.7	21.6	7.8	5.8	22.3	17.7	11.0	0.2	8.9	7.7	0.6	0.6
3500												
4000	41.8	22.7	11.9	6.7	29.7	24.3	10.0	0.6		10.0		
4500												
5000	44.9	27.9	11.9	5.4	30.0	22.3	10.7	0.8	7.5	12.5	0.9	0.7

TABLE 12

Experimental data for 1:4 slope, 40 mm D_{50}^{R}

TEST NO	170	171	172	173
$\bar{H}_3$ (mm)	121.7	104.5	90.2	69.5
$\bar{T}$ (s)	1.35	1.32	1.31	1.28
ϵ	0.50	0.51	0.51	0.48
d (mm)	610	610	610	610
BEDDING IN $\bar{H}_3$ (mm)	41.7	41.7	41.7	41.7
D_{50}^{R} (mm)	40	40	40	40
INITIAL t_R (mm)	80.6	78.9	78.2	79.8
WATER TEMP °C	17.5	17.0	15.5	15.2
N_Δ – NO OF WAVES				
500				
1000	21.3	9.0	6.4	3.0
1500				
2000	27.2	14.2	6.0	
2500				
3000	32.5	16.4	8.0	2.2
3500				
4000	38.3	23.3	9.2	
4500				
5000	45.1	24.2	7.4	2.3

TABLE 13

Experimental data for 1:6 slope, 20 mm D_{50}^{R}

TEST NO	141	142	143	144	145	146	147	148	149	150	151	152
$\bar{H}_3$ (mm)	117.6	83.1	62.0	102.6	40.5	90.5	75.5	64.9	48.6	70.6	62.1	46.8
$\bar{T}$ (s)	1.34	1.31	1.30	1.32	1.31	1.18	1.15	1.14	1.14	1.03	0.99	0.95
ϵ	0.50	0.51	0.51	0.51	0.51	0.49	0.50	0.51	0.50	0.45	0.47	0.49
d (mm)	610	610	610	610	610	610	610	610	610	610	610	610
BEDDING IN $\bar{H}_3$ (mm)	20.0	20.0	20.0	20.0	20.0	28.0	28.0	28.0	28.0	20.6	20.6	20.6
D_{50}^{R} (mm)	20	20	20	20	20	20	20	20	20	20	20	20
INITIAL t_R (mm)	41.3	41.6	43.0	40.4	40.6	42.9	43.1	39.2	37.8	38.5	38.6	38.9
WATER TEMP °C	14.0	14.0	15.1	16.0	17.2	17.5	18.0	17.4	17.0	16.2	15.6	15.0
N_Δ – NO OF WAVES												
500												
1000	63.6	12.2	14.9	24.0	7.9	25.2	32.3	14.5	7.8	9.6	13.3	9.7
1500												
2000	82.9	20.8	21.9	47.8		38.7	29.0	19.5	7.4	11.7	9.6	
2500												
3000	89.0	25.5	18.7	59.5	12.4	42.4	32.0	20.0	5.2	15.9	12.5	13.2
3500												
4000	118.3	28.6	21.4	77.4		53.2	37.7	21.4		21.2	27.2	
4500												
5000	107.3	37.5	26.9	99.2	8.1	63.5	47.1	22.8	4.7	20.1	22.0	0.5

TABLE 14

Experimental data for 1:6 slope, 30 mm D_{50}^R

TEST NO	153	154	155	156	157	158	159	160	161	162	163	164	165
$\bar{H}_3$ (mm)	109.2	78.9	53.6	81.4	90.5	90.9	80.3	62.1	78.2	62.9	41.9	55.3	51.9
$\bar{T}$ (s)	1.33	1.31	1.30	1.31	1.19	1.18	1.16	1.14	1.04	1.00	1.30	1.14	0.96
e	0.51	0.51	0.51	0.51	0.46	0.49	0.50	0.50	0.43	0.46	0.51	0.51	0.48
d (mm)	610	610	610	610	610	610	610	610	610	610	610	610	610
BEDDING IN $\bar{H}_3$ (mm)	19.9	19.9	19.9	19.9	27.5	27.5	27.5	27.5	30.4	30.4	19.9	27.5	30.4
D_{50}^R (mm)	30	30	30	30	30	30	30	30	30	30	30	30	30
INITIAL t_R (mm)	59.5	56.2	60.3	61.9	60.4	61.5	62.2	64.3	63.5	64.2	62.4	59.4	61.6
WATER TEMP °C		17.5			16.0		15.8	16.5	17.9	18.0	18.0	17.8	18.2
N_Δ – NO OF WAVES													
500													
1000	11.5		2.0	6.4	9.1	8.3	5.0	2.1	2.9	1.6	0.7	1.9	2.1
1500													
2000	16.1		3.5	8.7	11.6	9.3	6.5		4.0	2.5			
2500		U/S											
3000	20.3		6.4	10.3	11.4	8.5	4.7	3.5	5.0	3.8	2.4	2.9	1.7
3500													
4000	27.5		6.6	8.8	12.6	11.9	5.4		5.0	3.5			
4500													
5000	48.6		8.0	9.5	13.4	9.7	5.8	5.1	5.7	3.6	2.7	2.8	2.3

TABLE 15

Failure conditions

SLOPE I : —	TEST NO	D_{50}^{R} (mm)	$\bar{H}_3$ (mm)	$\bar{T}$ (s)	d (mm)	$\bar{N}$	N_Δ	t_R^{MIN} (mm)	t_R^{MIN}/D_{50}^{R}
2	70	20	42.6	1.31	610	3000	59.0	27.5	1.38
	74	20	47.7	1.15	610	2000	30.3	29.5	1.48
	75	20	48.2	1.15	610	3000	89.4	22.2	1.11
	79	20	52.7	0.98	610	1500	65.0	22.6	1.13
	82	20	41.6	0.99	305	5000	51.0	23.1	1.16
	88	30	67.7	1.31	610	5000	73.4	28.1	0.94
	90	30	74.8	1.16	610	3000	56.8	28.9	0.96
	94	30	76.9	1.04	610	5000	88.2	27.0	0.90
	98	40	93.4	1.31	610	4000	55.3	42.4	1.06
	OVERALL MEAN AND STANDARD DEVIATION						63.2 ± 18.6		1.12 ± 0.20
3	34	30	82.9	1.31	610	4000	75.2	35.6	1.19
	35	30	92.4	1.32	610	3000	98.0	24.9	0.83
	39	30	100.5	1.21	610	2000	81.2	32.3	1.08
	52	20	57.8	1.29	610	3000	71.0	26.2	1.31
	53	20	65.9	1.29	610	1000	100.0	22.9	1.15
	54	20	74.5	1.14	610	1500	111.1	22.0	1.10
	57	20	65.4	1.13	610	2000	85.3	21.4	1.07
	58	20	71.7	1.01	610	3000	87.4	25.6	1.28
	OVERALL MEAN AND STANDARD DEVIATION						88.7 ± 13.5		1.13 ± 0.15

TABLE 16

Design criteria

Criterion A: $\bar{H}_3/D^R_{50}$ **for no damage**

MEAN NO OF WAVES	1:2 SLOPE	1:3 SLOPE	1:4 SLOPE	1:6 SLOPE
1000	1.0	1.0	1.5	1.3
2000	1.0	1.0	1.5	1.2
3000	0.8	1.0	1.5	1.2
4000	0.8	1.0	1.4	1.2
5000	0.8	1.0	1.4	1.0

Criterion B: $\bar{H}_3/D^R_{50}$ **for 9** D^R_{50} **sized stones eroded**

1000	1.9	2.2	2.7	3.2
2000	1.7	1.8	2.3	2.7
3000	1.6	1.7	2.3	2.6
4000	1.6	1.6	2.2	2.5
5000	1.6	1.6	2.2	2.3
Damage as % of damage at failure	14%	10%	8%*	5%*

Criterion C: $\bar{H}_3/D^R_{50}$ **at 15% of damage at failure**

1000	1.9	2.4	3.1	4.5
2000	1.7	2.0	2.7	3.8
3000	1.6	2.0	2.6	3.6
4000	1.6	1.8	2.5	3.5
5000	1.6	1.8	2.5	3.4
N_Δ at 15% of damage at failure (to nearest whole number)	9	13	17*	25*

Criterion D: $\bar{H}_3/D^R_{50}$ **at failure (100% damage)**

1000	2.6	3.5	4.8*	7.8*
2000	2.5	3.4	4.5*	7.6*
3000	2.4	3.3	4.1*	7.6*
4000	2.3	3.1	4.0*	6.9*
5000	2.3	3.0	4.0*	6.5*
N_Δ at failure	63	86	114*	168*

* estimated

TABLE 17

Mixing details for riprap and filter grades

RIPRAP

STONE SIZE (mm)	% OF TOTAL BY WEIGHT		
	D_{50}^{R} = 20 mm	D_{50}^{R} = 30 mm	D_{50}^{R} = 40 mm
76.2 – 63.4			9.0
63.4 – 57.0			9.9
57.0 – 50.8		2.5	10.6
50.8 – 44.4		12.7	11.5
44.4 – 38.1		14.3	13.0
38.1 – 31.8	10.0	16.1	16.0
31.8 – 25.4	20.0	18.4	19.3
25.4 – 22.1	11.5	12.6	10.7
22.1 – 19.2	11.5	13.2	
19.2 – 16.0	18.5	10.2	
16.0 – 12.7	18.5		
12.7 – 11.1	10.0		
BULK DENSITY kg/m³	1510	1480	1480

FILTER

STONE SIZE (mm)	% OF TOTAL BY WEIGHT				
	GRADE				
	5/30	2	4/20	4/30	4/40
19.2 – 12.7					20
12.7 – 7.9		5		36	40
7.9 – 4.8	6	25	44	44	40
4.8 – 2.8	30	25	46	20	
2.8 – 1.7	29	27	10		
1.7 – 0.92	35	18			
BULK DENSITY kg/m³	1614	1633	1687	1632	1679

TABLE 18

Relationship between sieve size and weight

SIEVE SIZE (mm)	NO OF STONES IN SAMPLE	WEIGHT OF SAMPLE (g)	AVERAGE WEIGHT OF A STONE (g)	$W_R^{1/3}/\gamma_R^{1/3}D^R$
76.2 – 63.4	25	9765	390.6	0.75
63.4 – 57.0	25	7170	286.8	0.79
57.0 – 50.8	25	5200	208.0	0.79
50.8 – 44.4	50	8080	160.2	0.82
44.4 – 38.1	50	5320	106.4	0.83
38.1 – 31.8	50	3430	68.6	0.84
31.8 – 25.4	50	1765	35.3	0.83
25.4 – 22.1	50	1065	21.3	0.84
22.1 – 19.2	100	1340	13.4	0.83
19.2 – 16.0	100	850	8.5	0.83
16.0 – 12.7	200	900	4.5	0.83
12.7 – 11.1	200	560	2.8	0.85
			MEAN	0.82

TABLE 19

Summary of preliminary tests

TEST NO	EMBANKMENT	FILTER GRADE	SPECTRUM WITH $\bar{T}$ = 1.30 s	NOMINAL $\bar{H}_3$ (mm)	MEASURED $\bar{T}$ (s)	MEASURED $\bar{H}_3$ (mm)
1	PERMEABLE	2	MOSKOWITZ	92	1.38	90.4
2	"	"	"	"	1.39	96.9
3	"	"	"	"	1.38	91.8
4	"	"	"	"	1.36	90.5
5	"	"	"	140	1.34	129.9
6	"	"	"	80	1.37	79.9
7	"	"	"	60	1.36	58.8
8	IMPERMEABLE	2	MOSKOWITZ	92	1.35	88.7
9	"	"	"	140	1.34	127.9
10	"	"	"	80	1.36	79.0
11	"	"	"	60	1.35	59.4
12	"	2	NARROW	92	1.35	91.7
13	"	"	"	140	1.38	131.8
14	"	"	"	80	1.33	76.3
15	"	"	"	60	1.32	61.0
16	"	4/30	MOSKOWITZ	92	1.34	84.6
17	"	"	"	132	1.37	124.6
18	"	"	"	73	1.34	69.8
19	"	"	"	79	1.34	76.9
20	"	"	"	53	1.34	52.8
21	"	4/30	NARROW	92	1.33	90.8
22	"	"	"	132	1.35	136.8
23	"	"	"	79	1.32	80.8
24	"	"	"	73	1.33	73.4
25	"	4/30	MOSKOWITZ	92	1.30	90.3
26	"	"	"	79	1.30	80.8
27	"	"	"	73	1.29	71.2
28	"	"	"	53	1.30	53.9
29	"	5/30	MOSKOWITZ	92	1.31	90.7
30	"	"	"	79	1.30	77.4
31	"	"	"	73	1.30	70.6
32	"	"	"	53	1.30	53.2

TABLE 20

Experimental data from preliminary tests

TEST NO	1	2	3	4	5	6	7	8	9	10	11	12	13	14
$\bar{H}_3$ (mm)	90.4	96.9	91.8	90.5	129.9	79.9	58.8	88.7	127.9	79.0	59.4	91.7	131.8	76.3
$\bar{T}$ (s)	1.38	1.39	1.38	1.36	1.34	1.37	1.36	1.35	1.34	1.36	1.35	1.35	1.38	1.33
ϵ	0.48	0.49	0.47	0.45	0.38	0.48	0.48	0.44	0.36	0.49	0.47	0.10	0.20	0.12
INITIAL t_R (mm)														
N_Δ-NO OF WAVES														
250													112.9*	
500	18.3	6.2	7.8	28.4	92.5*	13.4		33.9	89.5*	29.4		57.4		31.3
1000	40.7	11.3	16.1	38.0		14.4	8.5	67.5		50.4	7.5	75.3*		38.0
1500	42.8	17.1	45.4	49.7		13.1		71.5*		52.5				45.3
1750														48.4*
2000	51.9	22.7	40.4	55.8		22.9	9.1			62.7	7.8			
2250														
2500	63.9	49.0	35.1	66.1		24.2				81.7*				
2750														
3000	70.6	62.7		81.5		28.1	9.1				10.2			
3500	72.2	53.0	34.9	85.4*		36.3								
4000	81.2*	53.1	37.7			47.9	9.2				13.6			
4500		63.3	60.8			46.4								
5000		64.6	58.0			50.1	6.6				18.4			
5500		64.9	62.3			49.0								
6000		79.4	65.5			53.7	9.6				24.4			
6500		83.2	72.7											
7000		84.3*	79.9*			57.7								
8000						58.9	13.6				24.5			
8250						59.4*								
9000														
10000							19.5				28.1			
12000							20.0				35.9			
12500														
14000							18.0				38.6			
16000							20.2				46.2			
18000							16.0				49.1			
20000											48.0			

* RIPRAP FAILED

TABLE 21

Experimental data from preliminary tests

TEST NO	15	16	17	18	19	20	21	22	23	24	25	26	27	28
$\bar{H}_3$ (mm)	61.0	84.6	124.6	69.8	76.9	52.8	90.8	136.8	80.8	73.4	90.3	80.4	71.2	53.9
$\bar{T}$ (s)	1.32	1.34	1.37	1.34	1.34	1.34	1.33	1.35	1.32	1.33	1.30	1.30	1.29	1.30
ϵ	0.10	0.49	0.42	0.50	0.48	0.49	0.14	0.16	0.10	0.12	0.48	0.47	0.46	0.49
INITIAL t_R (mm)		65.8	67.0	67.1	64.7	66.9	67.5	65.3	68.1	68.4	61.3	61.4	61.0	56.9
N_Δ-NO OF WAVES														
250														
500			113.2*	17.9	26.4		65.8	160.5*	33.4		32.0	20.4		
1000	11.6			31.4	36.5	5.5	93.3		50.0	46.0	56.1*	30.7	27.9	
1500				33.1	45.2		108.7		58.7			35.1		
1750														
2000	18.1	98.6		35.3	60.3	8.1	128.3		74.1	57.6		46.5	36.1	11.6
2250							136.4*							
2500		107.4		44.4	68.9				86.0			50.5		
2750		104.5*												
3000	23.7			40.5	78.8	8.7			84.9	66.7		60.0	41.5	
3500				48.0	91.8				93.4			67.3*		
4000	23.8			56.4	100.7	8.0			94.3	72.0			43.8	17.4
4500				62.5	102.8*				99.1					
5000	26.3			70.3		14.8			98.0					
5500				71.5					99.9					
6000	28.0			72.6					101.3	72.8			60.3	20.4
6500				74.2					108.5					
7000				76.0					111.2					
8000	32.3			78.4					116.3	84.4			64.1	20.8
8250									112.1*					
9000				79.6										
10000	38.7			80.2						95.0			58.9	20.8
12000	33.8													
12500													67.2*	
14000	37.9													
15000				84.9						104.5				
16000	38.4													
18000	39.7													
20000	39.6													

* RIPRAP FAILED

TABLE 22

Experimental data from preliminary tests

TEST NO	29	30	31	32
$\bar{H}_3$ (mm)	90.7	77.4	70.6	53.2
$\bar{T}$ (s)	1.31	1.30	1.30	1.30
ϵ	0.48	0.50	0.50	0.49
INITIAL t_R (mm)	57.4	58.0	58.1	60.2
N_Δ-NO OF WAVES				
250				
500	34.8	34.5	D	
1000	51.7*	46.5	A	
1500		61.4	T	
1750			A	
2000		62.4*		15.7
2250			U	
2500			/	
2750			S	
3000				
3500				
4000				20.5
4500				
5000				
5500				
6000				24.3
6500				
7000				
8000				26.2
8250				
9000				
10000				27.4
12000				
12500				
14000				
15000				
16000				
18000				
20000				

* RIPRAP FAILED

FIGURES

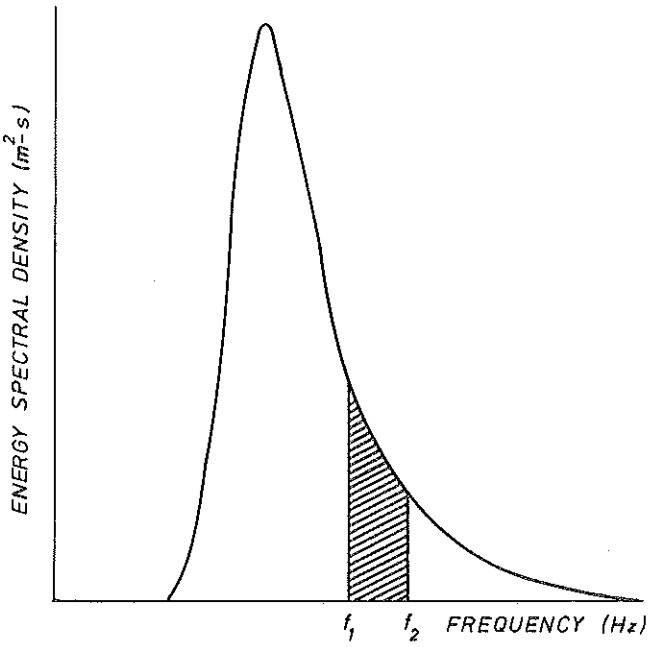

(a) THE ENERGY SPECTRUM

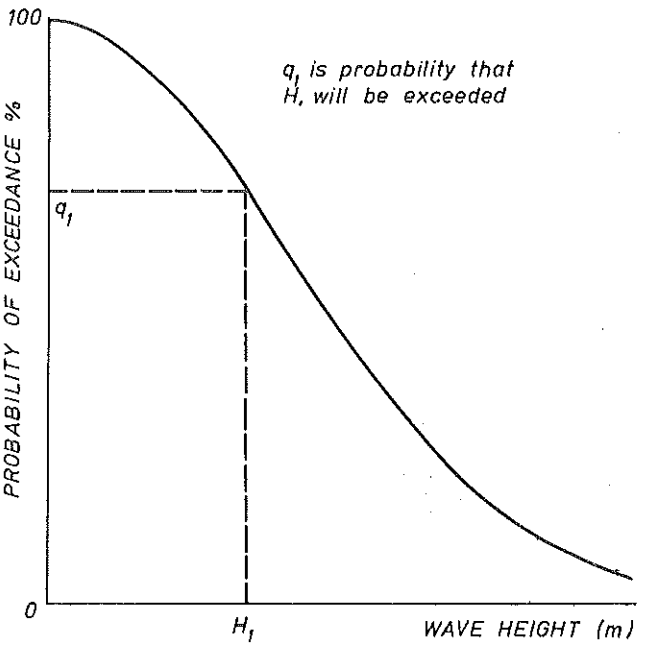

(b) CUMULATIVE PROBABILITY FUNCTION

THE ENERGY SPECTRUM AND CUMULATIVE PROBABILITY FUNCTION

FIG 1

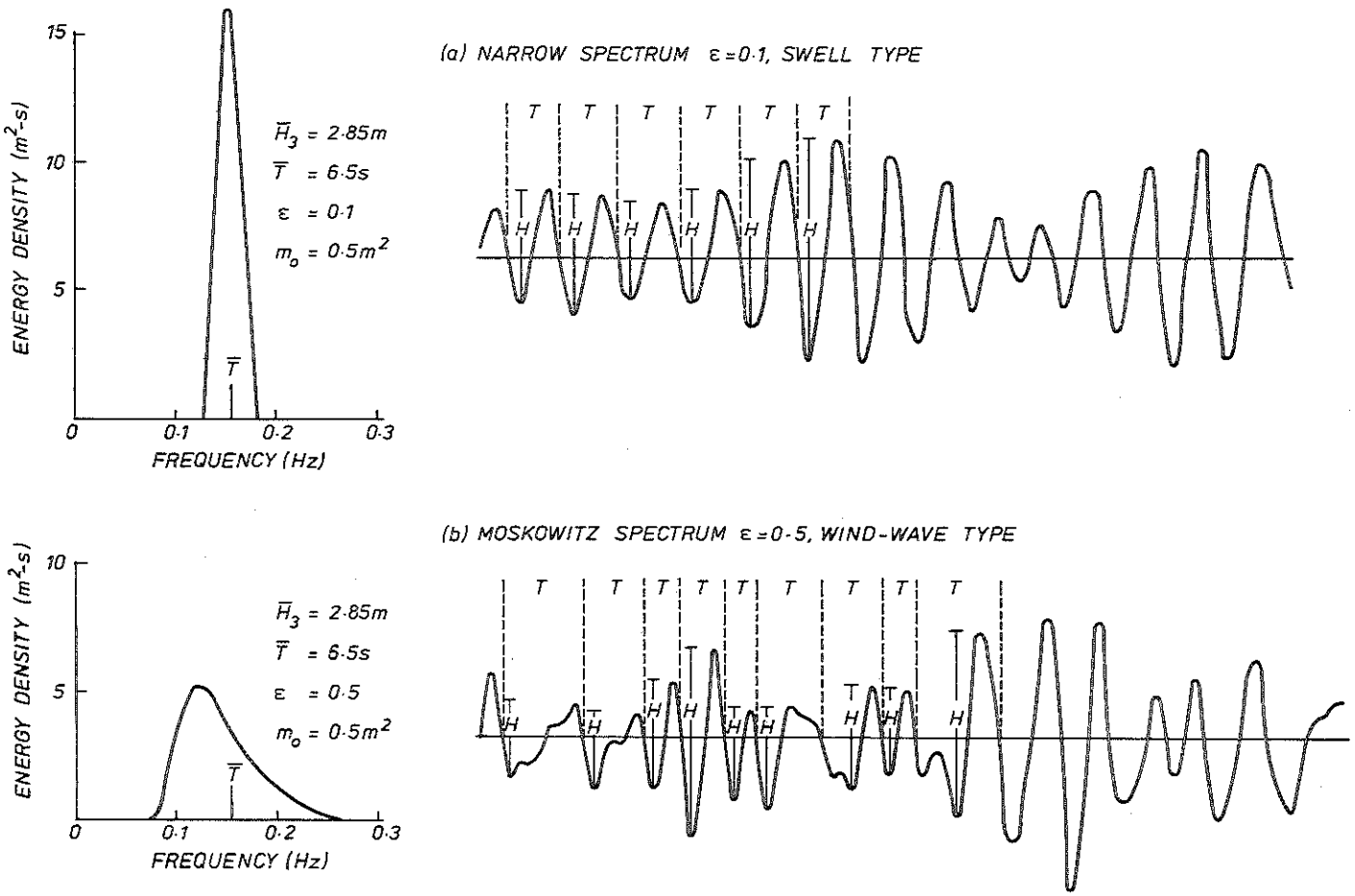

DEFINITION OF WAVES BY ZERO DOWN CROSSINGS

FIG 2

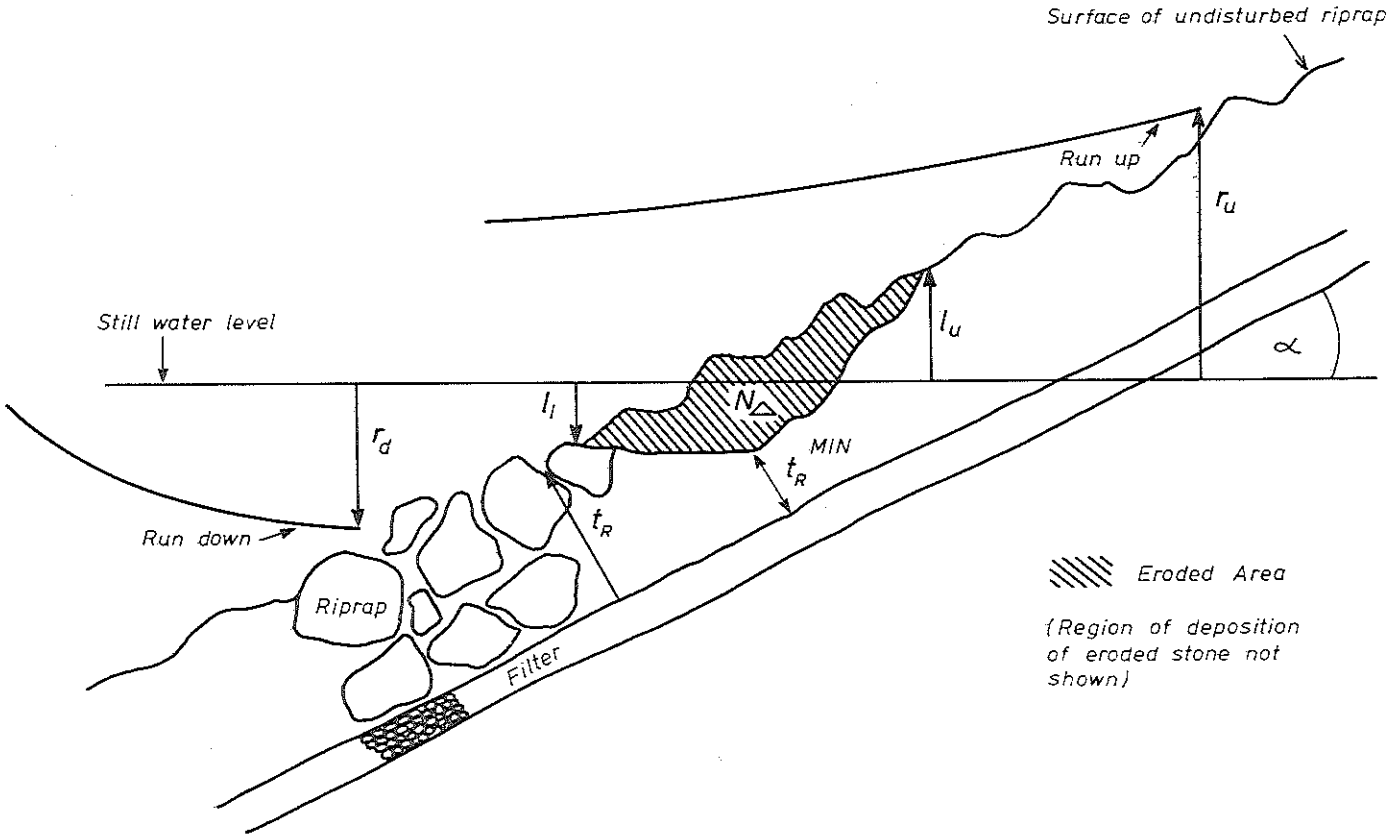

DEFINITION SKETCH OF RIPRAP SLOPE

FIG 3

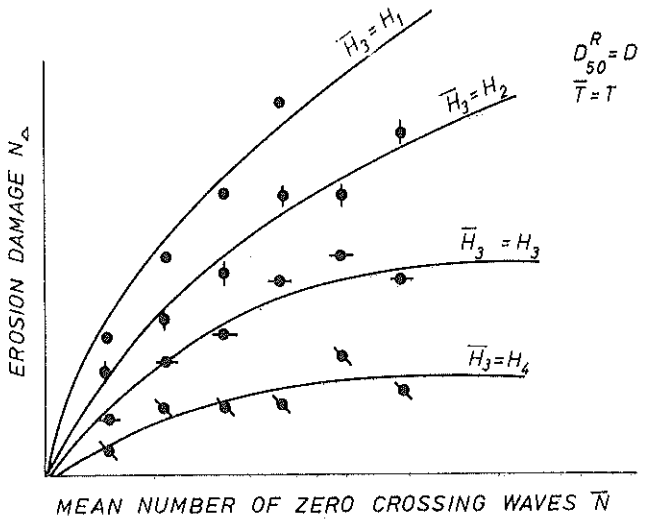

(a) DAMAGE HISTORIES IN ABSOLUTE UNITS

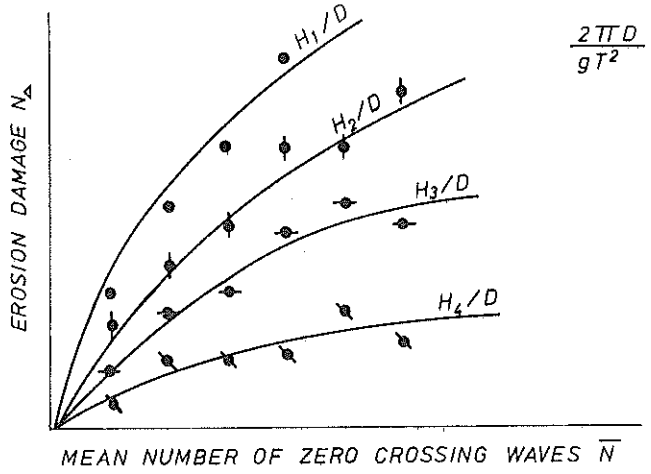

(b) DAMAGE HISTORIES IN DIMENSIONLESS TERMS

DAMAGE HISTORIES

FIG 4

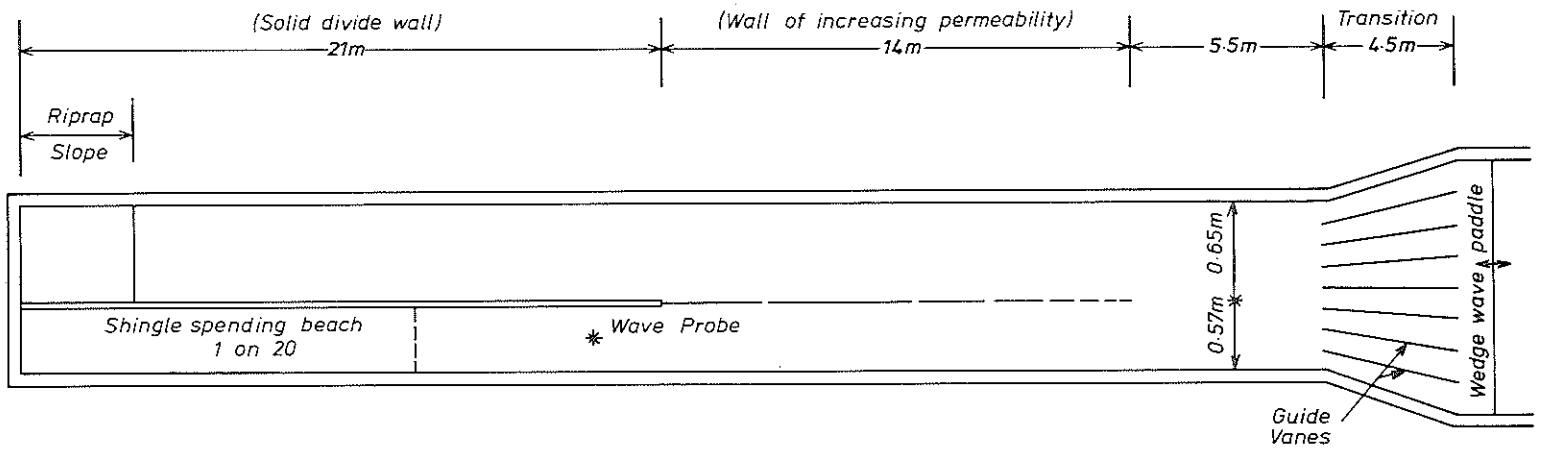

FLUME FOR RIPRAP TESTS

FIG 5

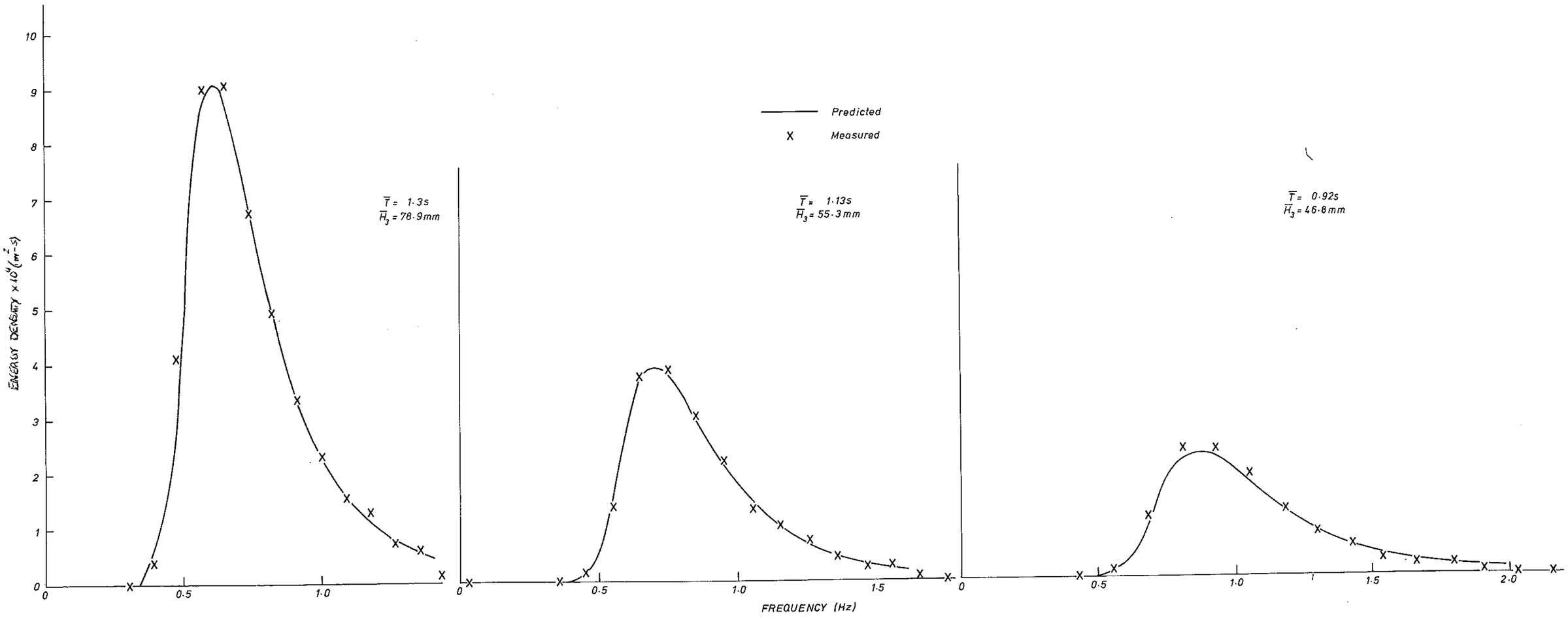

EXAMPLES OF MEASURED SPECTRA

FIG 6

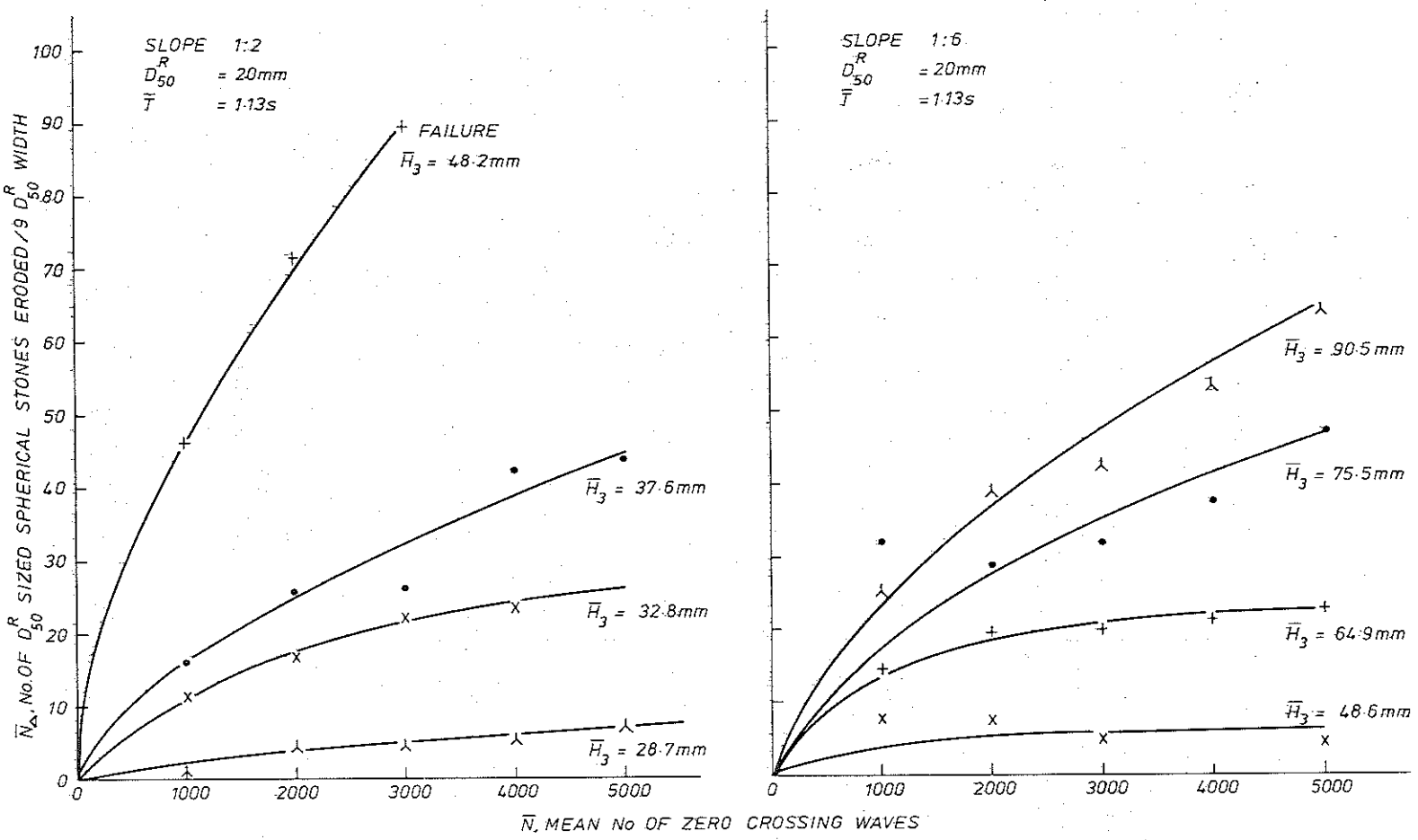

TYPICAL DAMAGE HISTORIES

FIG 7

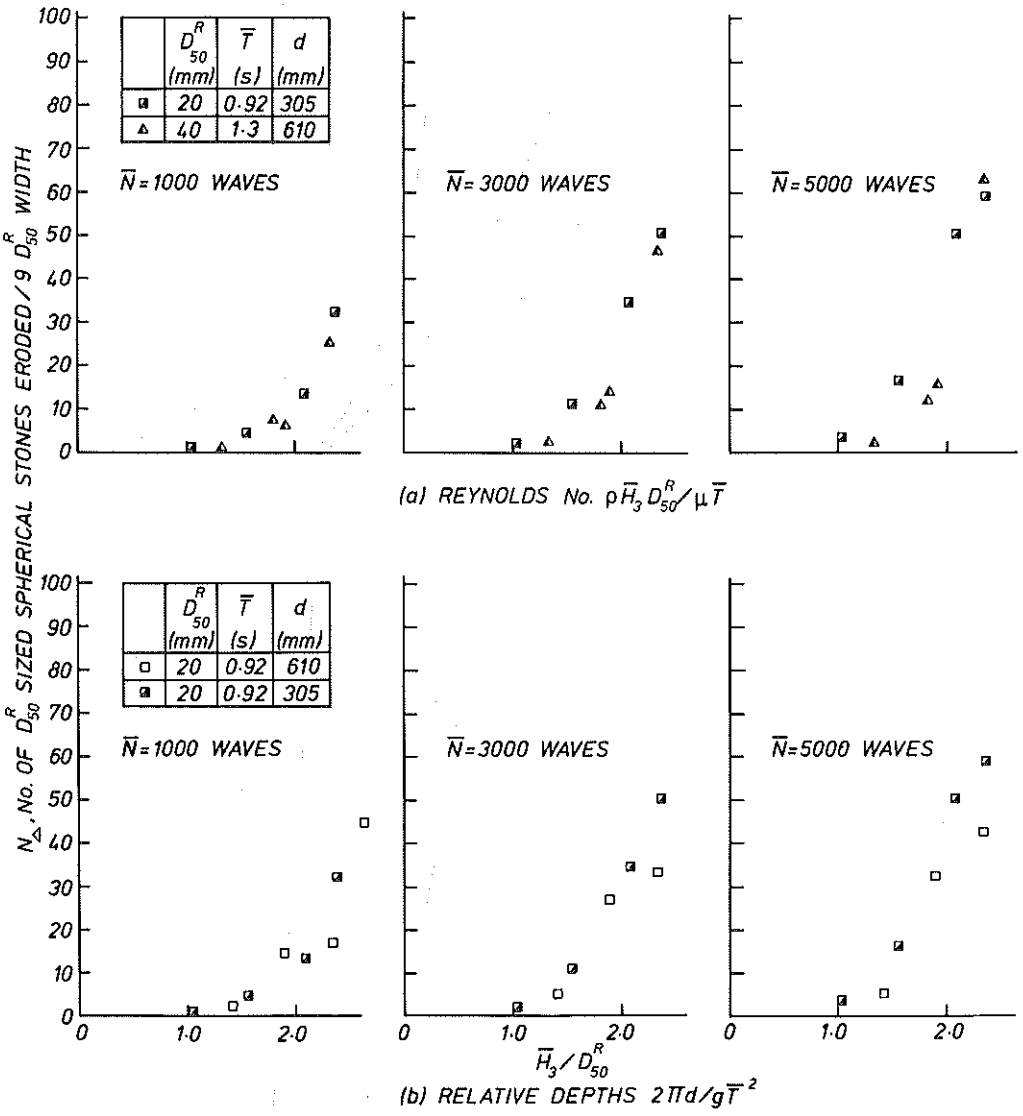

SCALE TESTS ON 1:2 SLOPE

FIG 8

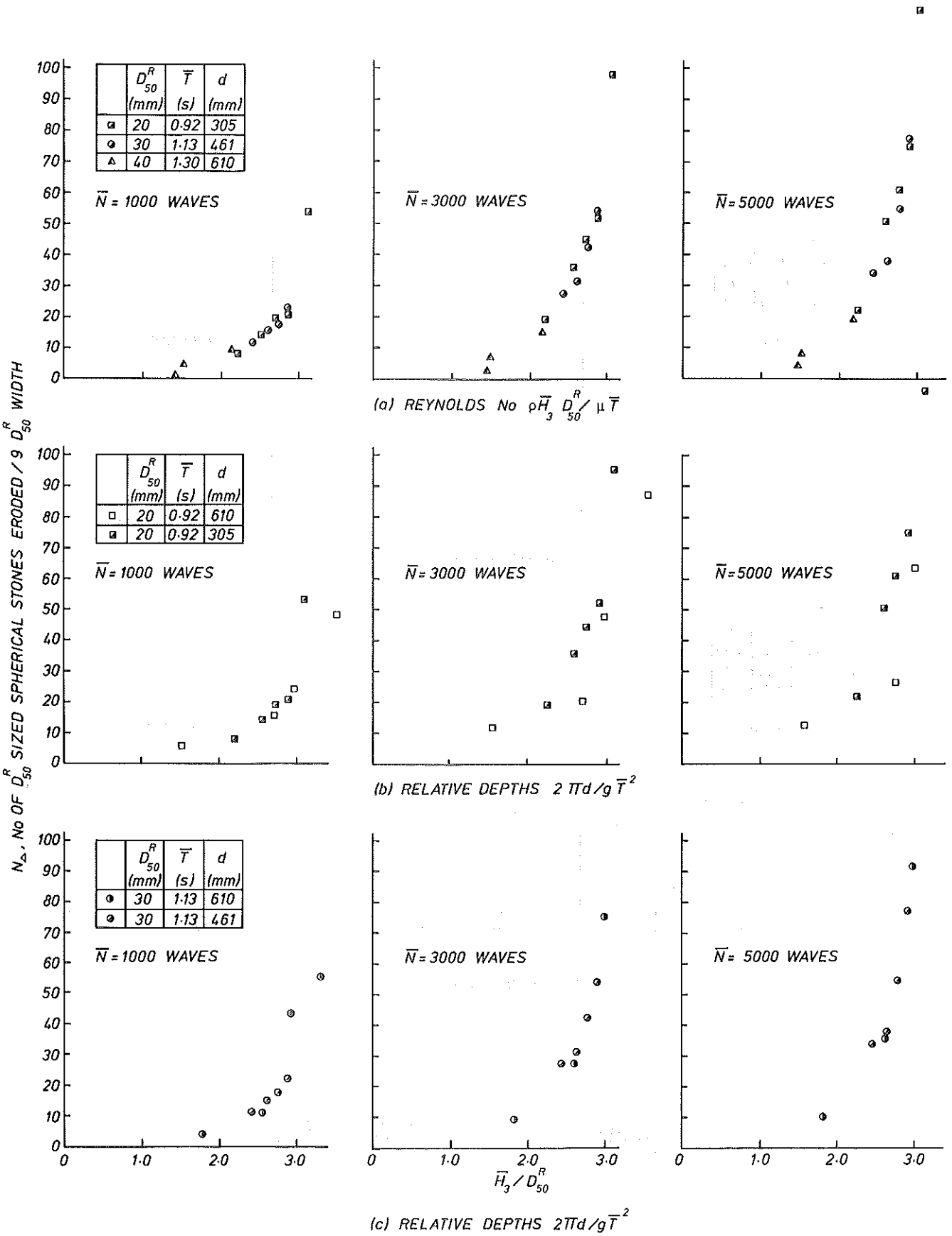

SCALE TESTS ON 1:3 SLOPE

FIG 9

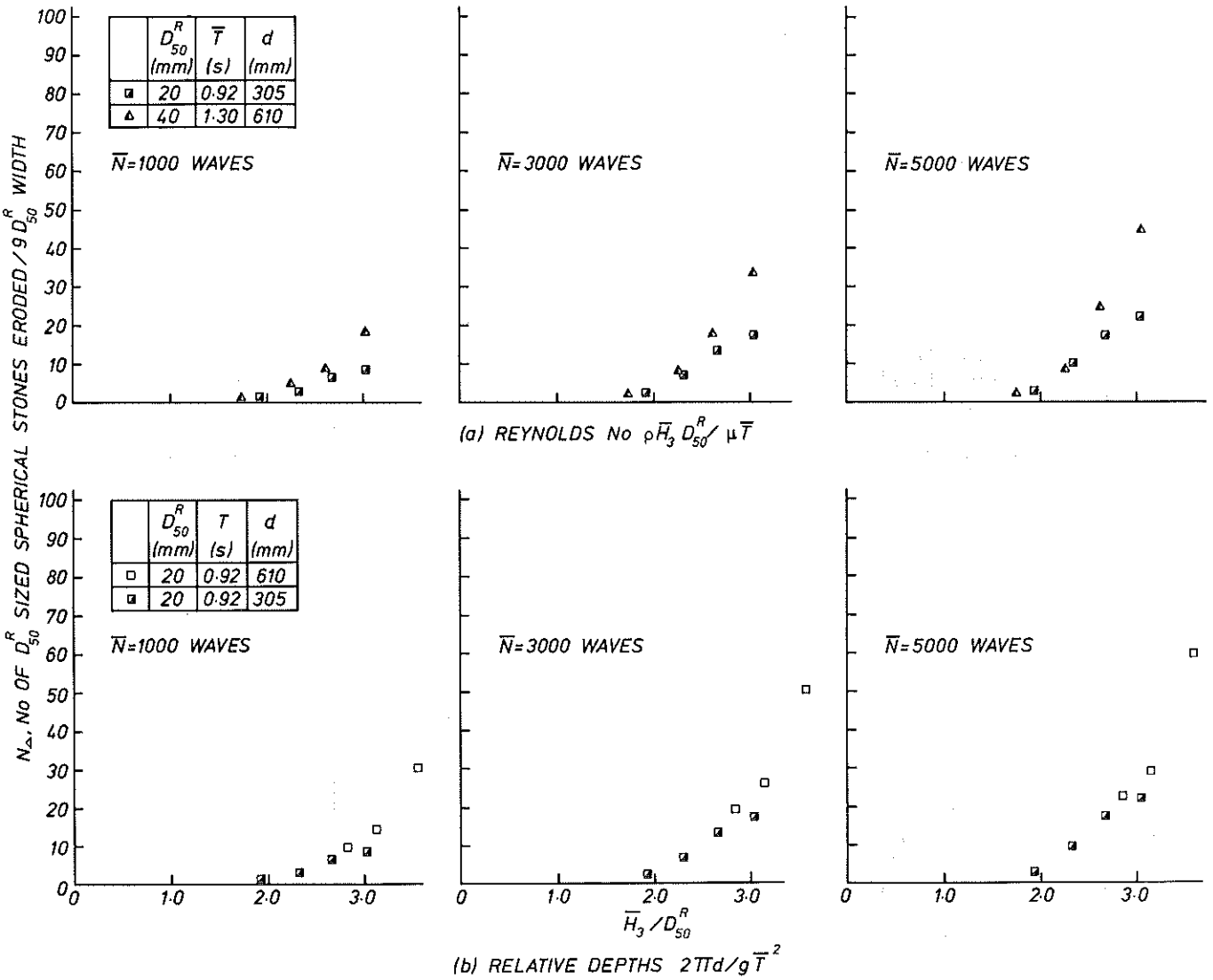

SCALE TESTS ON 1:4 SLOPE

FIG 10

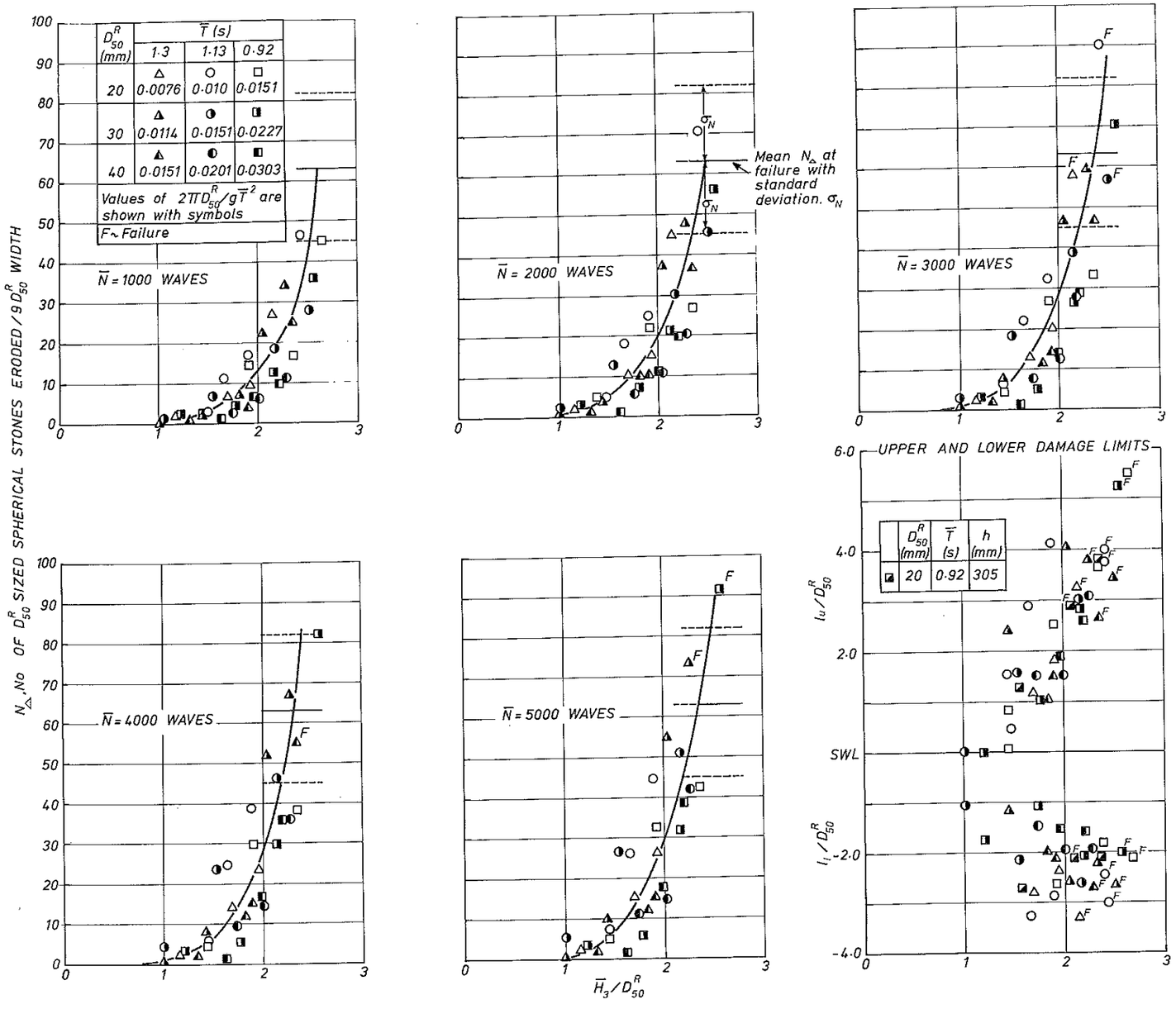

EROSION DAMAGE AND DAMAGE LIMITS ON THE 1:2 SLOPE

FIG 11

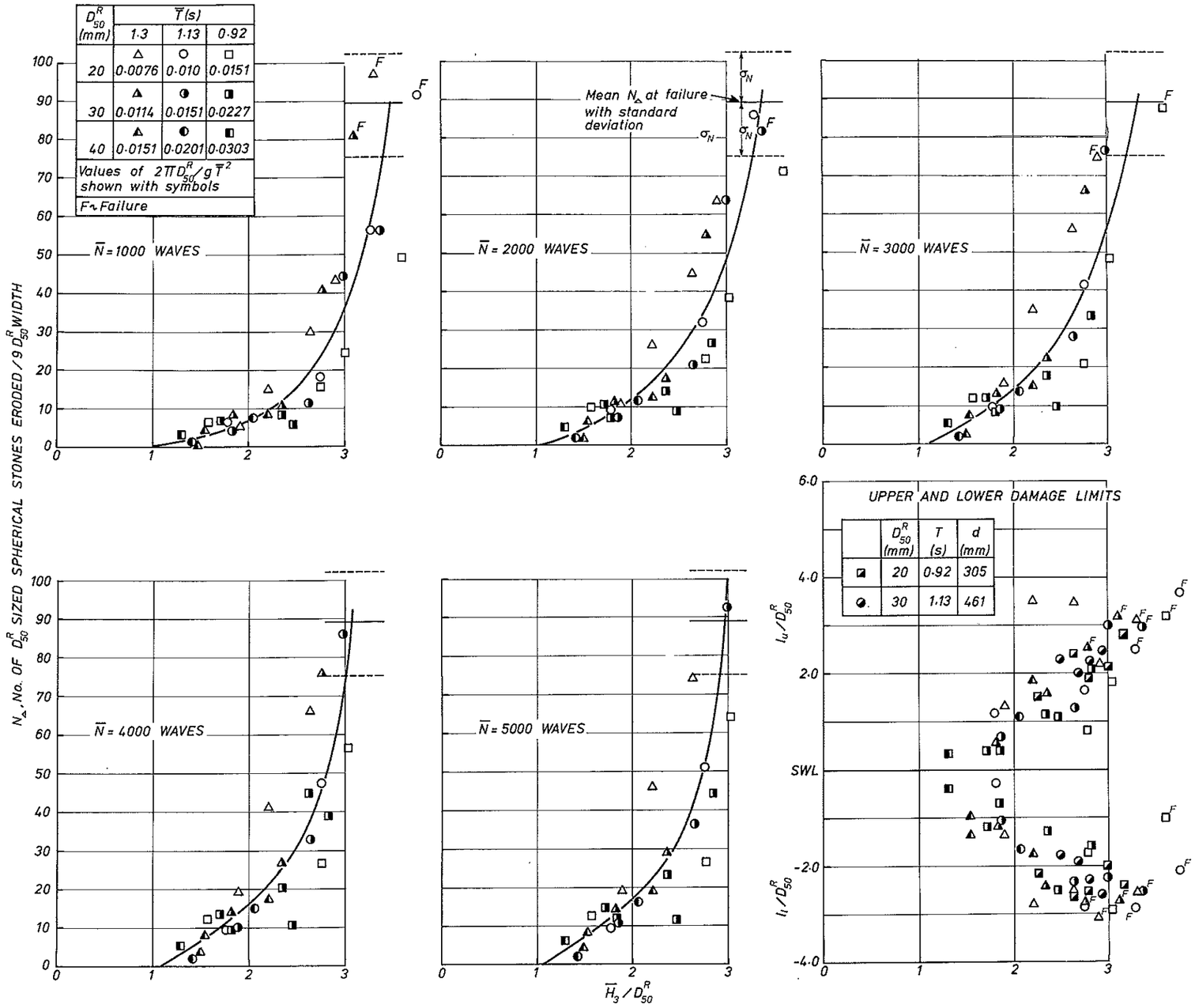

EROSION DAMAGE AND DAMAGE LIMITS ON THE 1:3 SLOPE

FIG 12

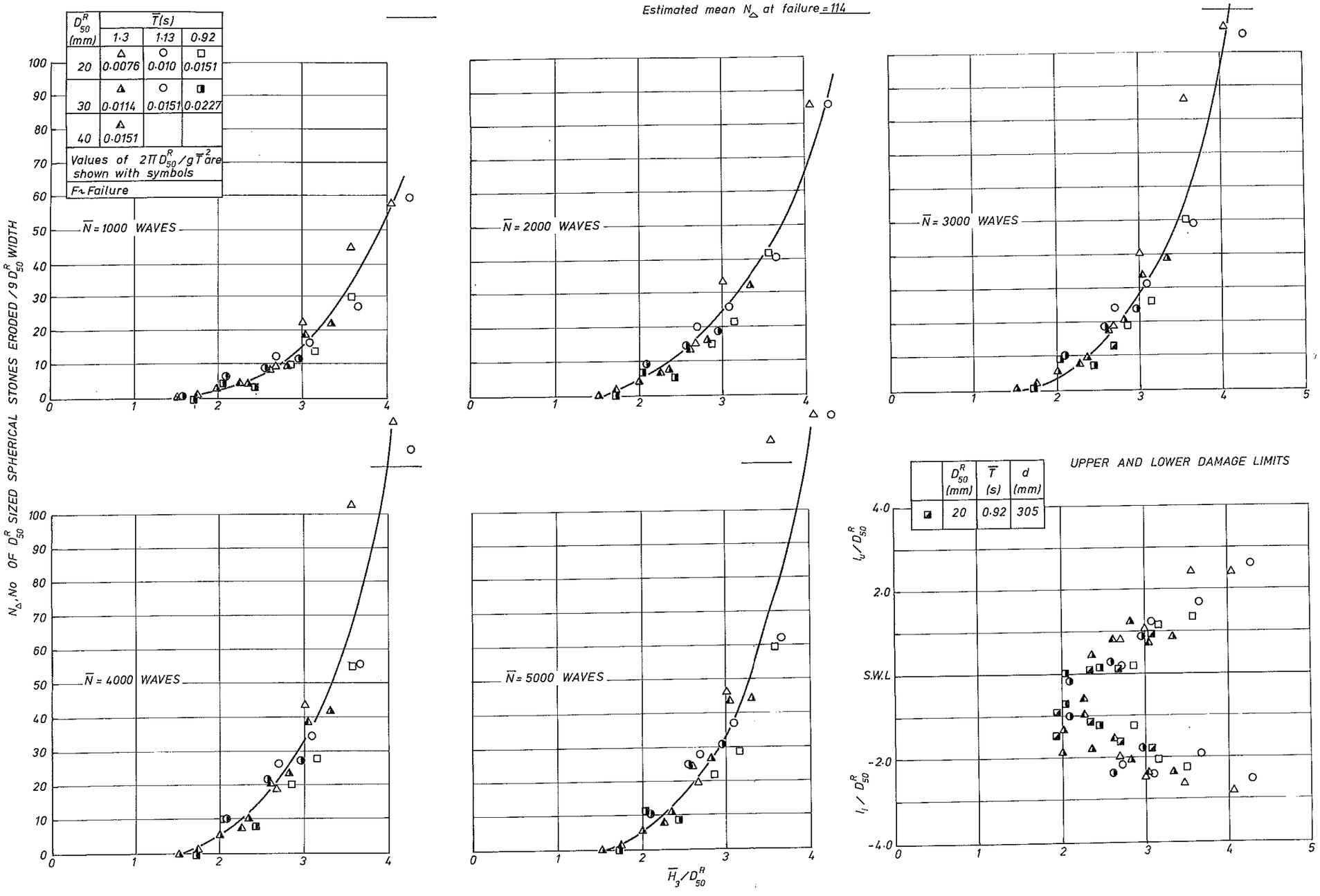

EROSION DAMAGE AND DAMAGE LIMITS ON THE 1:4 SLOPE

FIG 13

D_{50}^R (mm)	$\bar{T}$ (s) 1·3	1·13	0·92
20	△ 0·0076	○ 0·010	□ 0·0151
30	▲ 0·0114	◑ 0·0151	◧ 0·0227
40			

Values of $2\pi D_{50}^R / g\bar{T}^2$ are shown with symbols

F ~ Failure

$\bar{N}$=1000 WAVES

Estimated mean $N_\triangle$ at failure = 168

$\bar{N}$= 2000 WAVES

$\bar{N}$= 3000 WAVES

UPPER AND LOWER DAMAGE LIMITS

$N_\triangle$, No OF D_{50}^R SIZED SPHERICAL STONES ERODED / 9 D_{50}^R WIDTH

$\bar{N}$= 4000 WAVES

$\bar{N}$= 5000 WAVES

$\bar{H}_3 / D_{50}^R$

l_1 / D_{50}^R

SWL

l_1 / D_{50}^R

EROSION DAMAGE AND DAMAGE LIMITS ON THE 1:6 SLOPE

FIG 14

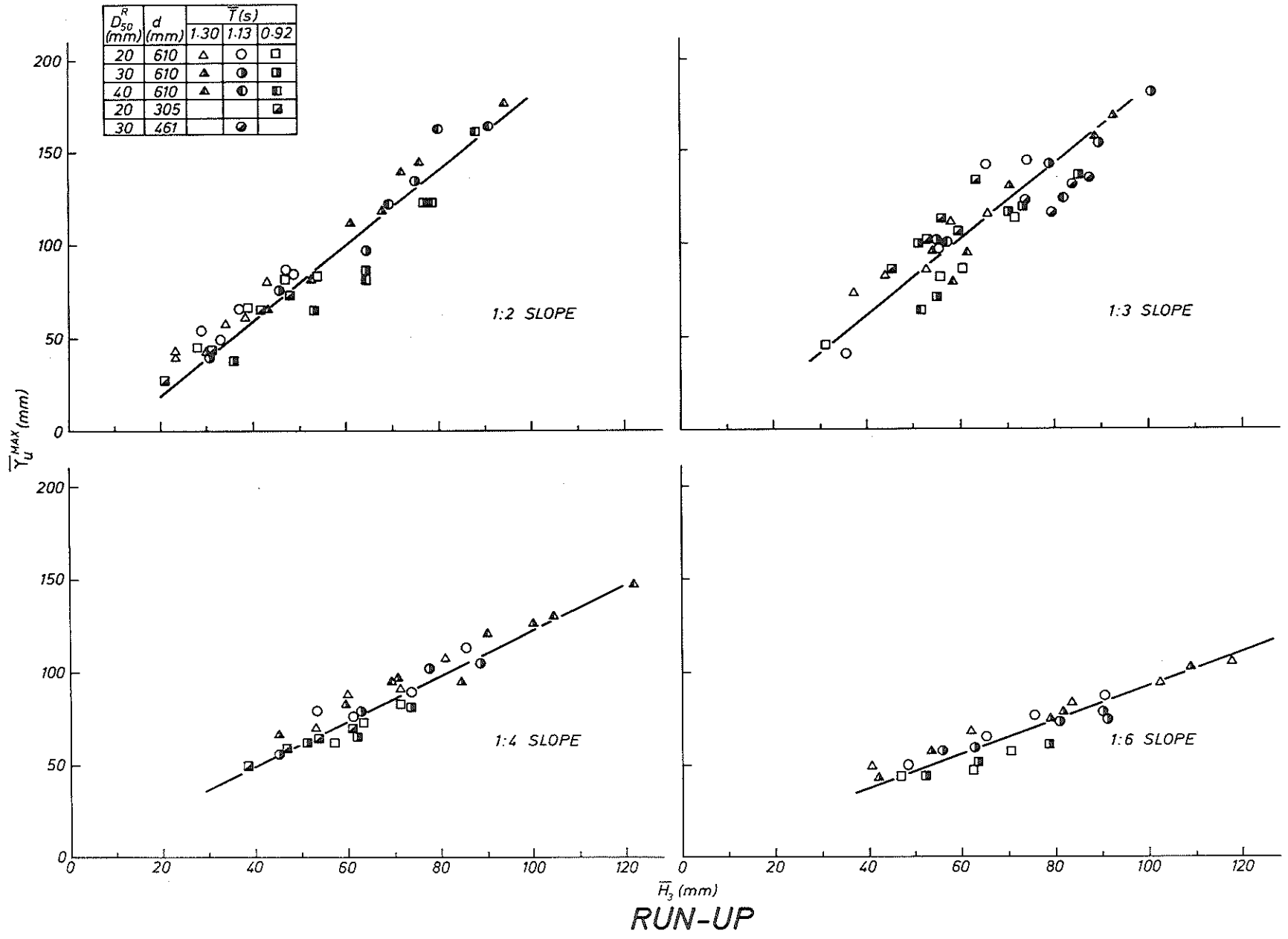
D_{50}^{R} (mm)
d (mm)
$\overline{T}$ (s)
1·30
1·13
0·92
20 610
30 610
40 610
20 305
30 461
1:2 SLOPE
1:3 SLOPE
1:4 SLOPE
1:6 SLOPE
$\overline{Y}_u^{MAX}$ (mm)
$\overline{H}_3$ (mm)
0
50
100
150
200
20
40
60
80
120

RUN-UP

FIG 15

D_{50}^{R} (mm)	d (mm)	T(s) 1.30	1.13	0.92
20	610	△	○	□
30	610	◭	◑	◨
40	610	◭	◐	◧
20	305			◪
30	461		◕	

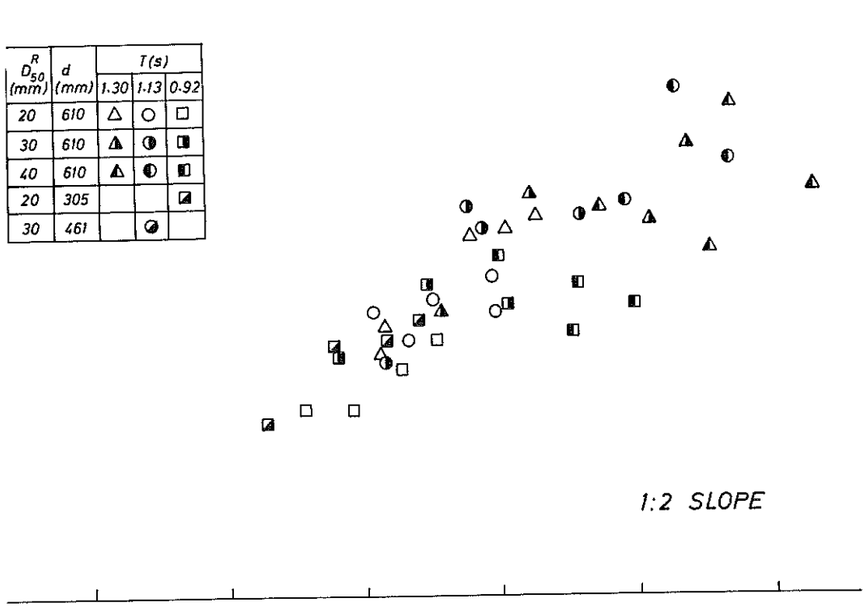

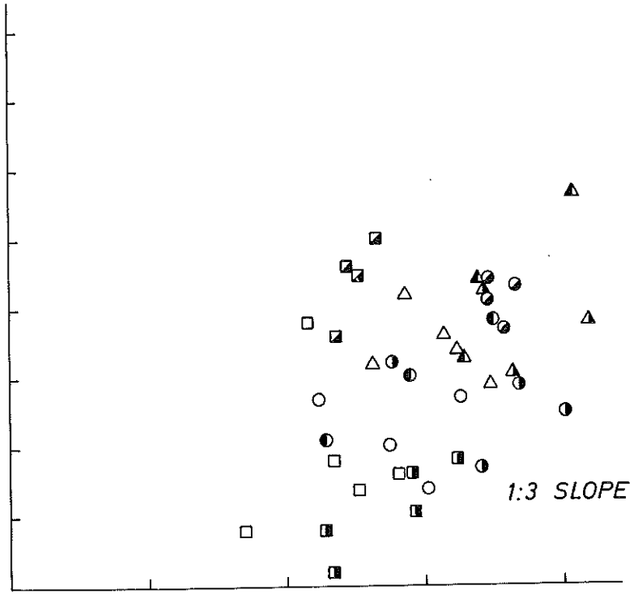

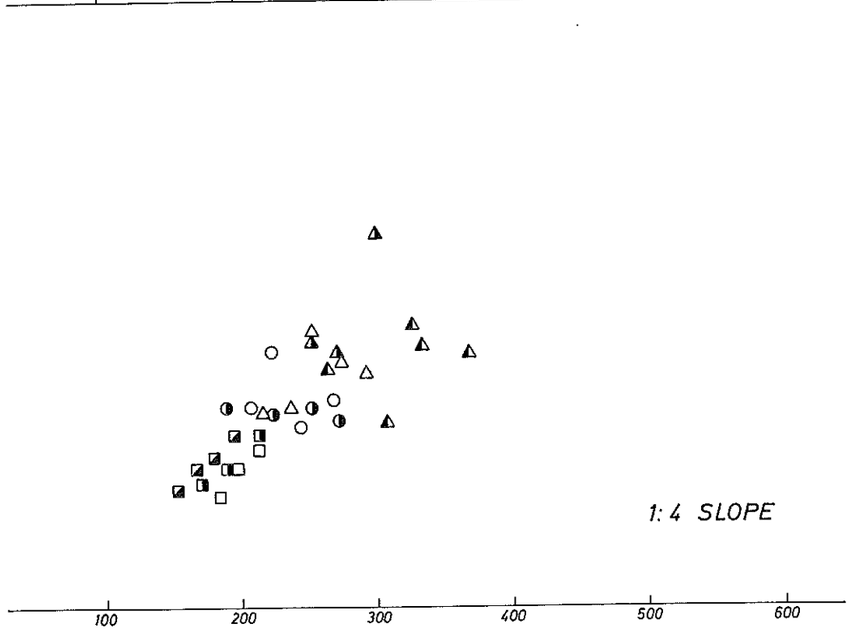

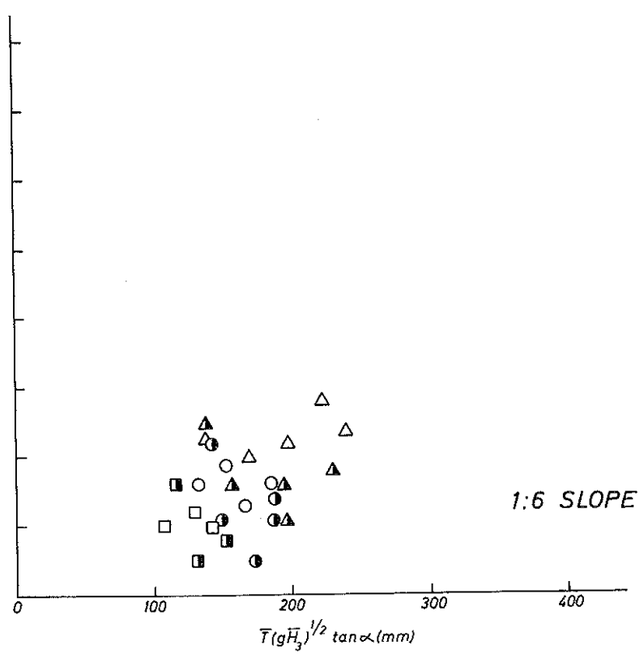

	SLOPE
Y	1:2
+	1:3
X	1:4
人	1:6

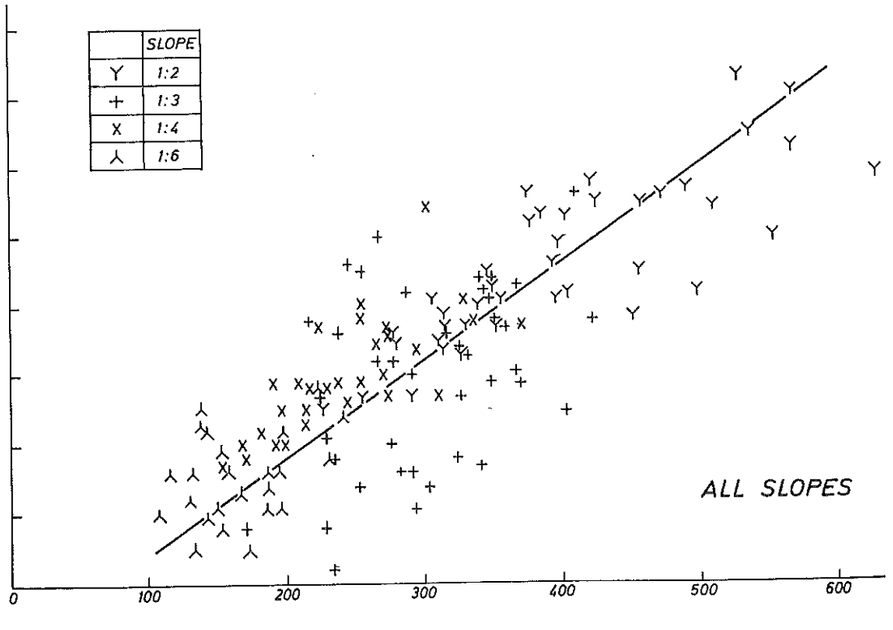

RUN-DOWN

FIG 1(

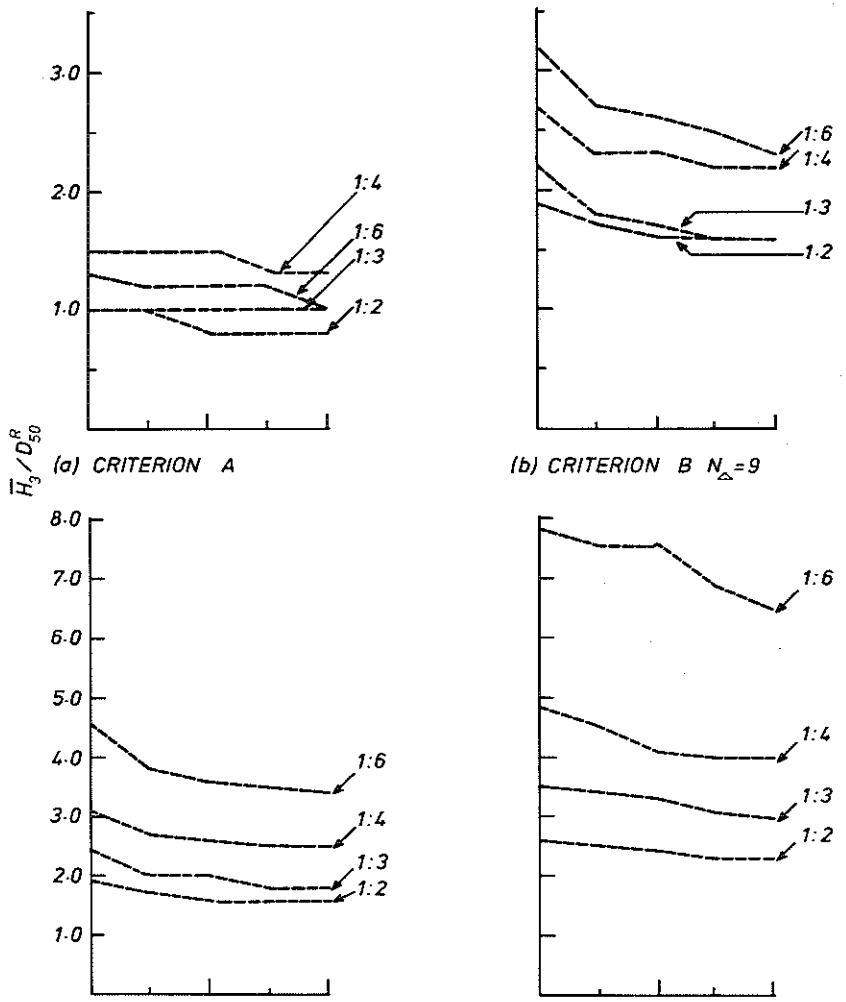

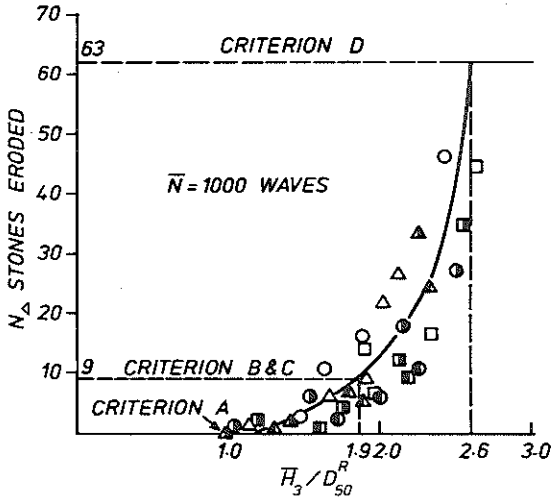

(e) EXAMPLE OF THE $\overline{H}_3 / D_{50}^R$ VALUES CORRESPONDING TO THE DIFFERENT DAMAGE CRITERIA ON THE 1:2 SLOPE AT 1000 WAVES

DESIGN CRITERIA

FIG 17

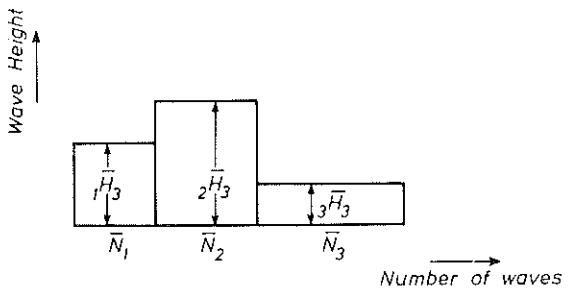

(a) DESIGN STORM

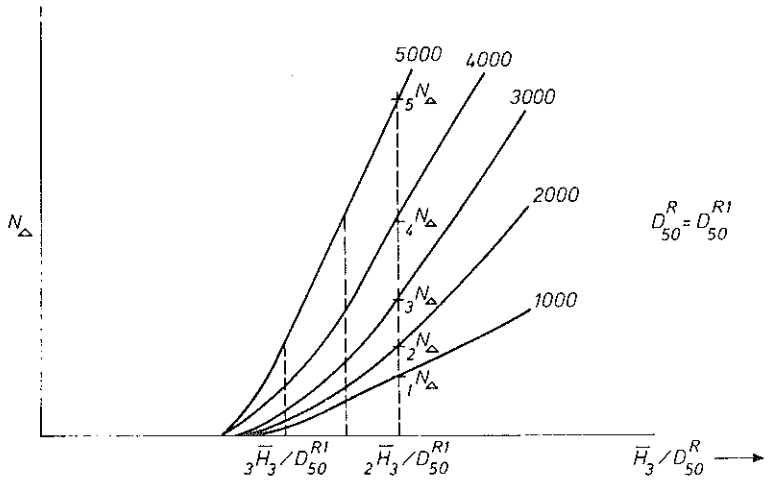

(b) DAMAGE CURVES

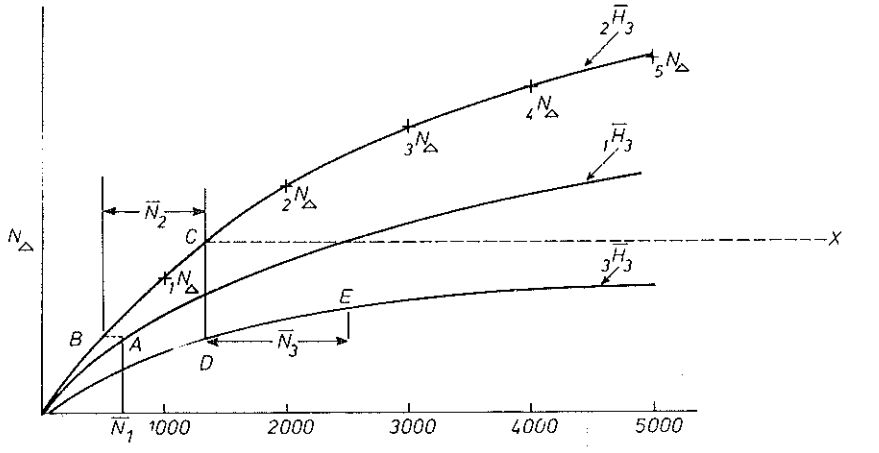

(c) RECONSTRUCTED DAMAGE HISTORIES FOR D_{50}^{R1}

AN EXAMPLE OF DESIGN METHOD 2

FIG 18

Filter 4/20 is used with 20mm riprap
" 4/30 " " " 30 " "
" 4/40 " " " 40 " "

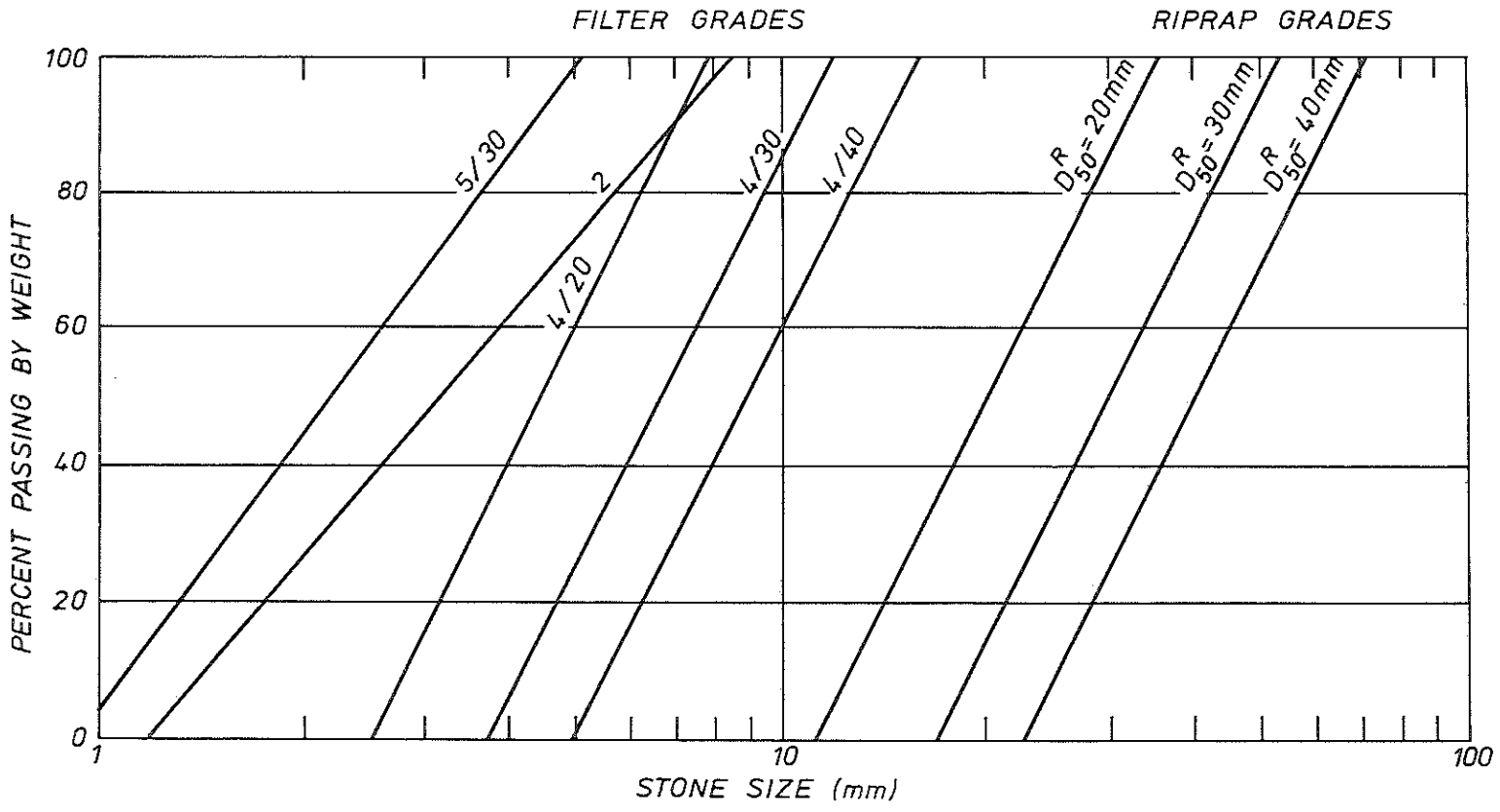

GRADING CURVES FOR RIPRAP AND FILTER LAYERS

FIG 19

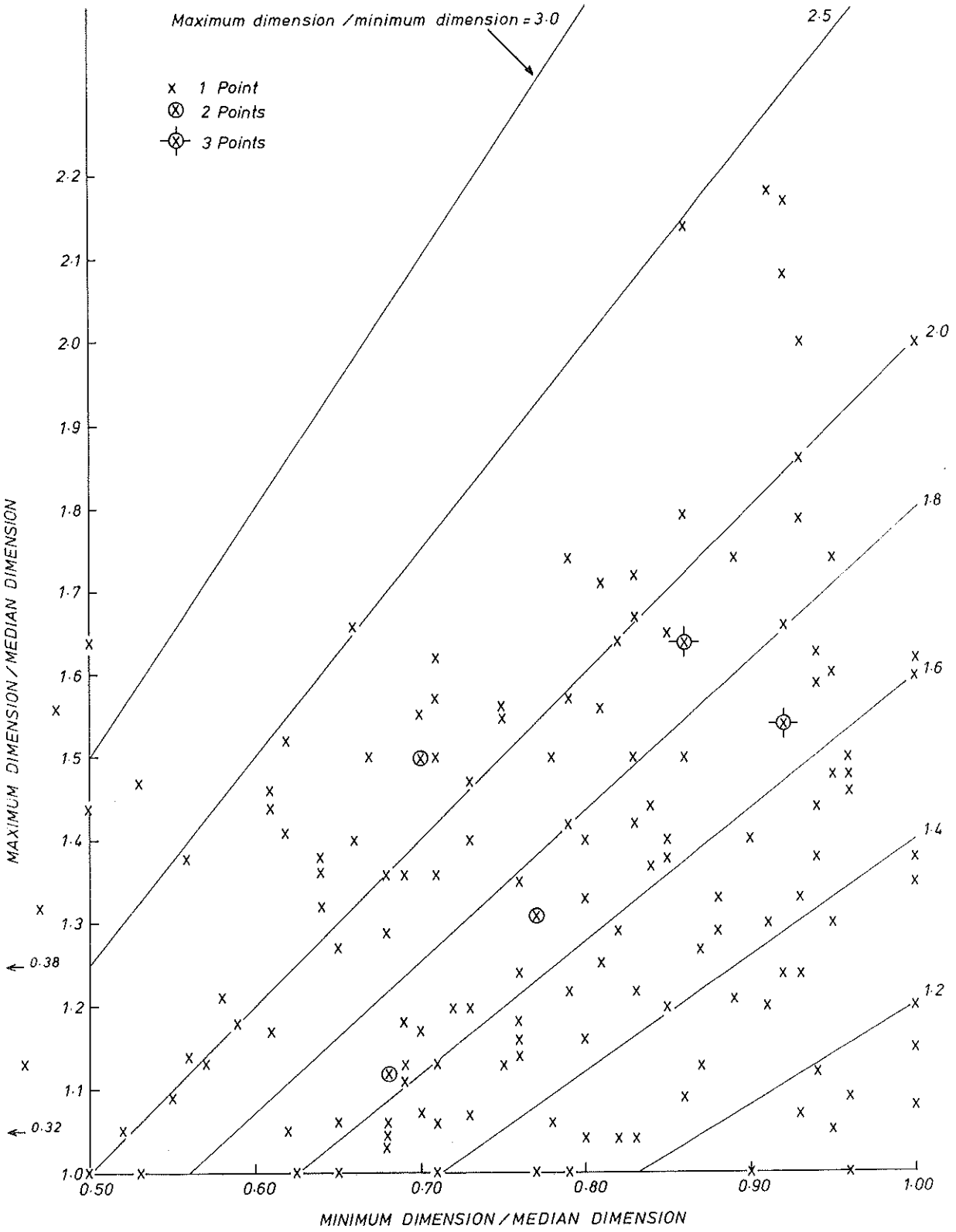

SHAPE ANALYSIS FOR 20mm D_{50}^{R} RIPRAP

FIG 20

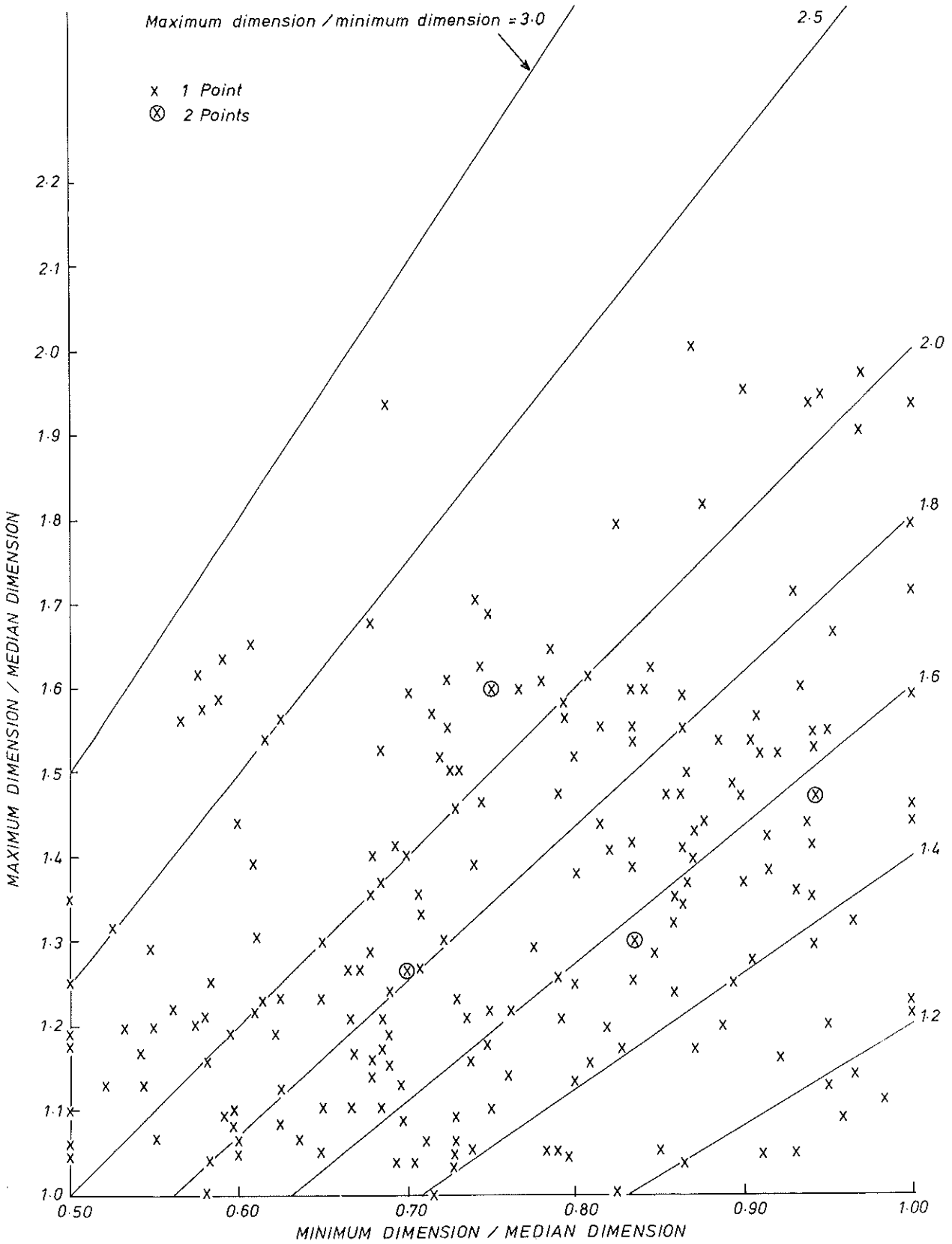

SHAPE ANALYSIS FOR 30mm D_{50}^{R} RIPRAP

FIG 21

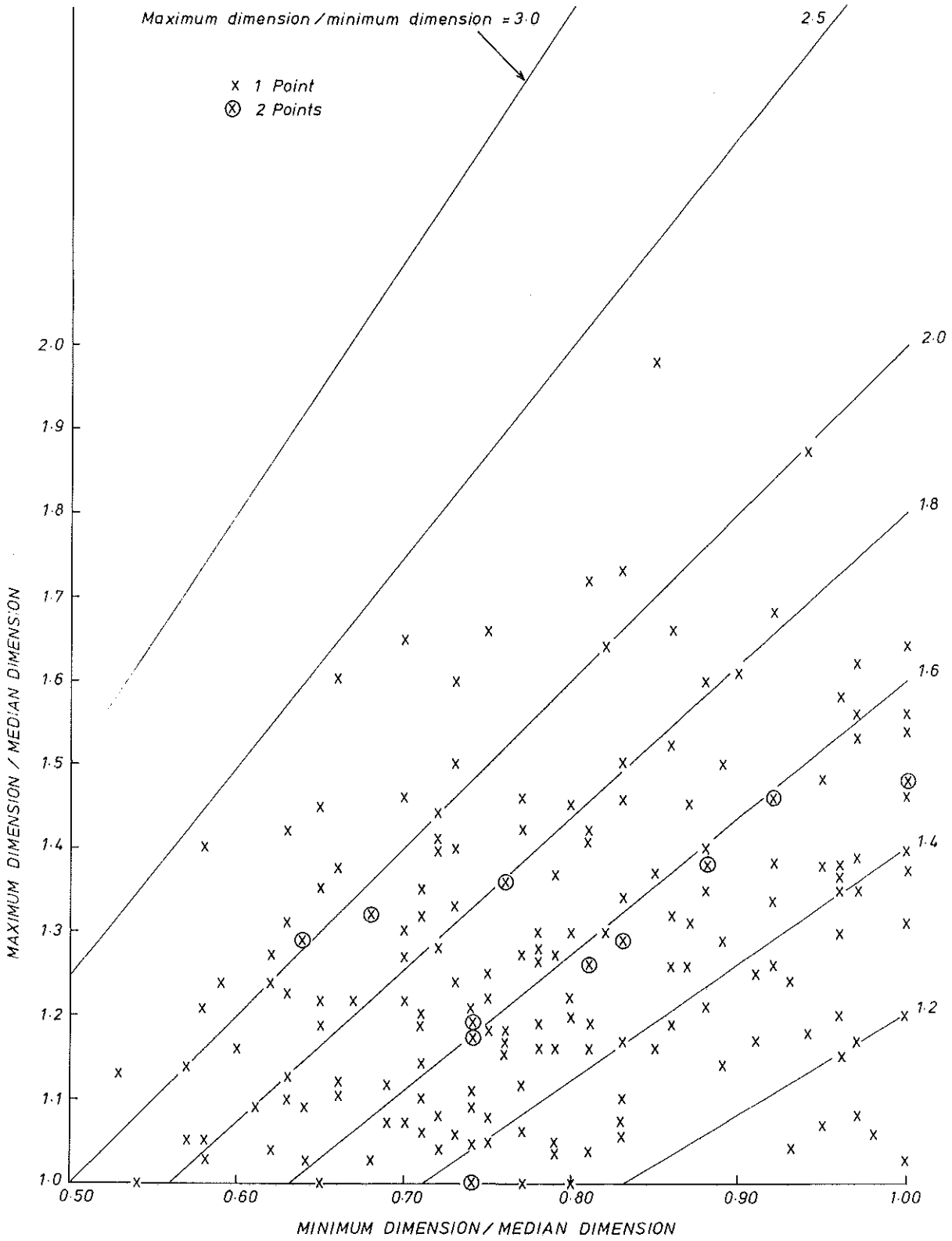

SHAPE ANALYSIS FOR 40mm D_{50}^{R} RIPRAP

FIG 22

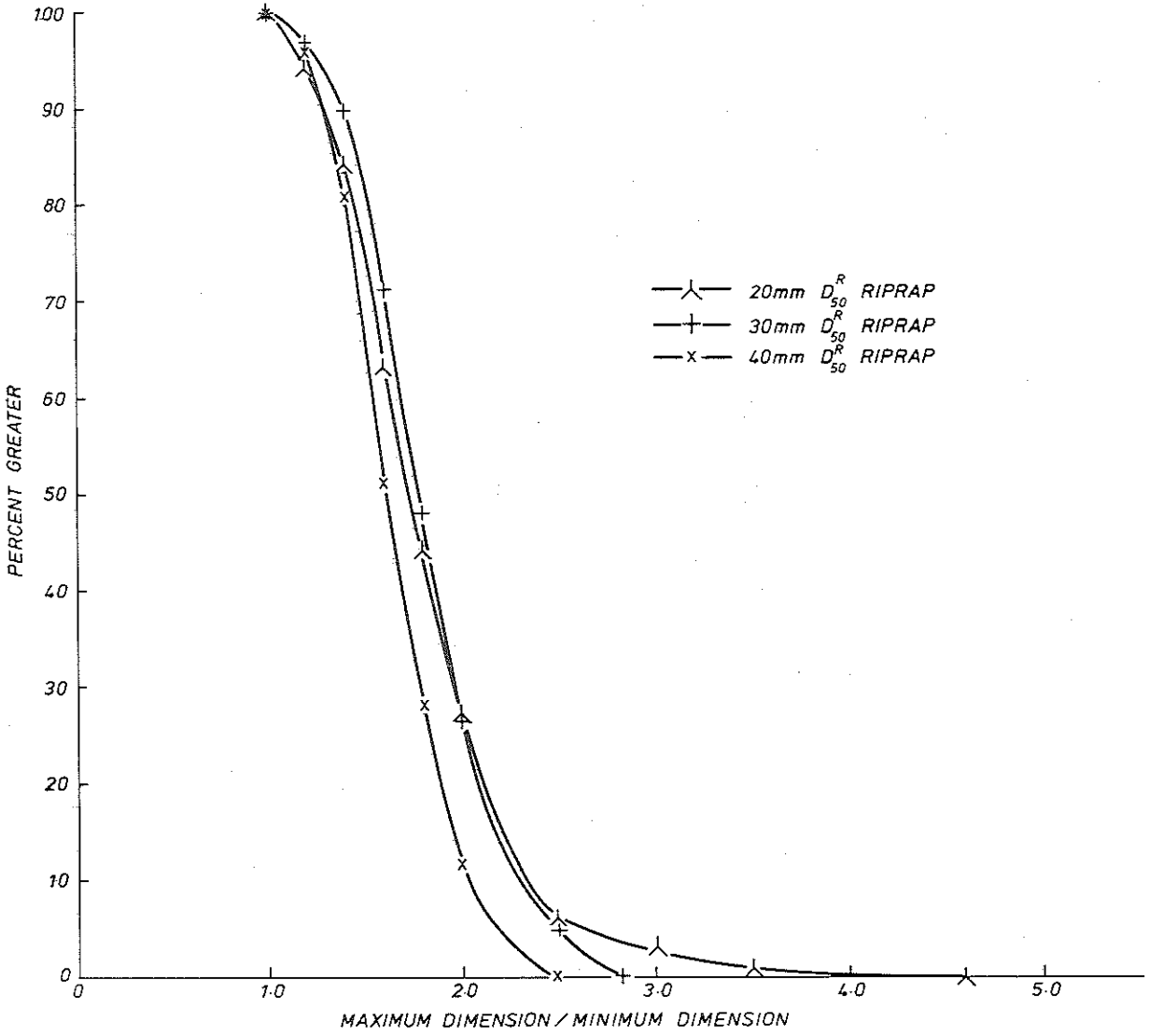

DISTRIBUTION OF STONE SHAPES

FIG 23

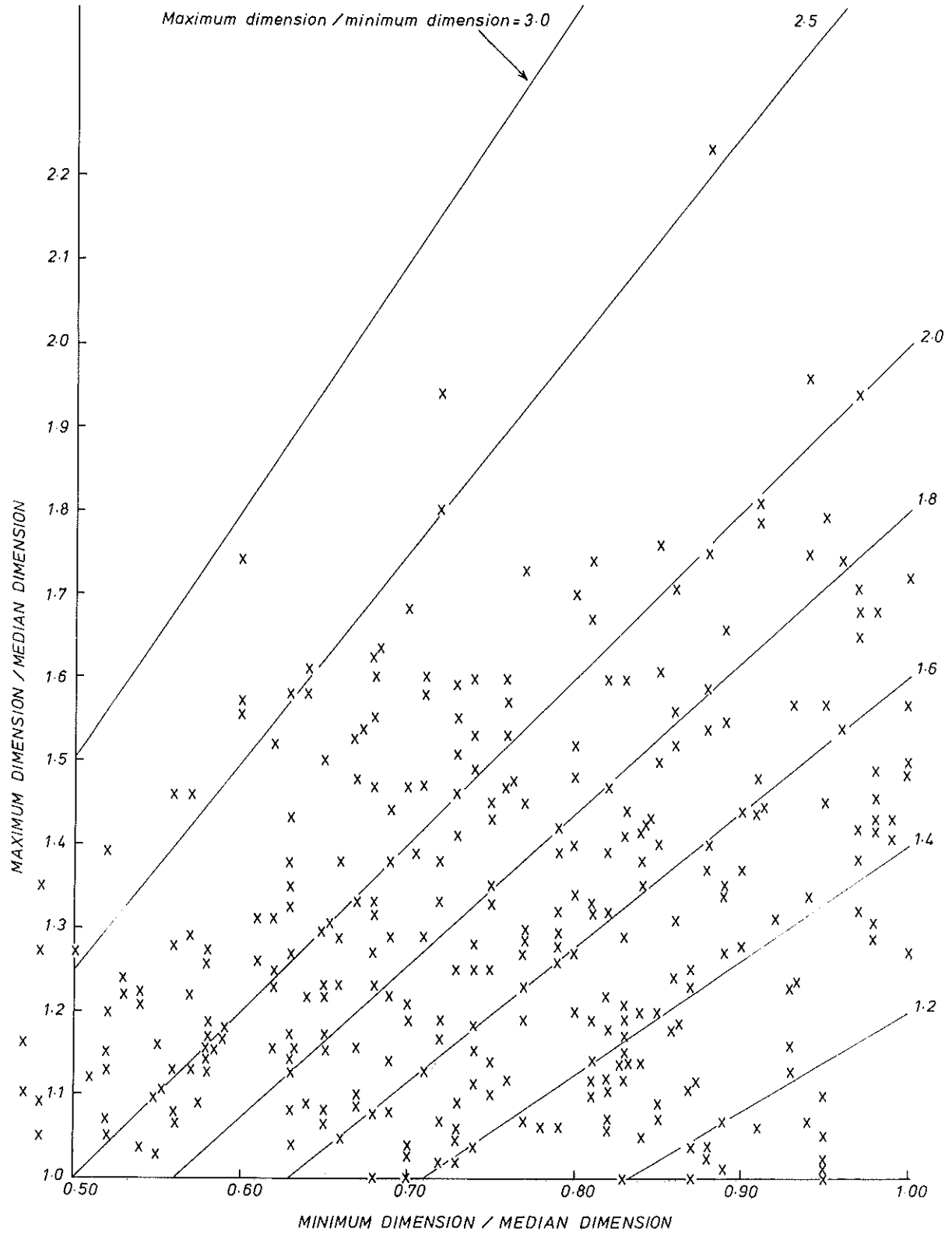

SHAPE ANALYSIS OF 30mm D_{50}^{R} AFTER TESTS

FIG 24

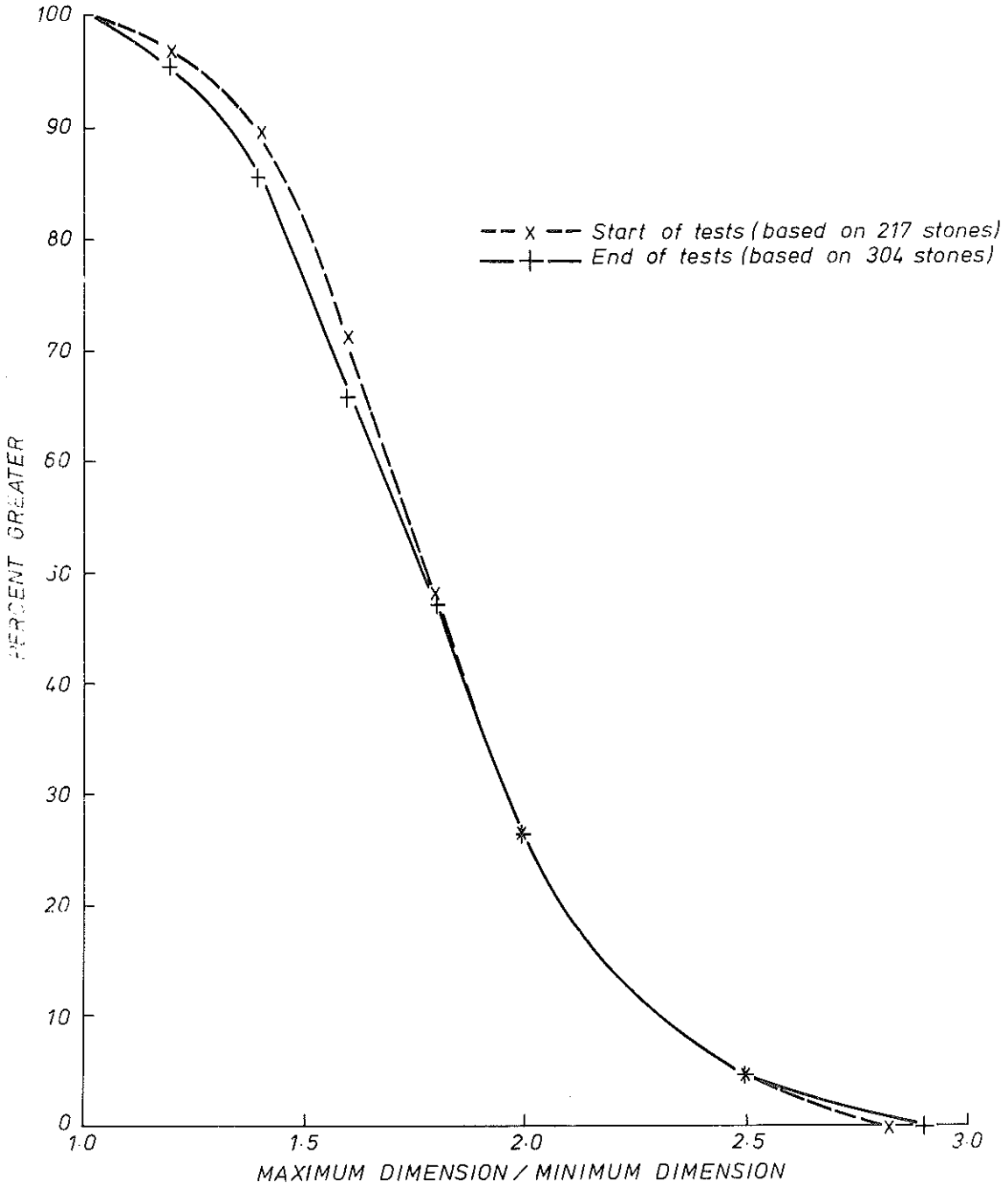

DISTRIBUTION OF STONE SHAPES
BEFORE AND AFTER TESTS FOR 30mm D_{50}^{R} RIPRAP

FIG 25

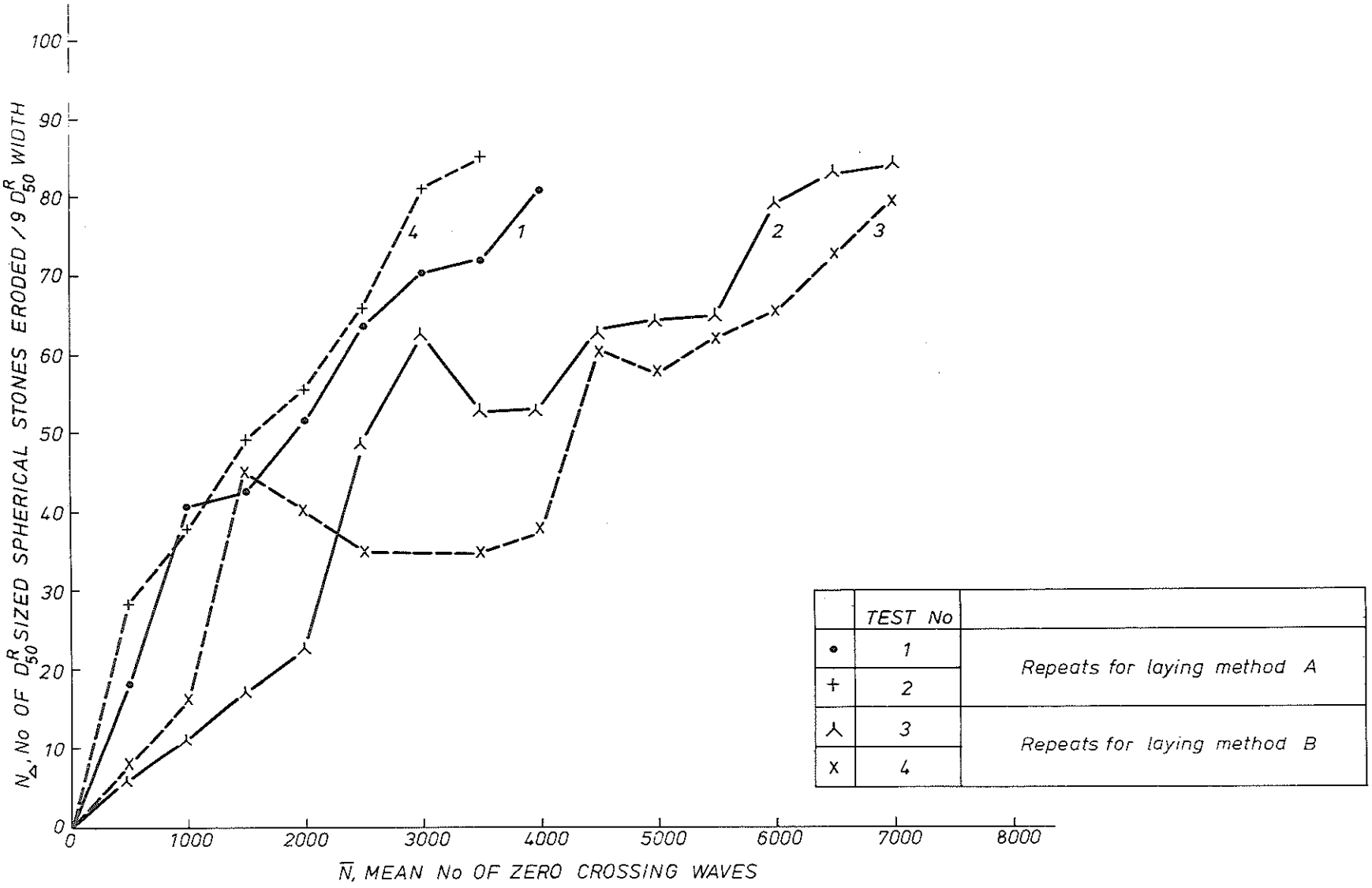

DAMAGE HISTORIES, REPEAT TESTS 1-4

FIG 26

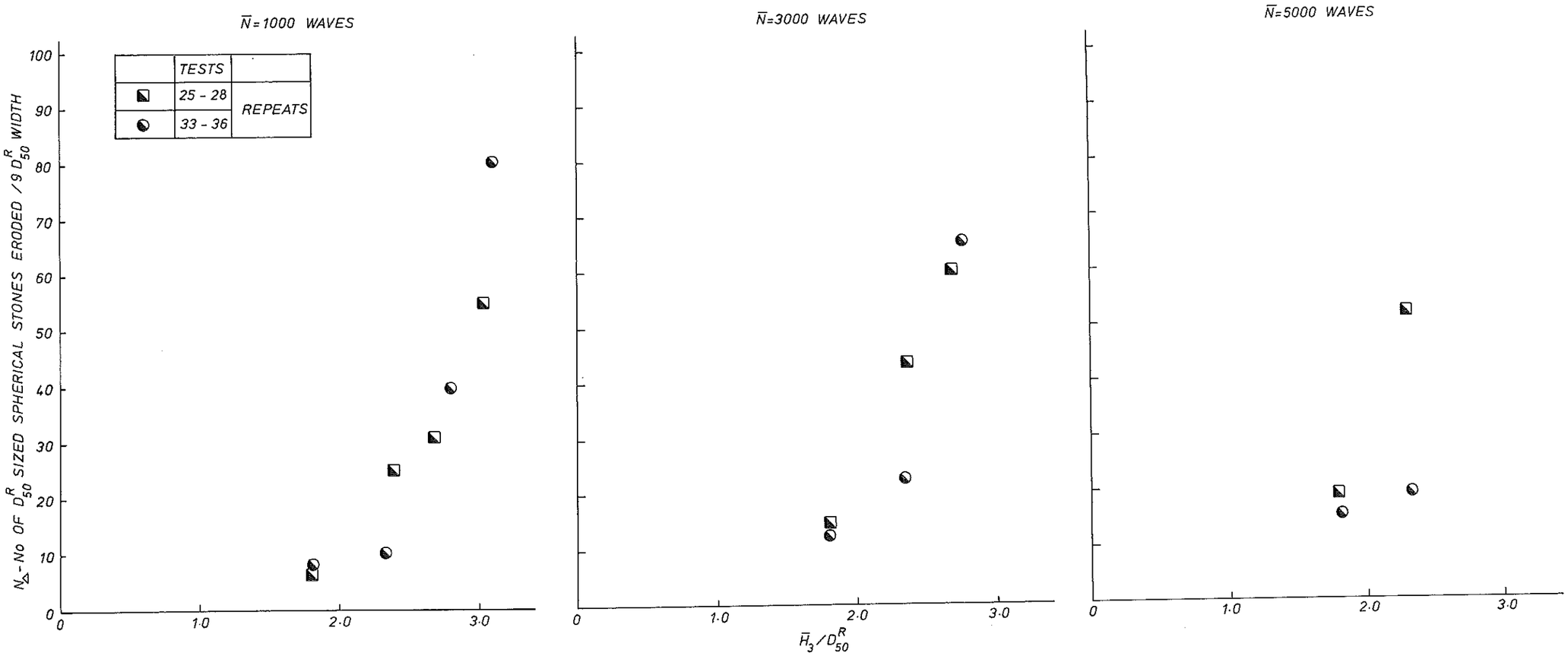

EROSION DAMAGE FOR REPEAT TESTS

FIG 27

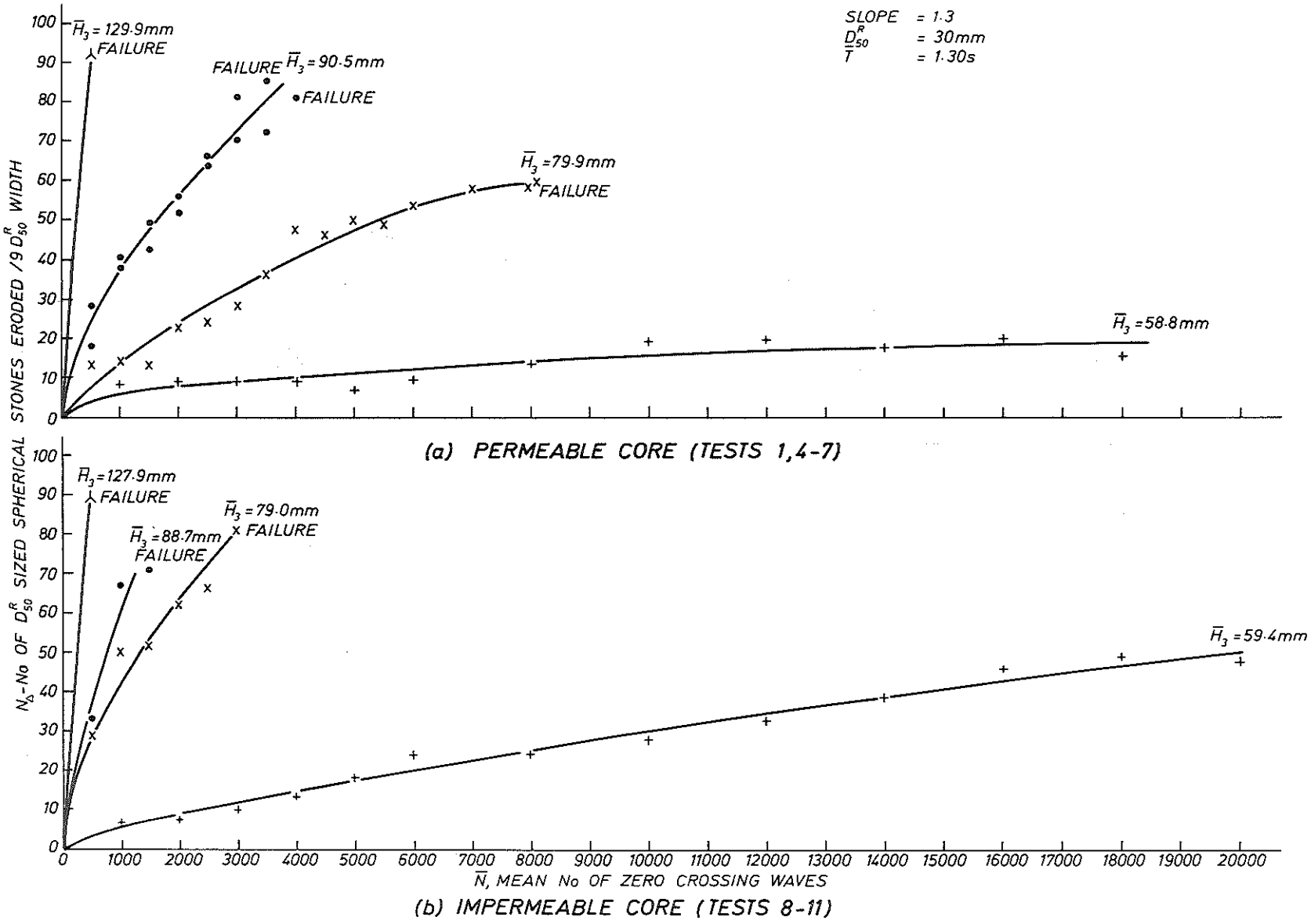

DAMAGE HISTORIES, TESTS 1,4-11

FIG 28

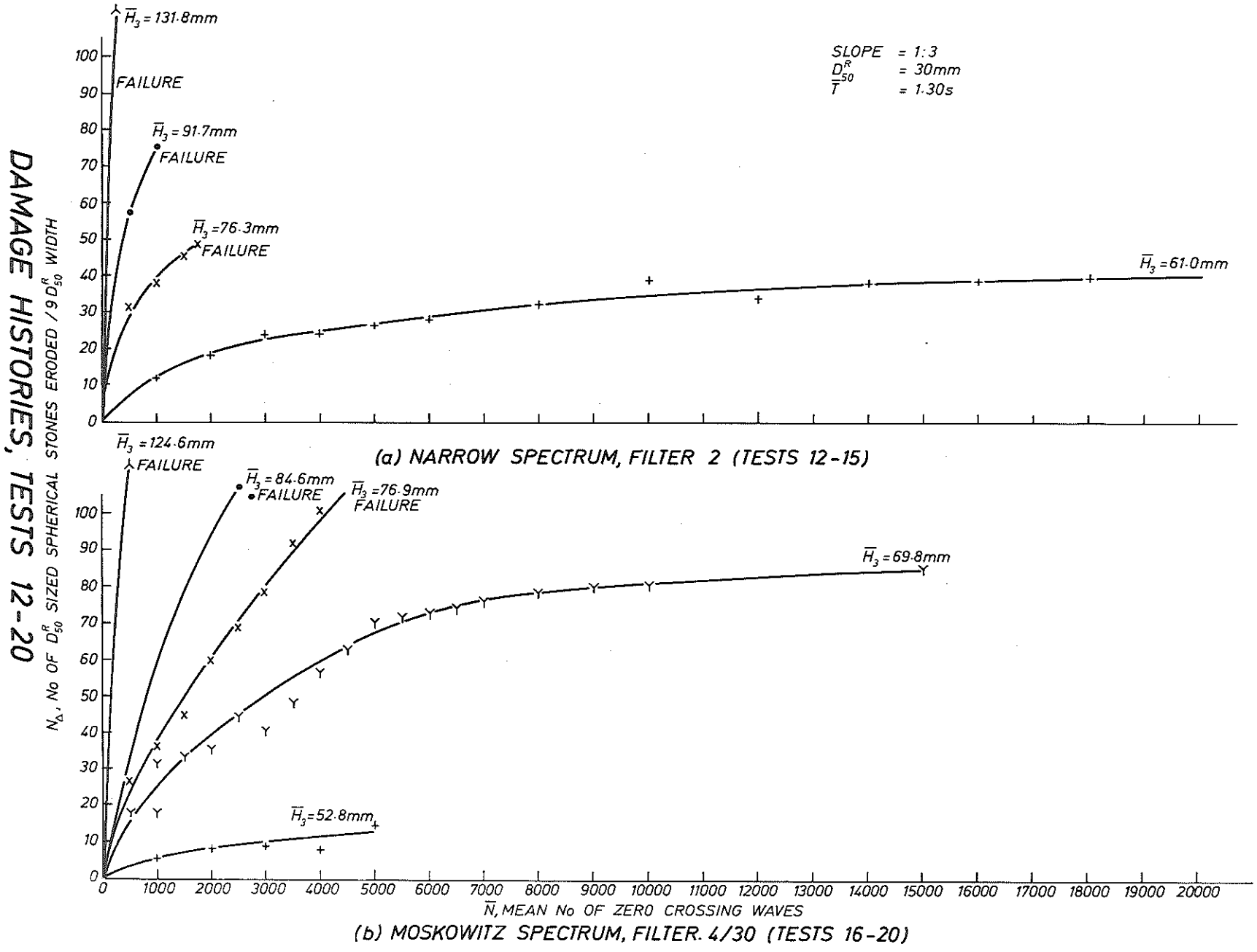
DAMAGE HISTORIES, TESTS 12-20
N_Δ, No OF D_{50}^R SIZED SPHERICAL STONES ERODED / 9 D_{50}^R WIDTH
SLOPE = 1:3
D_{50}^R = 30mm
$\overline{T}$ = 1.30s
$\overline{H}_3$ = 131·8mm
FAILURE
$\overline{H}_3$ = 91·7mm
FAILURE
$\overline{H}_3$ = 76·3mm
FAILURE
$\overline{H}_3$ = 61·0mm
(a) NARROW SPECTRUM, FILTER 2 (TESTS 12-15)
$\overline{H}_3$ = 124·6mm
FAILURE
$\overline{H}_3$ = 84·6mm
FAILURE
$\overline{H}_3$ = 76·9mm
FAILURE
$\overline{H}_3$ = 69·8mm
$\overline{H}_3$ = 52·8mm
$\overline{N}$, MEAN No OF ZERO CROSSING WAVES
(b) MOSKOWITZ SPECTRUM, FILTER. 4/30 (TESTS 16-20)

FIG 29

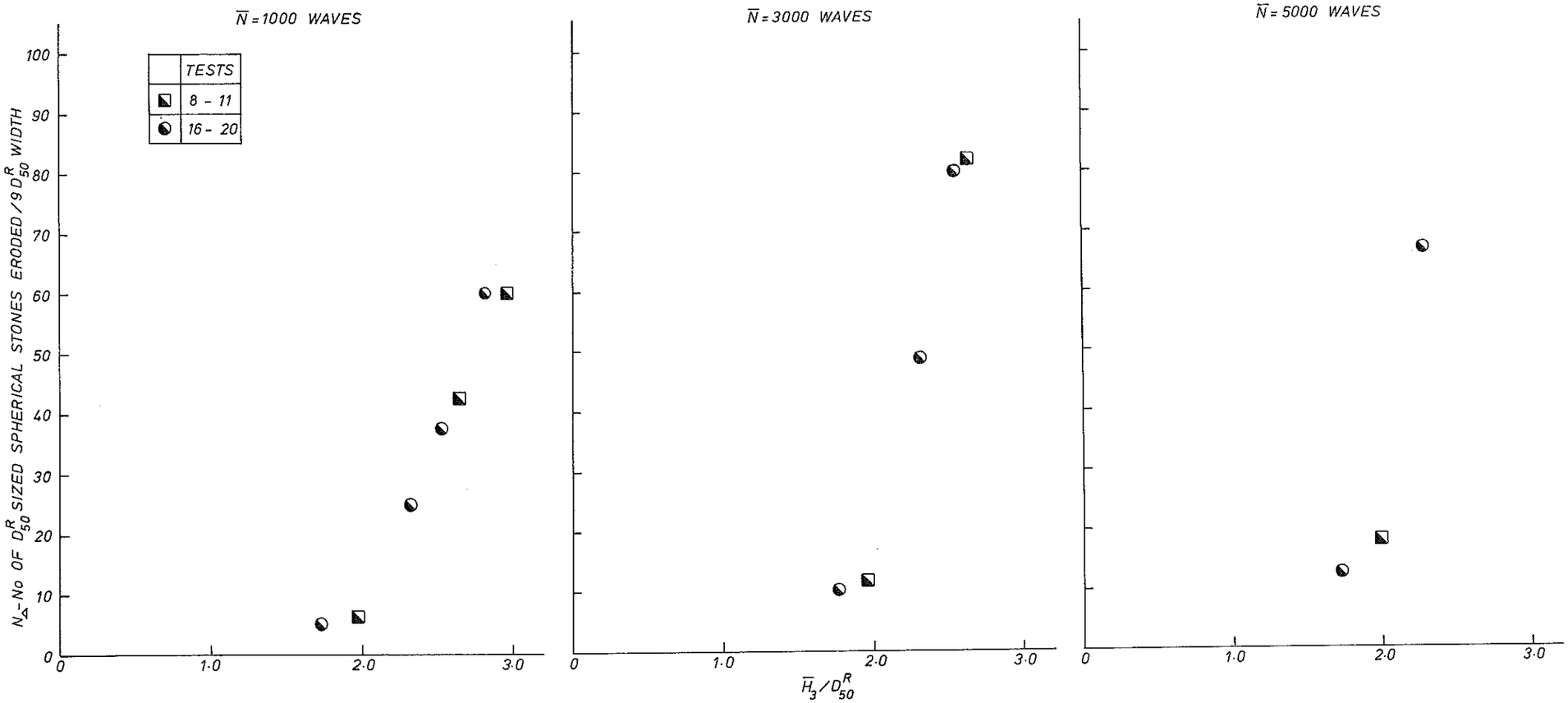

EROSION DAMAGE

FIG 30

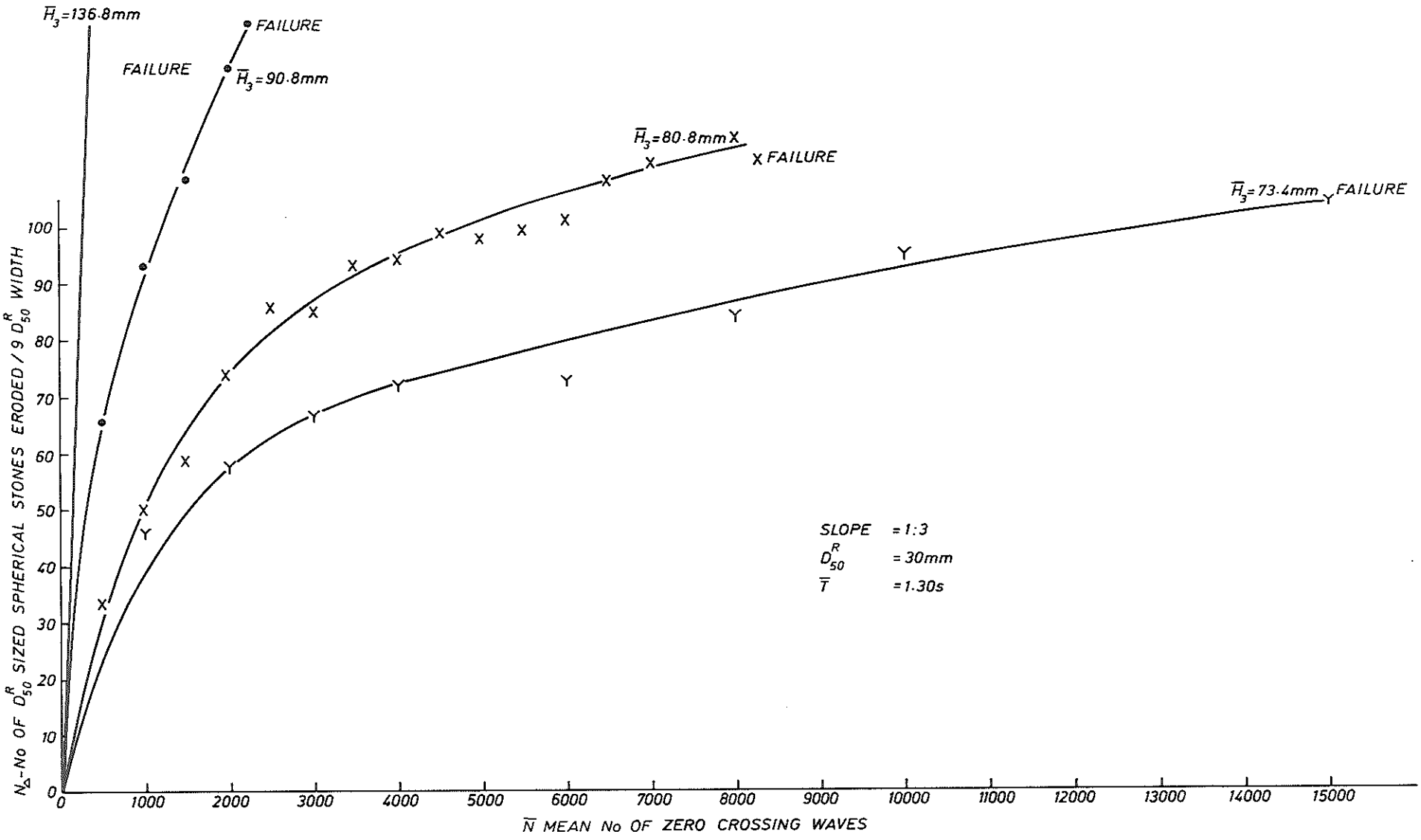

DAMAGE HISTORIES, TESTS 21-24

FIG 31

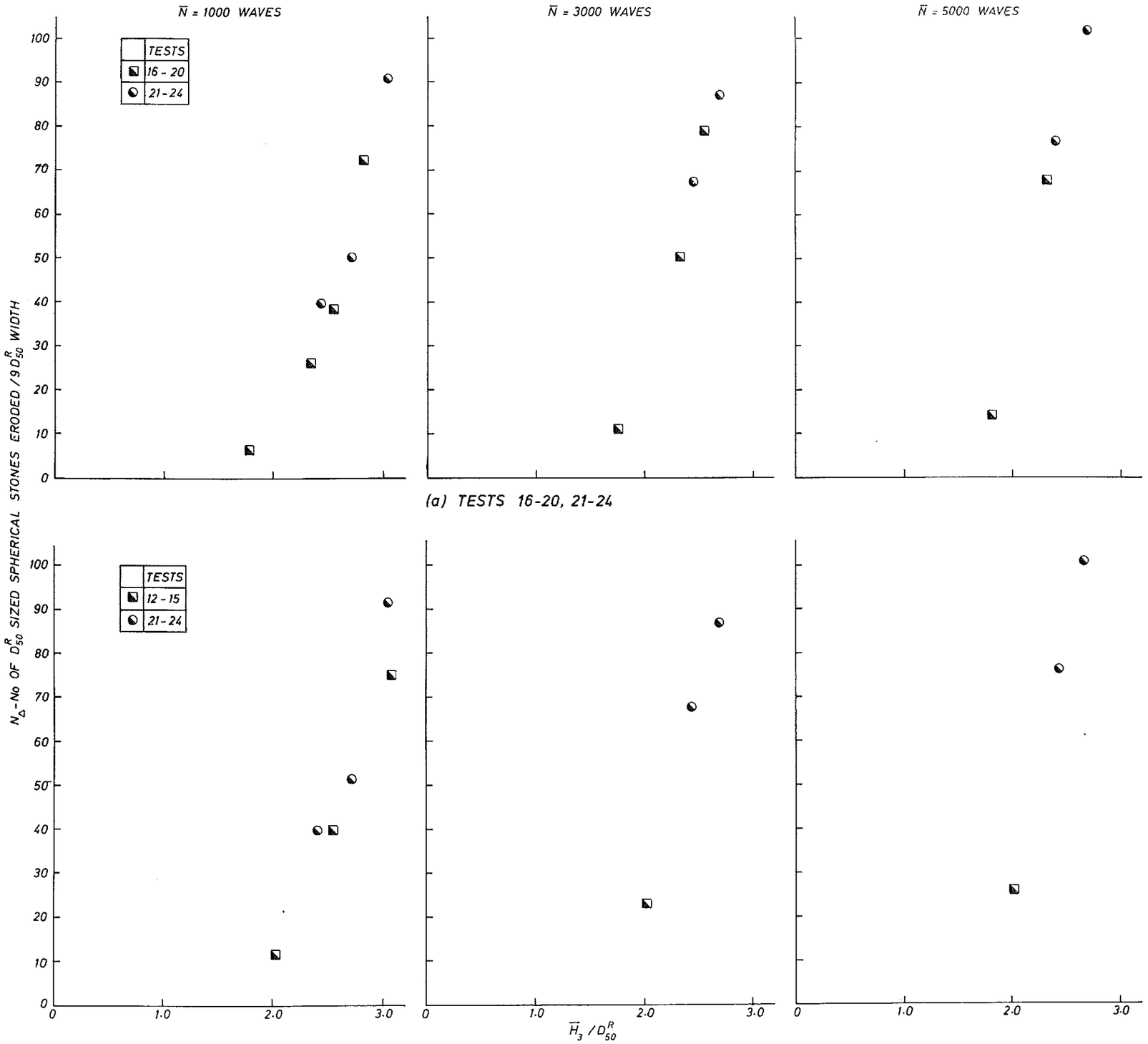

(a) TESTS 16-20, 21-24

(b) TESTS 12-15, 21-24

EROSION DAMAGE

FIG 32

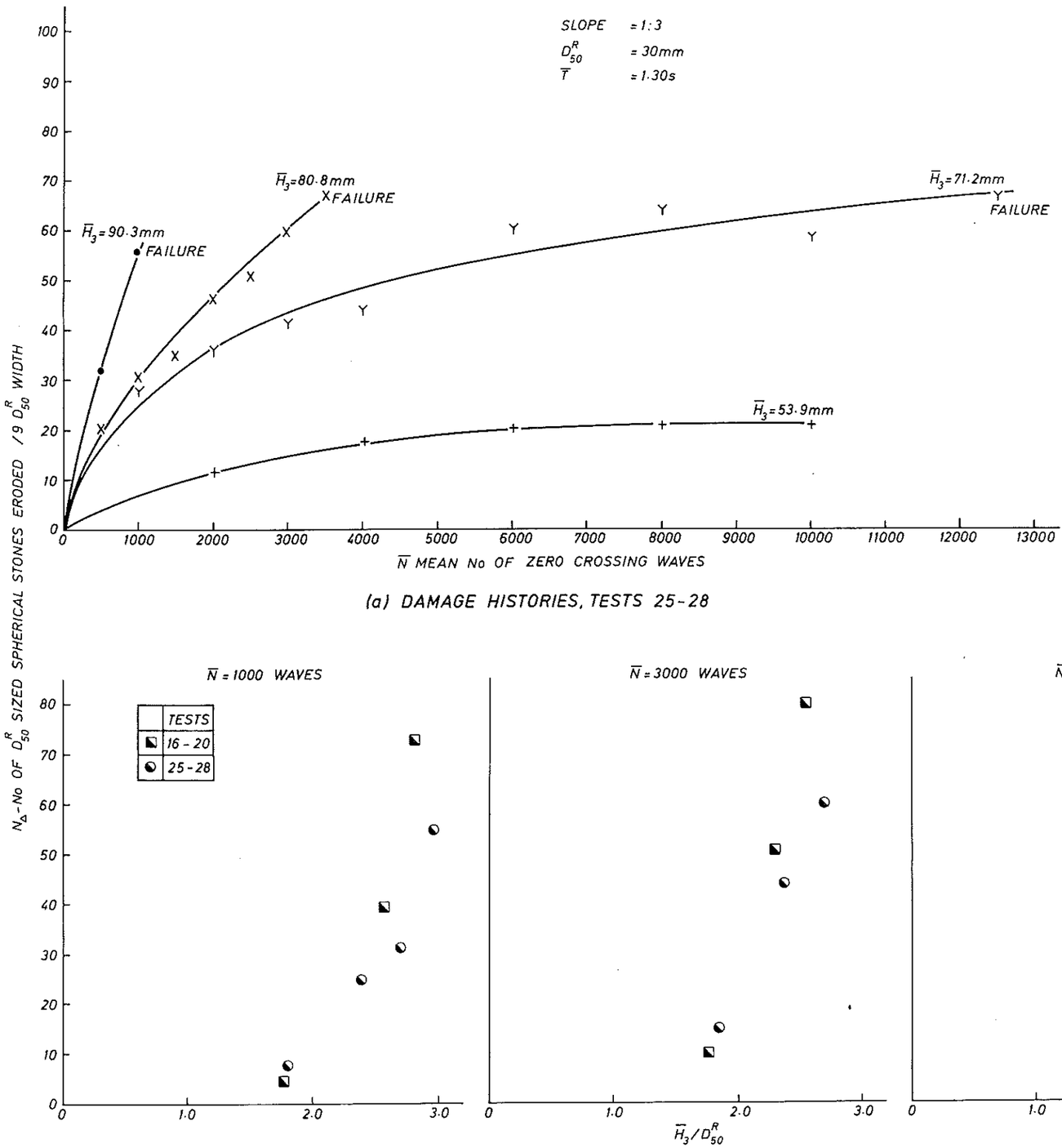

(a) DAMAGE HISTORIES, TESTS 25-28

(b) EROSION DAMAGE, TESTS 16-20, 25-28

DAMAGE RESULTS

FIG 33

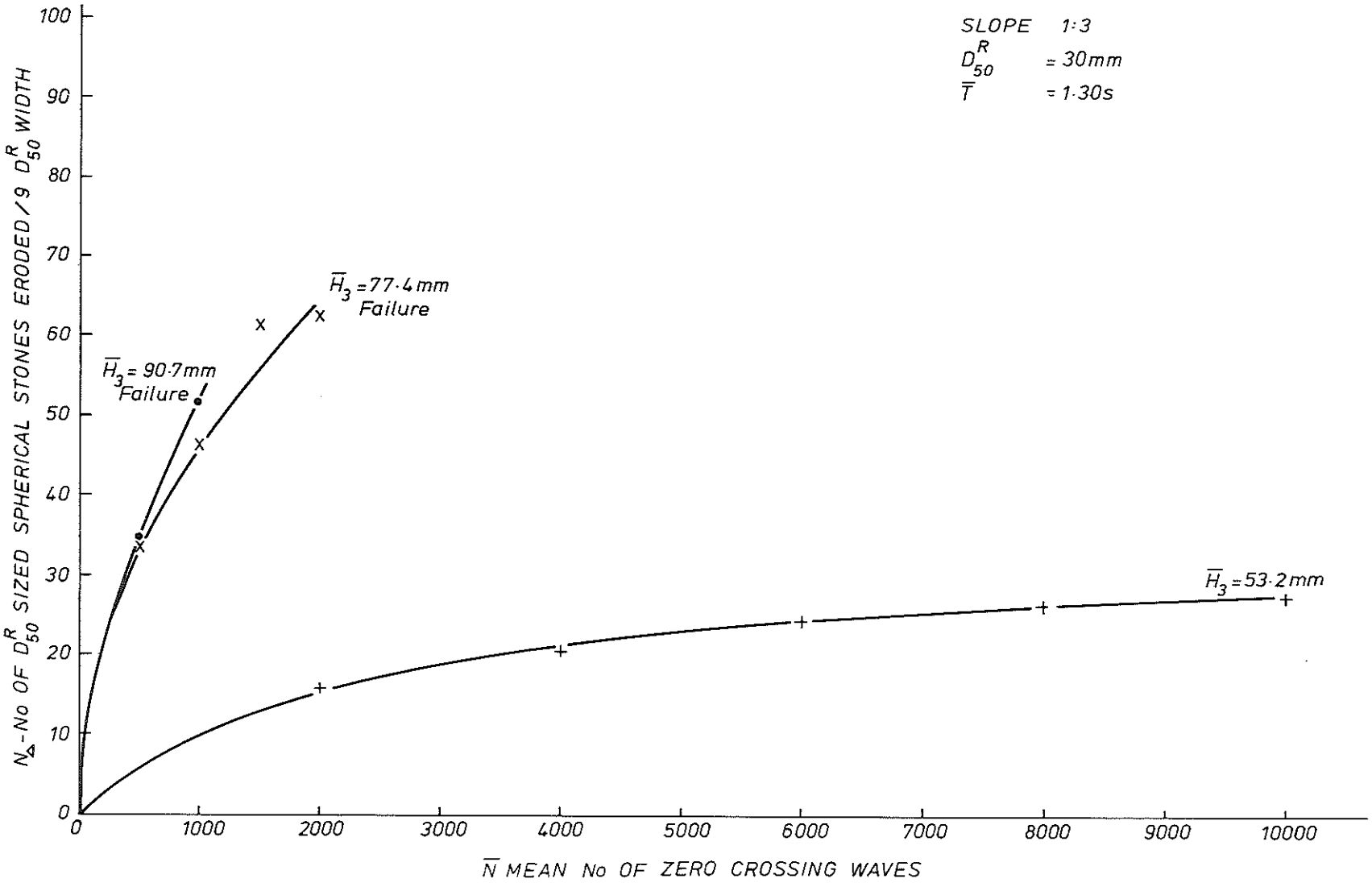

DAMAGE HISTORIES, TEST 29-32

FIG 34

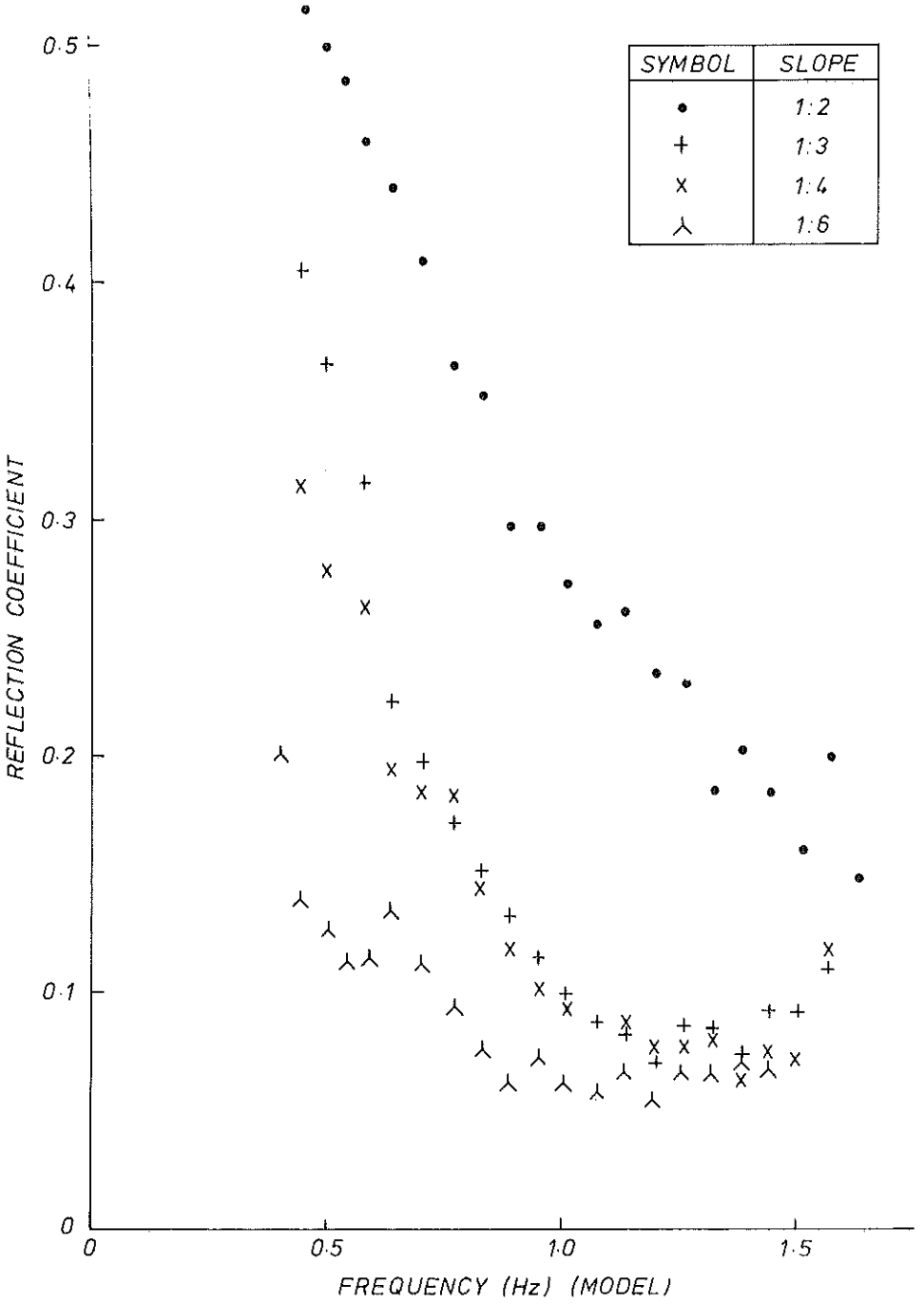

REFLECTION COEFFICIENTS FOR 30mm D_{50}^{R} RIPRAP

FIG 35

PLATES

PLATE 1 Methods of placing

METHOD A Stone laid in strips (tipping up-slope). Each strip adjusted for level before laying next.

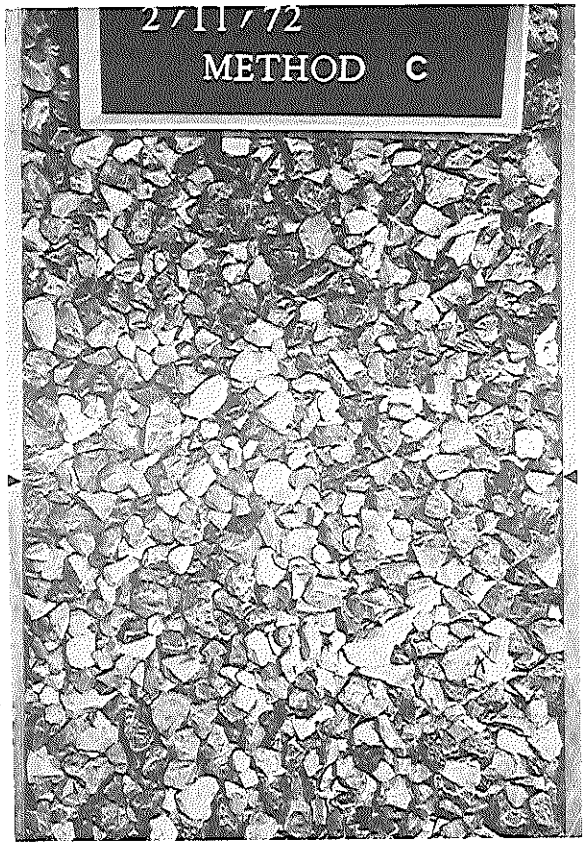

METHOD C Stone laid in strips (tipping down slope). Each strip adjusted for level before laying next.

METHOD B Stone laid in strips (tipping up-slope). All strips laid before adjusting for level.

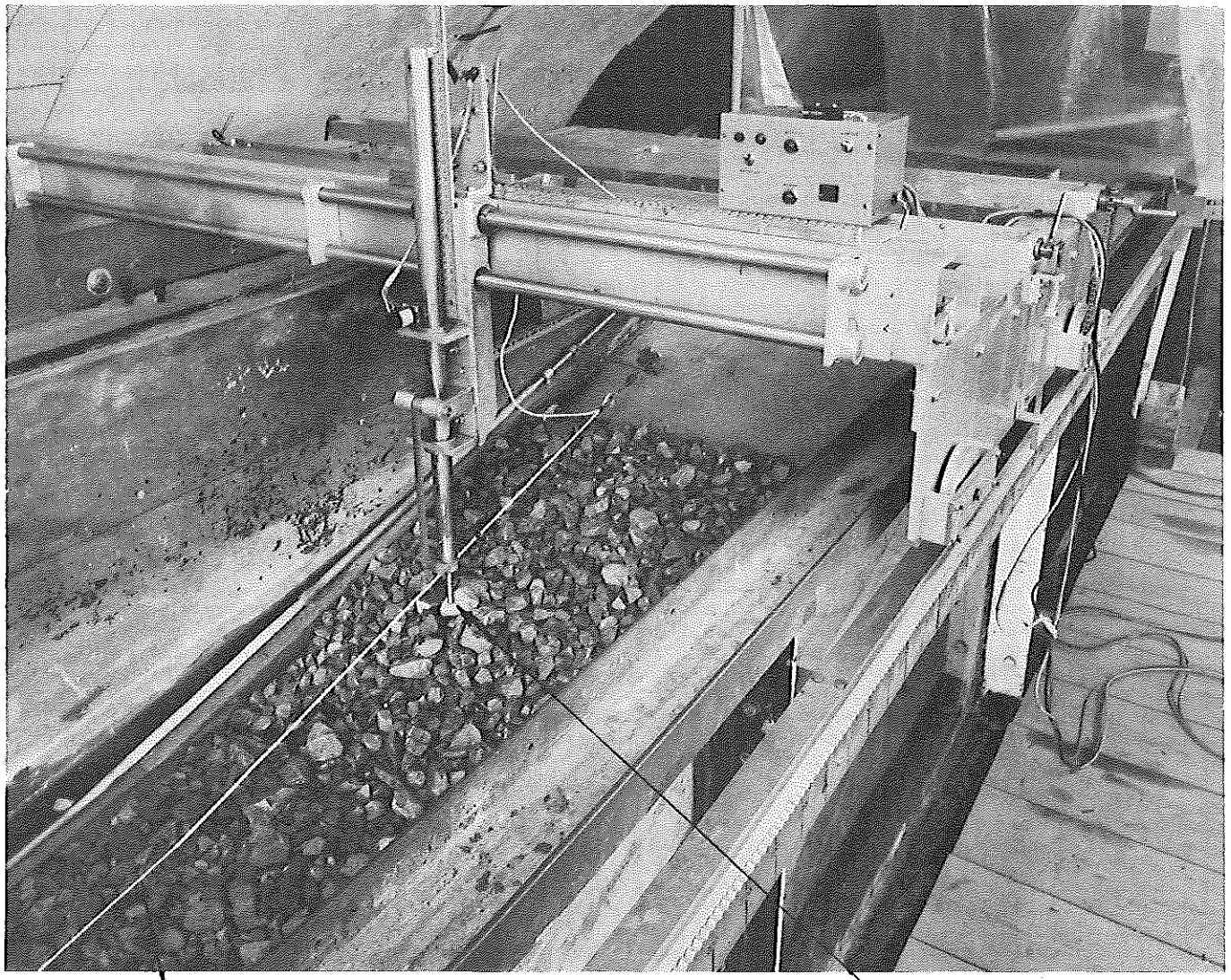

PLATE 2 Experimental facility showing the surface profiler and the run-up recorder

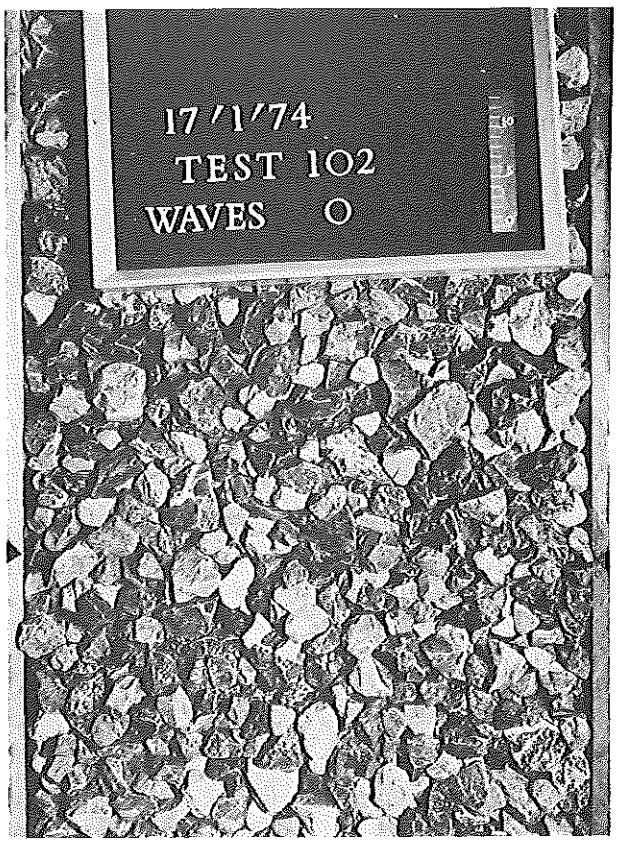

D_{50}^{R} = 40mm

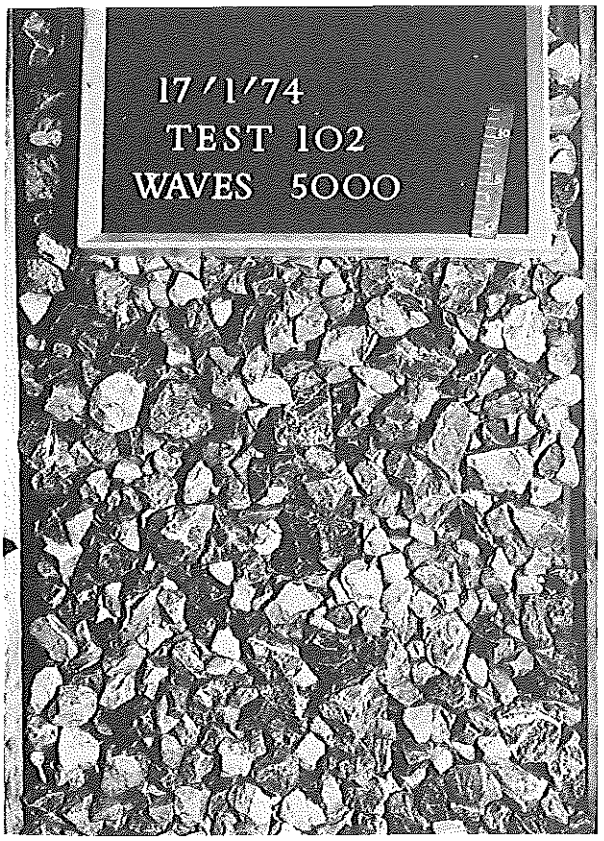

1:2 Slope

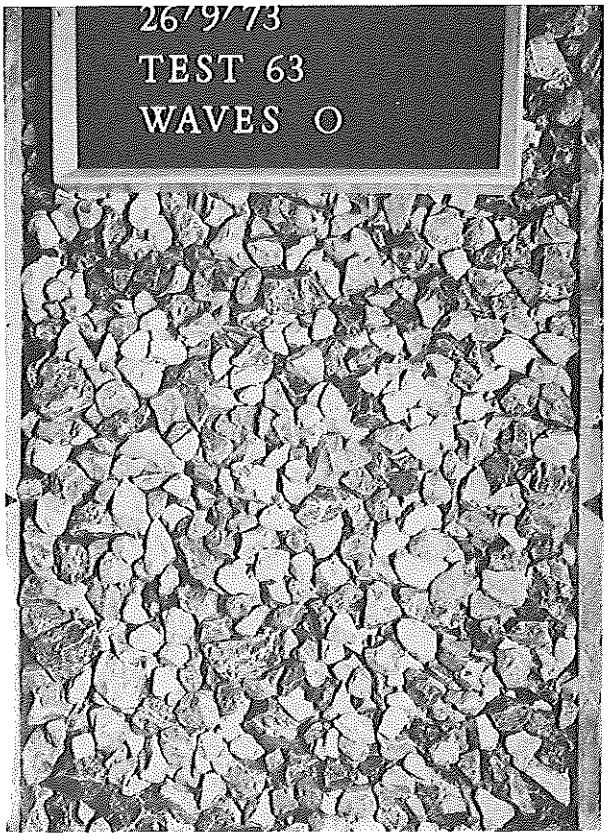

D_{50}^{R} = 40mm

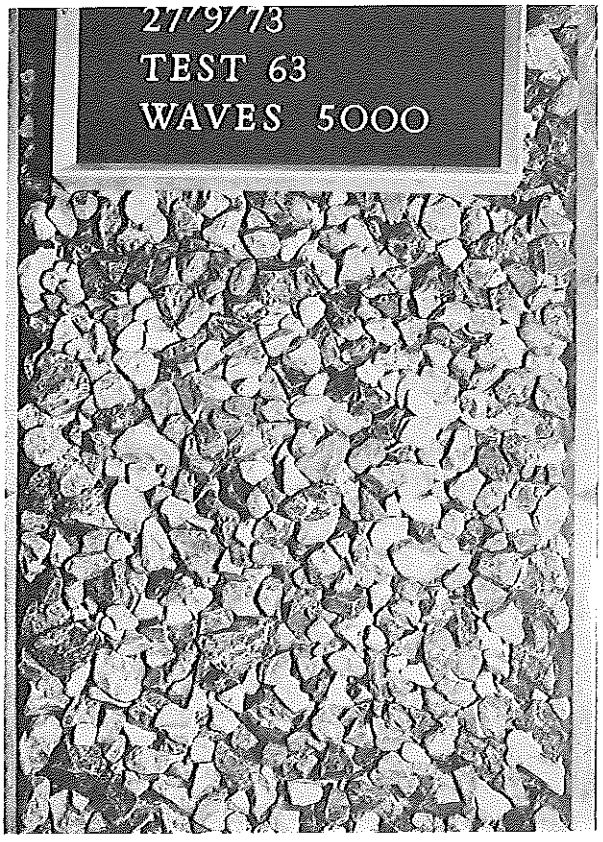

1:3 Slope

PLATE 3 The riprap before and after 5000 waves where failure did not occur

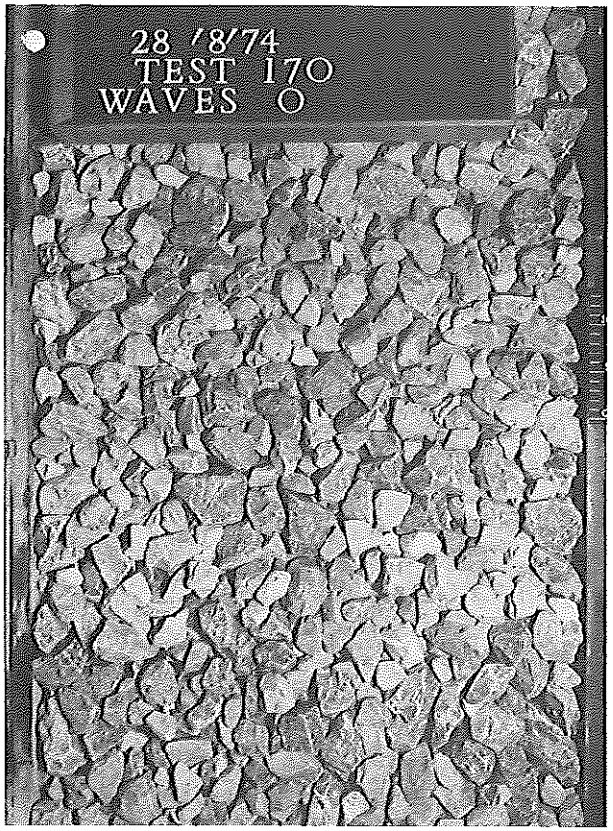

D_{50}^{R} = 40mm

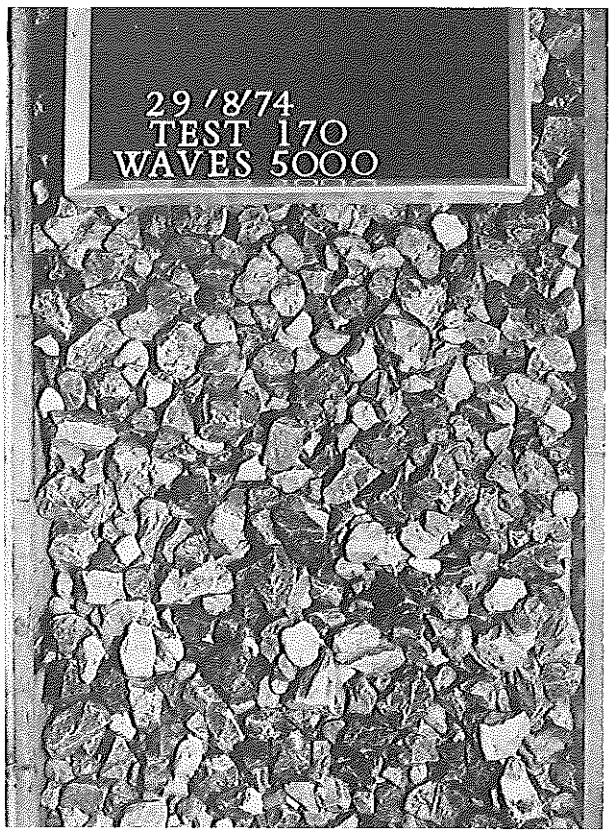

1:4 Slope

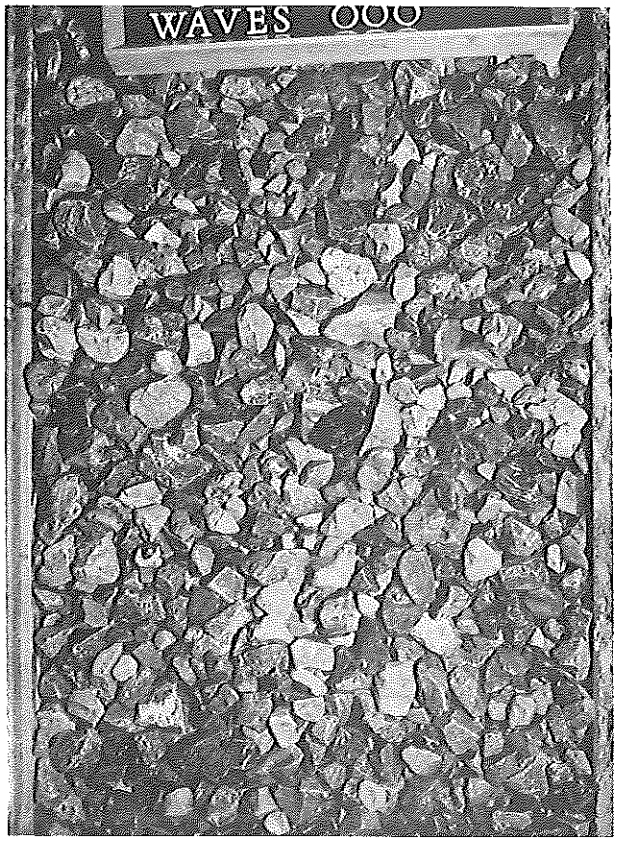

D_{50}^{R} = 30mm

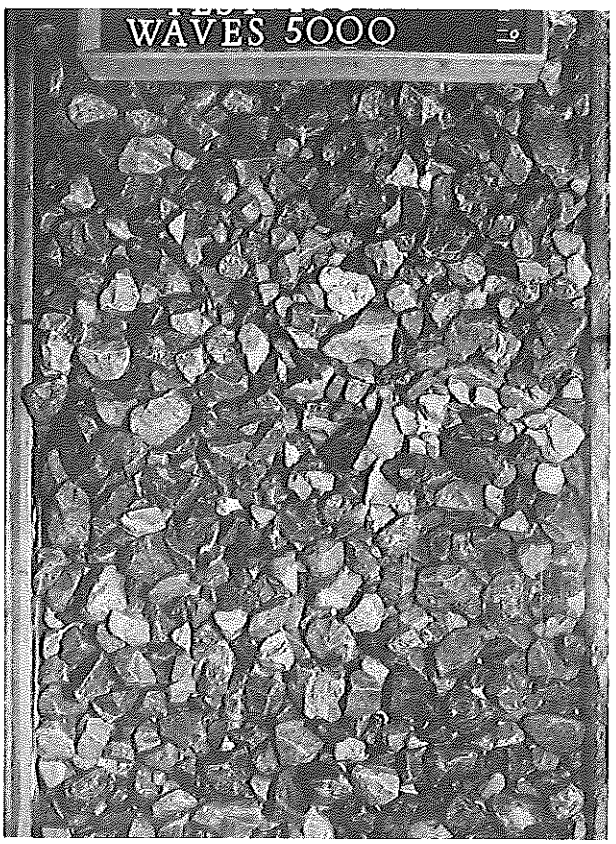

1:6 Slope

PLATE 4 The riprap before and after 5000 waves where failure did not occur

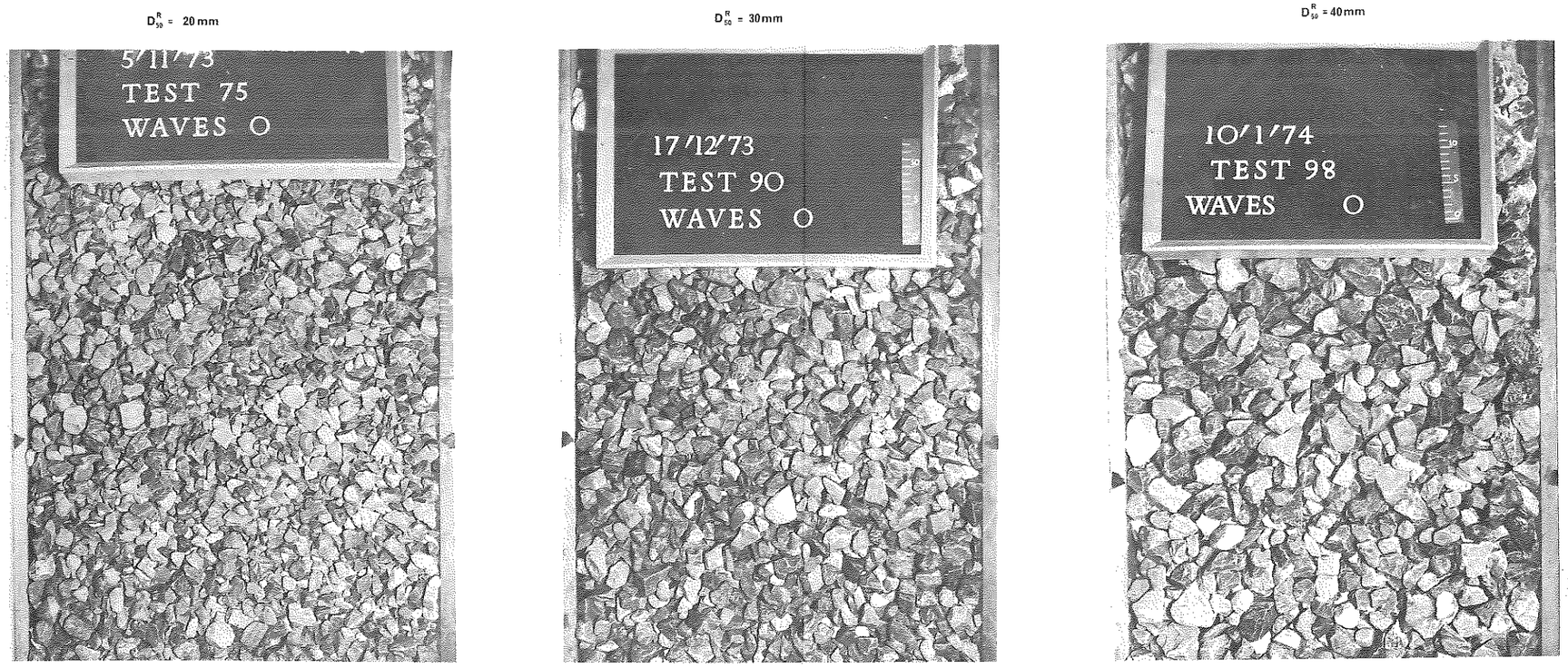

PLATE 5 Typical failures on the 1:2 slope

D_{50}^{R} = 20mm

D_{50}^{R} = 30mm

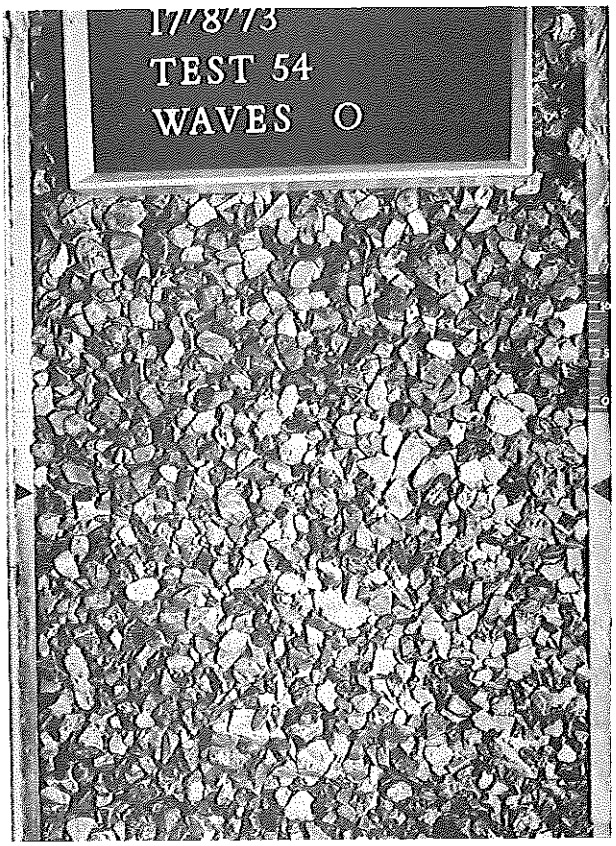

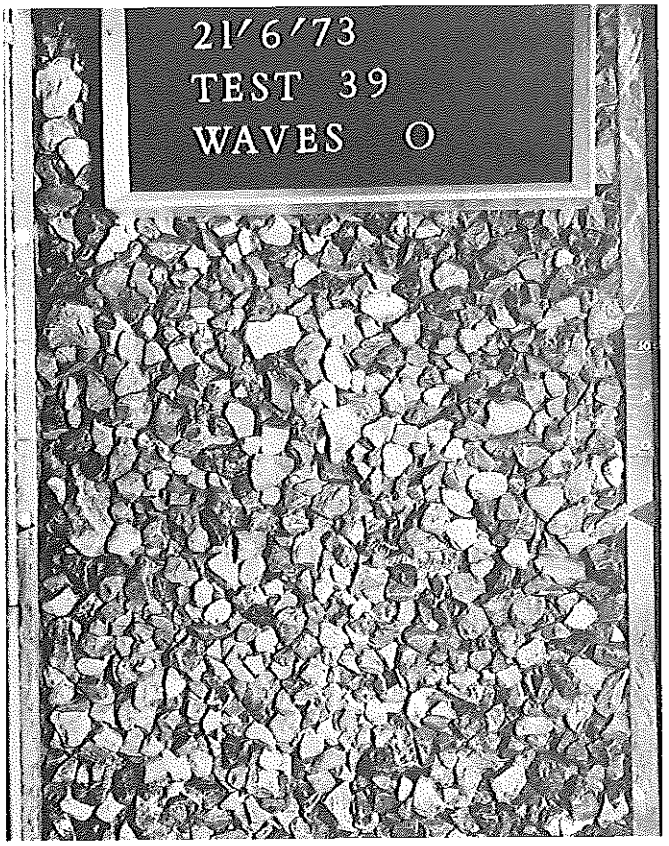

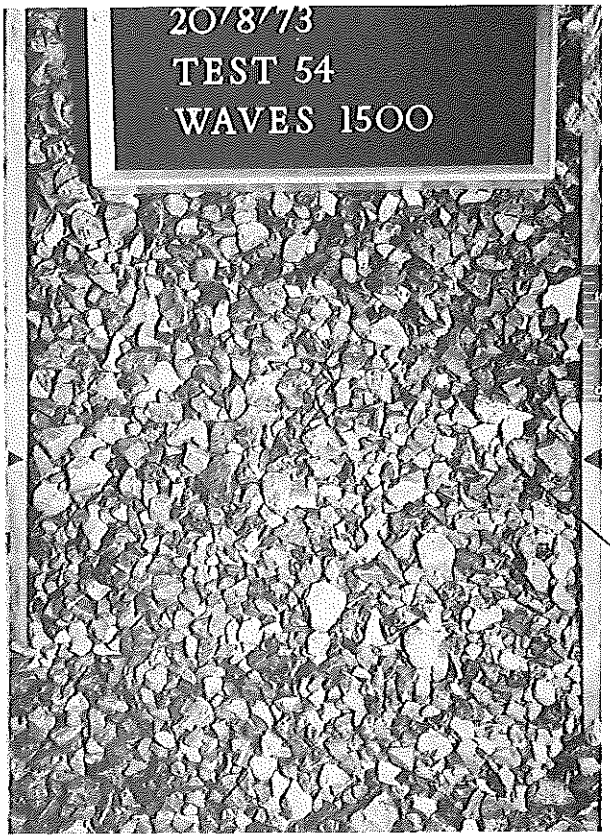

Failure

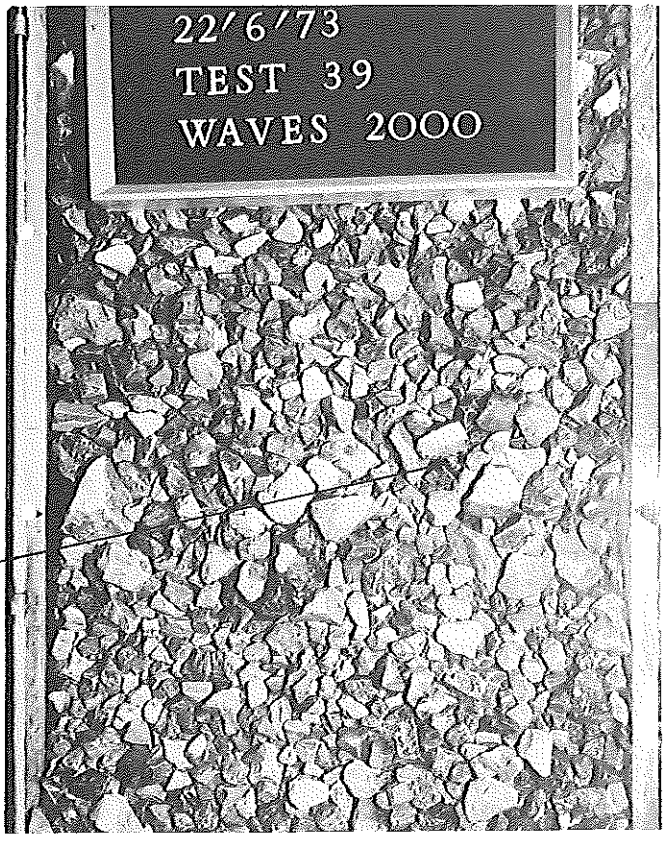

PLATE 6 Typical failures on the 1:3 slope

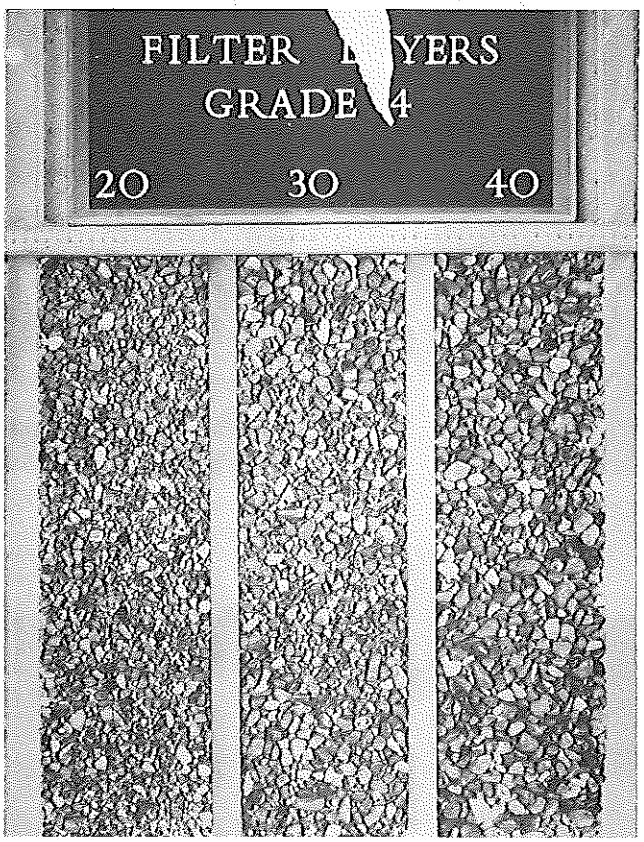

PLATE 7 Filter grades 4/20, 4/30, 4/40 as laid

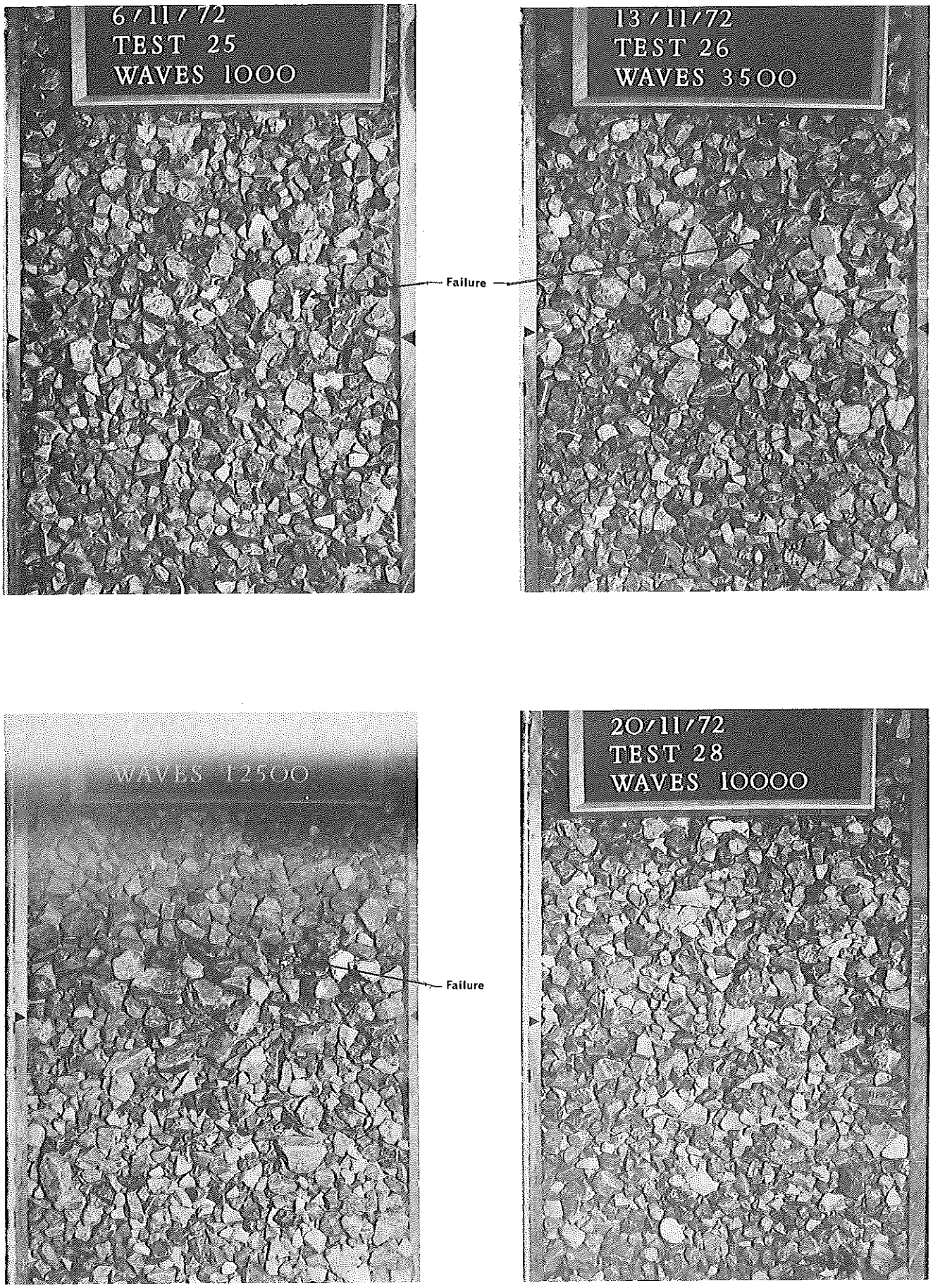

PLATE 8 Exposure of filter layer at failure

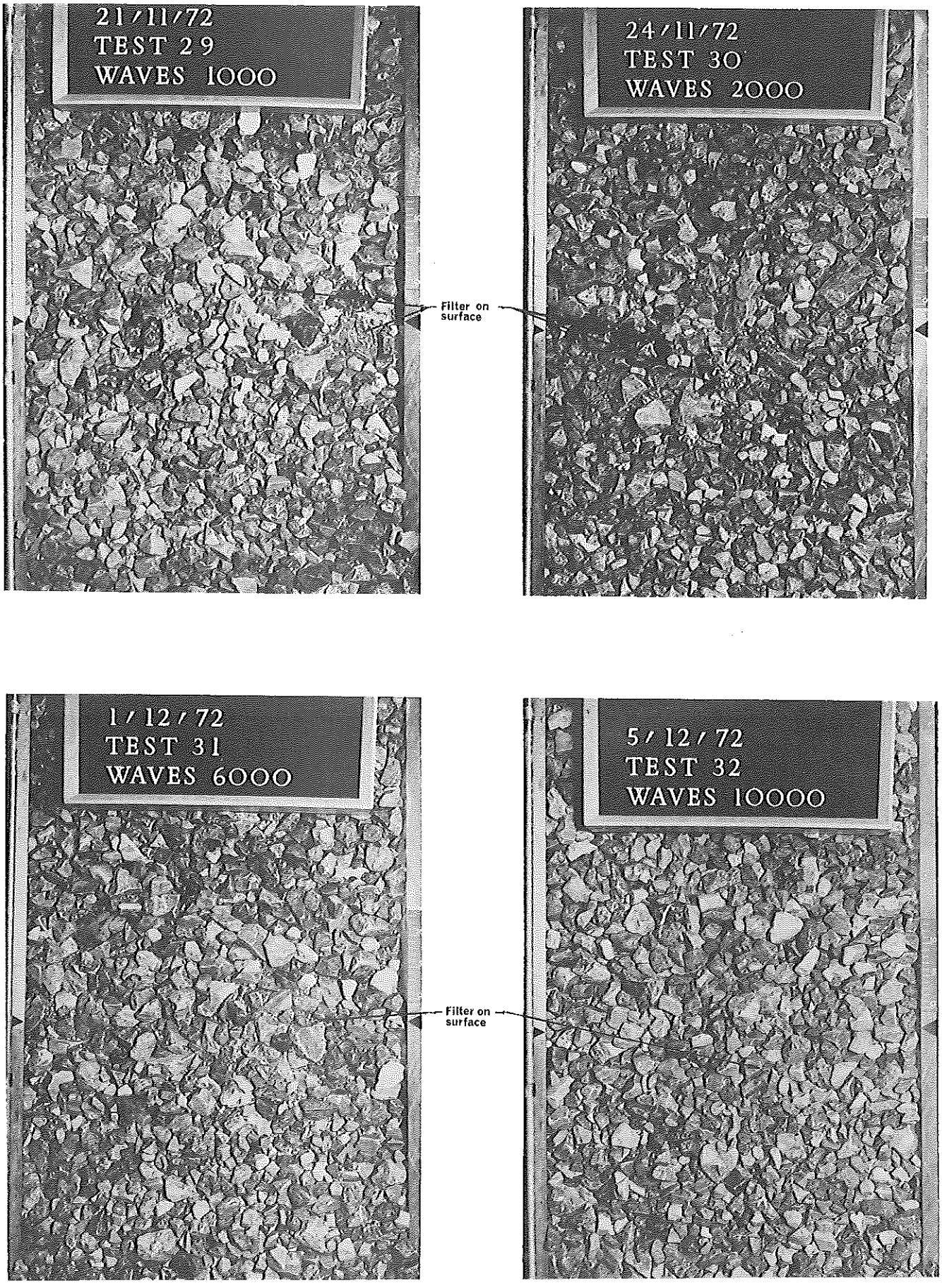

PLATE 9 Tests using fine filter material